

ISME Communications

Interpreting UniFrac with Absolute Abundance: A Conceptual and Practical Guide --Manuscript Draft--

Manuscript Number:	ISMECOMMUN-D-25-00391R3
Full Title:	Interpreting UniFrac with Absolute Abundance: A Conceptual and Practical Guide
Article Type:	Brief Communication
Keywords:	Microbial ecology; Beta Diversity; Absolute Abundance; Bioinformatics; UniFrac
Corresponding Author:	Marian L. Schmidt, PhD Cornell University Ithaca, New York UNITED STATES
Corresponding Author's Institution:	Cornell University
Other Authors:	Augustus R. Pendleton
Abstract:	<p>β-diversity is central to microbial ecology, yet commonly used metrics overlook changes in microbial load (or “absolute abundance”), limiting their ability to detect ecologically meaningful shifts. Popular for incorporating phylogenetic relationships, UniFrac distances currently default to relative abundance and therefore omit important variation in microbial abundances. As quantifying absolute abundance becomes more accessible, integrating this information into β-diversity analyses is essential. Here, we introduce Absolute UniFrac (UA), a variant of Weighted UniFrac that incorporates absolute abundances. Using simulations and a reanalysis of four 16S rRNA metabarcoding datasets (from a nuclear reactor cooling tank, the mouse gut, a freshwater lake, and the peanut rhizosphere), we demonstrate that Absolute UniFrac captures microbial load, composition, and phylogenetic relationships. While this can improve statistical power to detect ecological shifts, we also find Absolute UniFrac can be strongly correlated to differences in cell abundances alone. To balance these effects, we also incorporate absolute abundance into the generalized extension (GUA) that has a tunable, continuous ecological parameter (α) that modulates the relative contribution of rare versus abundant lineages to β-diversity calculations. Finally, we benchmark GUA and show that although computationally slower than conventional alternatives, GUA is comparably sensitive to noise in load estimates compared to conventional alternatives like Bray-Curtis dissimilarities, particularly at lower α. By coupling phylogeny, composition, and microbial load, Absolute UniFrac integrates three dimensions of ecological change, better equipping microbial ecologists to quantitatively compare microbial communities.</p>
Additional Information:	
Question	Response
Please state the numeric word count of your manuscript, counting from the beginning of the abstract to the end of the main manuscript (excluding references and figure legends). If substantially longer than the limit (e.g., 5,000 words for an Article), you may be asked to reduce the manuscript’s length, before or after review. Word counts for various publication types are detailed in our Author Instructions .	3750
Has this manuscript been submitted to this journal previously?	Yes
Please indicate the manuscript number for the previous submission.	25-00391

as follow-up to "Has this manuscript
been submitted to this journal previously?"

1 **Interpreting UniFrac with Absolute Abundance: A Conceptual and Practical Guide**

2 Augustus Pendleton^{1*} & Marian L. Schmidt^{1*}

3 ¹Department of Microbiology, Cornell University, 123 Wing Dr, Ithaca, NY 14850, USA

4 **Corresponding Authors:** Augustus Pendleton: arp277@cornell.edu; Marian L. Schmidt:

5 marschmi@cornell.edu; MarianL.Schmidt@gmail.com

6 **Physical Mailing Address:** Augustus Pendleton or Marian L. Schmidt, Department of
7 Microbiology, Cornell University, 123 Wing Drive, Ithaca, NY, 14853, United States

8 **Running Title:** A Guide to Absolute-Abundance UniFrac

9 **Abstract**

10 β -diversity is central to microbial ecology, yet commonly used metrics overlook changes in
11 microbial load (or “absolute abundance”), limiting their ability to detect ecologically meaningful
12 shifts. Popular for incorporating phylogenetic relationships, UniFrac distances currently default
13 to relative abundance and therefore omit important variation in microbial abundances. As
14 quantifying absolute abundance becomes more accessible, integrating this information into β -
15 diversity analyses is essential. Here, we introduce *Absolute UniFrac* (U^A), a variant of Weighted
16 UniFrac that incorporates absolute abundances. Using simulations and a reanalysis of four 16S
17 rRNA metabarcoding datasets (from a nuclear reactor cooling tank, the mouse gut, a freshwater
18 lake, and the peanut rhizosphere), we demonstrate that Absolute UniFrac captures microbial load,
19 composition, and phylogenetic relationships. While this can improve statistical power to detect
20 ecological shifts, we also find Absolute UniFrac can be strongly correlated to differences in cell
21 abundances alone. To balance these effects, we also incorporate absolute abundance into the
22 generalized extension (GU^A) that has a tunable, continuous ecological parameter (α) that
23 modulates the relative contribution of rare versus abundant lineages to β -diversity calculations.
24 Finally, we benchmark GU^A and show that although computationally slower than conventional
25 alternatives, GU^A is comparably sensitive to noise in load estimates compared to conventional
26 alternatives like Bray-Curtis dissimilarities, particularly at lower α . By coupling phylogeny,
27 composition, and microbial load, Absolute UniFrac integrates three dimensions of ecological
28 change, better equipping microbial ecologists to quantitatively compare microbial communities.

29

30 **Keywords:** Microbial Ecology - Beta Diversity - Absolute Abundance - Bioinformatics -
31 UniFrac

32 **Main Text**

33 Microbial ecologists routinely compare communities using β -diversity metrics derived
34 from relative abundances. Yet this approach overlooks a critical ecological dimension: microbial
35 load. High-throughput sequencing produces compositional data, in which each taxon's
36 abundance is constrained by all others [1]. However, quantitative profiling studies show that cell
37 abundance, not only composition, can drive major community differences [2]. In low-biomass
38 samples, relying on relative abundance can allow contaminants to appear biologically
39 meaningful despite absolute counts too low for concern [3].

40 Sequencing-based microbiome studies therefore rely on relative abundance even when
41 the hypotheses of interest implicitly concern absolute changes in biomass. This creates a
42 mismatch between ecological framing (growth, bloom magnitude, pathogen proliferation,
43 disturbance recovery, or colonization pressure) and the information the β -diversity metric
44 encodes [4]. As a result, β -diversity is often treated as if it includes biomass, even when absolute
45 abundance is either not measured at all or is measured but excluded from the calculation (as in
46 conventional UniFrac). Many studies therefore test biomass-linked hypotheses using a metric
47 that normalizes biomass away [4]. A conceptual correction is needed in which β -diversity is
48 understood as variation along three axes: composition, phylogeny and absolute abundance.

49 Absolute microbial load measurements are now increasingly obtainable through flow
50 cytometry, qPCR, and genomic spike-ins, allowing biomass to be quantified alongside taxonomic
51 composition [4, 5]. These approaches improve detection of functionally relevant taxa and
52 mitigate the compositional constraints imposed by sequencing [1, 2]. Most studies that
53 incorporate absolute abundance counts currently rely on Bray-Curtis dissimilarity, which can
54 capture load but does not consider phylogenetic similarity [5–7]. Unifrac distances provide the
55 opposite strength, incorporating phylogeny but discarding absolute abundance, as they are
56 restricted to relative abundance data by construction [8]. This leaves no phylogenetically
57 informed β -diversity metric that operates on absolute counts, despite the fact that biomass is
58 central to many ecological hypotheses.

59 To evaluate the implications of incorporating absolute abundance into phylogenetic β -
60 diversity, we use both simulations and reanalysis of four 16S rRNA amplicon datasets. The

61 simulations use a simple four-taxon community with controlled abundance shifts to directly
62 compare both Bray-Curtis and UniFrac in their relative and absolute forms, illustrating how each
63 metric responds when abundance, composition, or evolutionary relatedness differ. We then
64 reanalyze four real-world datasets spanning nuclear reactor cooling water [5], the mouse gut [3],
65 a freshwater lake [9], and rhizosphere soil [10]. These differ widely in richness, biomass range,
66 and ecological context, allowing us to test when absolute abundance changes align with or
67 diverge from phylogenetic turnover. Together, these simulations and reanalyses provide the
68 empirical foundation for interpreting Absolute UniFrac relative to existing β -diversity measures
69 across the three axes of ecological difference: abundance, composition, and phylogeny.

70 We also extend Absolute UniFrac as was proposed by [11] to Generalized Absolute
71 UniFrac that incorporates a tunable ecological dimension, α , and evaluate its impact across
72 simulated and real-world datasets. As α increases, β -diversity is increasingly correlated with
73 differences in absolute abundance, allowing researchers to fine tune the relative weight their
74 analyses place on microbial load versus composition.

75 Defining Absolute UniFrac

76 The UniFrac distance was first introduced by Lozupone & Knight (2005) and has since
77 become enormously popular as a measure of β -diversity within the field of microbial ecology
78 [12]. A benefit of the UniFrac distance is that it considers phylogenetic information when
79 estimating the distance between two communities. After first generating a phylogenetic tree
80 representing species (or amplicon sequence variants, “ASVs”) from all samples, the UniFrac
81 distance computes the fraction of branch-lengths which is *shared* between communities, relative
82 to the total branch length represented in the tree. UniFrac can be both unweighted, in which only
83 the incidence of species is considered, or weighted, wherein a branch’s contribution is weighted
84 by the proportional abundance of taxa on that branch [8]. The Weighted UniFrac is derived:

$$85 U^R = \frac{\sum_{i=1}^n b_i |p_i^a - p_i^b|}{\sum_{i=1}^n b_i (p_i^a + p_i^b)}$$

86 where the contribution of each branch length, b_i , is weighted by the difference in the relative
87 abundance of all species (p_i) descended from that branch in sample a or sample b . Here, we
88 denote this distance as U^R , for “Relative UniFrac”. Popular packages which calculate weighted

89 UniFrac—including the diversity-lib QIIME plug-in and the R packages phyloseq and
90 GUUniFrac—run this normalization by default [11, 13, 14].

91 Importantly, U^R is most sensitive to changes in abundant lineages, which can sometimes
92 obscure compositional differences driven by rare to moderately-abundant taxa [11]. To address
93 this weakness, Chen et al. (2012) introduced the generalized UniFrac distance (GU^R), in which
94 the impact of abundant lineages can be mitigated by decreasing the parameter α :

$$95 \quad GU^R = \frac{\sum_{i=1}^n b_i (p_i^a + p_i^b)^\alpha \left| \frac{p_i^a - p_i^b}{p_i^a + p_i^b} \right|}{\sum_{i=1}^n b_i (p_i^a + p_i^b)^\alpha}$$

96 where α ranges from 0 (close to Unweighted UniFrac) up to 1 (identical to U^R , above). However,
97 if one wishes to use absolute abundances, both U^R and GU^R can be derived without normalizing
98 to proportions:

$$99 \quad U^A = \frac{\sum_{i=1}^n b_i |c_i^a - c_i^b|}{\sum_{i=1}^n b_i (c_i^a + c_i^b)} \quad GU^A = \frac{\sum_{i=1}^n b_i (c_i^a + c_i^b)^\alpha \left| \frac{c_i^a - c_i^b}{c_i^a + c_i^b} \right|}{\sum_{i=1}^n b_i (c_i^a + c_i^b)^\alpha}$$

100 Where c_i^a and c_i^b denote for the absolute counts of species descending from branch b_i in
101 communities a and b , respectively. We refer to these distances as *Absolute UniFrac* (U^A) and
102 *Generalized Absolute UniFrac* (GU^A). Although substituting absolute for relative abundances is
103 mathematically straightforward, to our knowledge there is no prior work that examines UniFrac
104 in the context of absolute abundance, either conceptually or in application. Incorporating
105 absolute abundances introduces a third axis of ecological variation: beyond differences in
106 composition and phylogenetic similarity, U^A also captures divergence in microbial load. This
107 makes interpretation of U^A nontrivial, particularly in complex microbiomes.

108 Demonstrating β -diversity metrics' behavior with a simple simulation

109 To clarify how U^A behaves relative to existing β -diversity metrics, we first constructed a
110 simple four-taxon simulated community arranged in a small phylogeny (Fig. 1A). By varying the
111 absolute abundance of each ASV (1, 10, or 100), we generated 81 samples and 3,240 pairwise
112 comparisons. For each pair, we computed four dissimilarity metrics: Bray-Curtis with relative

113 abundance (BC^R), Bray-Curtis with absolute abundance (BC^A), Weighted UniFrac with relative
114 abundance (U^R), and Weighted UniFrac with absolute abundance (U^A). These comparisons help
115 to illustrate how each axis of ecological difference—abundance, composition, and phylogeny—is
116 expressed by the different metrics.

117 U^A does not consistently yield higher or lower distances compared to other metrics, but
118 instead varies depending on how abundance and phylogeny intersect (Fig. 1B). In the improbable
119 scenario that all branch lengths are equal, U^A is always less than or equal to BC^A (Fig. S1).
120 These comparisons emphasize that once branch lengths differ, incorporating phylogeny and
121 absolute abundance alters the structure of the distance space. The direction and magnitude of that
122 change depend on which branches carry the abundance shifts. U^A is also usually smaller than
123 BC^A and is more strongly correlated with BC^A (Pearson's $r = 0.82$, $p < 0.0001$) than with BC^R (r
124 = 0.41) and U^R ($r = 0.55$).

125 To better understand how these metrics diverge, we examined individual sample pairs
126 (Fig. 1C). Scenario 1 (gold star) illustrates the classic advantage of UniFrac: ASV_1 and ASV_2
127 are phylogenetically close, so U^R and U^A discern greater similarity between samples than BC^R
128 and BC^A , which ignore phylogenetic structure. Scenario 2 (red star) highlights a limitation of
129 relative metrics: two samples with identical relative composition but a 100-fold difference in
130 biomass appear identical to BC^R and U^R , but not to their absolute counterparts. In Scenario 3
131 (green star), incorporating absolute abundance decreases dissimilarity. BC^A and U^A are lower
132 than their relative counterparts because half the community is identical in absolute abundance,
133 even though their proportions differ. In contrast, Scenario 4 (blue star) shows that U^A can exceed
134 BC^A when abundance differences occur on long branches, amplifying phylogenetic dissimilarity.

135 These scenarios demonstrate that U^A integrates variation along three ecologically
136 relevant axes: composition, phylogenetic similarity, and microbial load, rather than isolating any
137 single dimension. Because a given U^A value can reflect multiple drivers of community change,
138 interpreting it requires downstream analyses to disentangle the relative contributions of these
139 three axes. To evaluate how this plays out in real systems we next reanalyzed four previously
140 published datasets spanning diverse microbial environments.

141

142 **Application of Absolute UniFrac to Four Real-World Microbiome Datasets**

143 To illustrate the sensitivity of U^A to both variation in composition and absolute
144 abundance, we re-analyzed four previously published datasets from diverse microbial systems.
145 These datasets included: (i) nuclear reactor cooling water sampled across three reactor cycle
146 phases [5]; (ii) the mouse gut sampled across multiple regions and between two diets [3]; (iii)
147 depth-stratified freshwater communities sampled across two months [9]; and (iv) peanut
148 rhizospheres under two crop rotation schemes (conventional rotation (CR) vs. sod-based rotation
149 (SBR)), plant maturities, and irrigation treatments [10]. Absolute abundance was quantified by
150 flow cytometry for the cooling water and freshwater datasets, droplet digital PCR for the mouse
151 gut, and by qPCR for the rhizosphere dataset. Together these span a wide range of richness—from
152 215 ASVs in the cooling water to 24,000 ASVs in the soil—and microbial load—from as low as
153 4×10^5 cells/ml (cooling water) up to 2×10^{12} 16S rRNA copies/gram (mouse gut). Additional
154 details of the re-analysis workflow, including ASV generation and phylogenetic inference, are
155 provided in the Supporting Methods.

156 We first calculated four β -diversity metrics for all sample pairs in each dataset and
157 compared them to U^A (Fig. 2). The degree of concordance between U^A and other metrics was
158 highly context dependent. In the cooling water dataset, U^A closely tracked all three alternatives,
159 whereas in the remaining systems it diverged substantially. U^A also spanned a similar or wider
160 range of distances than the other metrics. For example, in the soil dataset BC^R and U^R occupied a
161 narrow range relative to the broad separation observed under U^A .

162 U^A generally reported distances that were similar to or greater than U^R , consistent with
163 the simulations shown in Fig. 1B. This reflects the ability of U^A to discern dissimilarity due to
164 differences in microbial load, even when community composition is conserved. In contrast, U^A
165 yielded distances that were similar to or lower than BC^A , again matching the simulated behavior
166 in Fig 1B. In these cases, phylogenetic proximity between abundant, closely-related ASVs leads
167 U^A to register greater similarity than BC^A .

168 Given these differences, we next quantified how well each metric discriminates among
169 categorical sample groups. For each dataset, we ran PERMANOVAs to measure the proportion
170 of variance (R^2) and statistical power (*pseudo-F*, *p*-value) attributable to group structure, using
171 groupings that were determined to be significant in the original publications. To evaluate how

172 strongly absolute abundance contributed to this discrimination, we also calculated GU^A across a
173 range of α values. The resulting R^2 values are displayed in Fig. 3A, with the corresponding
174 *pseudo-F* statistics and *p*-values provided in Fig. S2.

175 As in Fig. 2, the performance of each metric was strongly context dependent (Fig. 3A). In
176 the mouse gut and freshwater datasets, absolute-abundance-aware metrics (BC^A and GU^A)
177 explained the greatest proportion of variance (R^2), and R^2 generally increasing as α increased. In
178 contrast, relative metrics captured more variation in the cooling water dataset (again at higher α),
179 and all metrics explained comparably little variance in the soil dataset. Taken at face value, these
180 trends might suggest that higher α values typically improve group differentiation.

181 However, this comes with a major caveat: at high α values, GU^A becomes strongly
182 correlated with total cell count alone (Fig. 3B). Mantel tests confirmed that absolute-abundance
183 metrics are far more sensitive to differences in microbial load than their relative counterparts.
184 This behavior is intuitive, and to some extent desirable, because these metrics are designed to
185 detect changes in microbial load even when composition remains constant. Yet at $\alpha = 1$, U^A
186 approaches a proxy for sample absolute abundance itself. In ordination space (Fig. S3), this can
187 cause Axis 1 to correlate with absolute abundance and in some cases (freshwater and soil)
188 produces strong horseshoe effects [15], potentially distorting ecological interpretation. Beyond
189 tuning α to modify the influence of abundances, approaches such as NMDS or partial ordination
190 can also be used to modulate the sensitivity of ordinations to microbial load [16].

191 We recommend calibrating α based on research goals, modulating this effect by using
192 GU^A across a range of α rather than relying on U^A ($\alpha = 1$). Researchers should consider how
193 much emphasis they want their dissimilarity metric to place on microbial load (Box 1). When
194 biomass differences are central to the hypothesis being tested (for example, detecting
195 cyanobacterial blooms), high α are recommended. In contrast, if microbial load is irrelevant or
196 independent of the hypothesis in question, low α (or U^R) may be preferred; for example in the
197 soil dataset, fine-scale differences in composition may be obscured by random variation in
198 microbial load.

199 In many systems, microbial biomass is one piece of the story, likely correlated to other
200 variables being tested. If the importance of microbial load in the system is unknown, one

201 potential approach is to calculate correlations as demonstrated in Fig. 3B and select an α prior to
202 any ordinations or statistical testing. Again, correlation to cell count is valuable and is intrinsic to
203 absolute abundance-aware measures, especially when microbial load is relevant to the
204 hypotheses being tested. Correlations to cell count in BC^4 , an accepted approach in the literature,
205 ranged from ~0.5 up to ~0.8. As a general recommendation from these analyses, we recommend
206 α values in an intermediate range from 0.1 up to 0.6, wherein GU^A has similar correlation to cell
207 count as BC^4 .

208 **Computational and Methodological Considerations**

209 Applying GU^A in practice raises several considerations related to sequencing depth,
210 richness, and computational cost. Both Bray-Curtis and UniFrac can be sensitive to sequencing
211 depth because richness varies with read count [17–19]. To address this, we provide a workflow
212 and accompanying code describing how we incorporated rarefaction into our own analyses (Box
213 2; available code). This approach minimizes sequencing-depth biases while preserving
214 abundance scaling for downstream β -diversity analysis.

215 To explore the sensitivity of GU^A to rarefaction, we calculated GU^A using rarefaction at
216 multiple sequencing depths, and used Mantel tests to assess the correlation between the rarefied
217 GU^A distance matrices the non-rarefied control (Fig. S4; supplemental methods). GU^A was
218 largely insensitive to rarefaction at high α values, even at depths as low as 250 reads per sample,
219 but sensitivity increased as α decreased (Fig. S4). When rarefying to the minimum sequencing
220 depth, as recommended, the effect of rarefaction was negligible (all Mantel's R > 0.95, Fig. S4).

221 GU^A is slower to compute than both BC^4 and U^R because it must traverse the phylogenetic
222 tree to calculate branch lengths for each iteration. Computational time of GU^A increases
223 quadratically with ASV number and is 10-20 times slower, though up to 50 times slower, than
224 BC^4 (Fig. 4A-B). The number of samples or α values, however, have relatively little effect on
225 runtime (Fig. S5). For a dataset of 24,000 ASVs, computing on a single CPU is still reasonable
226 (1.4 minutes), but repeated rarefaction increases runtime substantially because branch lengths are
227 redundantly calculated with each iteration. Allowing branch-length objects to be cached or
228 incorporated directly into the GUnifrac workflow would considerably improve computational
229 efficiency.

We also evaluated the sensitivity of GU^A to measurement error in absolute abundance due to uncertainty arising from the quantification of cell number or 16S copy number. To assess the sensitivity of GU^A and BC^A to measurement error, we added random error to the 16S copy number measurements from the mouse gut dataset, limiting our analyses to the stool samples where copy numbers varied by an order of magnitude. Across 50 iterations, each copy number could randomly vary by a given percentage of error in either direction. We re-calculated β -diversity (BC^A and GU^A at $\alpha = 1$ and $\alpha = 0.2$) and compared these measurements to the original dataset.

Introducing random variation into measured 16S copy number altered GU^A values only modestly, and the effect was proportional to the magnitude of the added noise (Fig. 4C–D). At $\alpha = 1$, each 1% of quantification error introduced an average difference of 0.0022 in GU^A ; at $\alpha = 0.2$, GU^A was even less sensitive. Thus, moderate α values provide a balance between interpretability and robustness to noise in absolute quantification. The max deviation from true that added error could inflict on a given metric was also proportional (and always less) than the magnitude of the error itself (Fig. 4D). A more rigorous approach to assessing error propagation within these metrics, including mathematical proofs of the relationships estimated above, is outside the scope of this paper but would be helpful.

GU^A was also insensitive to normalization approaches that adjust ASV abundances based on the predicted 16S rRNA gene copy number (Fig. S6; supplemental methods). We used PICRUSt2 (v2.6) to normalize ASV abundances within each dataset based on predicted 16S copy number per genome, and then applied our standard rarefaction pipeline prior to GU^A calculation (Box 2) [20, 21]. Correlations between GU^A distance matrices calculated from 16S copy number-normalized datasets and those from the original, non-normalized datasets were consistently near unity across all datasets (Mantel's R > 0.98, Fig. S6A), demonstrating that 16S copy number-normalization had a negligible effect on GU^A . Sensitivity of GU^A to 16S copy number-normalization generally decreased with increasing values of α in the cooling reactor, freshwater, and soil datasets, but not in the mouse gut dataset (Fig. S6A). In the mouse gut dataset, several highly abundant ASVs belonging to the genus *Faecalibaculum* had predicted 16S copy numbers of seven copies per genome, explaining the relatively greater (though still weak) sensitivity of this dataset to copy number-normalization (Fig. S6B). Finally, we note that 16S copy number-

260 normalization does not account for variation in genome copies per cell (ploidy), which can vary
261 across several orders of magnitude between species and growth phase [22–24].

262 Ecological Interpretation and conceptual significance

263 Absolute UniFrac reframes the interpretation of β -diversity by making biomass an explicit
264 ecological axis rather than an unmeasured or normalized-away quantity. Conventional UniFrac
265 captures composition and shared evolutionary history but implicitly invites interpretation as if it
266 also encodes differences on microbial load. By incorporating absolute abundance directly,
267 Absolute UniFrac helps to resolve this mismatch and restores alignment between ecological
268 hypotheses and the quantities represented in the metric. In this view, β -diversity becomes a three-
269 axis ecological measure, incorporating composition, phylogeny and biomass, rather than a two-
270 axis approximation. That said, the additional dimension of microbial load also increases the
271 complexity of applying and interpreting this metric.

272 There are many cases where the incorporation of absolute abundance allows microbial
273 ecologists to assess more realistic, ecologically-relevant differences in microbial communities,
274 especially when microbial load is mechanistically central. Outside of the datasets re-analyzed
275 here [3, 5, 9, 10]; the temporal development of the infant gut microbiome involves both a rise in
276 absolute abundance and compositional changes [6]; bacteriophage predation in wastewater
277 bioreactors can be understood only when microbial load is considered [25]; and antibiotic-driven
278 declines in specific swine gut taxa were missed using relative abundance approaches [26]. As β -
279 diversity metrics (and UniFrac specifically) remain central to microbial ecology, these findings
280 highlight how interpretation changes once biomass is incorporated. Broader adoption of absolute
281 abundance profiling will also depend on data availability. Few studies currently make absolute
282 quantification data publicly accessible, underscoring the need to deposit absolute measurements
283 alongside sequencing reads for reproducibility, ideally as metadata within SRA submissions.

284 While demonstrated here with 16S rRNA data, the approach should extend to other marker
285 genes or (meta)genomic features, provided absolute abundance estimates are available. In this
286 sense, GU^A offers a more ecologically grounded view of lineage turnover by jointly reflecting
287 variation in biomass and phylogenetic structure.

288 No single metric (or α in GU^A), however, is universally “best”. Each β -diversity metric
289 emphasizes a different dimension of community change. Researchers should therefore select
290 metrics based on the ecological quantity that is hypothesized to matter most (Box 1). Here, we
291 demonstrate not that GU^A outperforms other measures, but that it faithfully incorporates the three
292 axes of variation it was designed to incorporate: composition, phylogenetic similarity, and
293 absolute abundance (Fig. 1 and Fig. 2). As with any β -diversity analysis, interpretation requires
294 matching the metric to the ecological question at hand, and exploring sensitivity across different
295 metrics where appropriate [27]. By providing demonstrations and code for the application and
296 interpretation of U^A/GU^A , we hope to encourage the use of these metrics as a tool of microbial
297 ecology.

298 **Conclusion**

299 By explicitly incorporating absolute abundance, Absolute UniFrac shifts phylogenetic β -
300 diversity from a two-axis approximation to a three-axis ecological measure. This reframing
301 connects the metric to the underlying biological questions that motivate many microbiome
302 studies. As methods for quantifying microbial load continue to expand, the ability to interpret β -
303 diversity in a biomass-aware framework will become increasingly important for distinguishing
304 true ecological turnover from proportional change alone. In this way, Absolute UniFrac is not
305 simply an alternative distance metric but a tool for aligning statistical representation with
306 ecological mechanism.

307 **Author Contribution Statement:** Both authors contributed equally to the manuscript.

308 **Preprint servers:** This article was submitted to *bioRxiv* (doi: 10.1101/2025.07.18.665540) under
309 a CC-BY-NC-ND 4.0 International license.

310 **Data Availability:** All data and code used to produce the manuscript are available at
311 https://github.com/MarschmiLab/Pendleton_2025_Absolute_Unifrac_Paper, in addition to a
312 reproducible renv environment. All packages used for analysis are listed in Table S1.

313 **Funding Statement:** This work was supported by a NOAA Margaret A. Davidson Fellowship to
314 AP (NA24NOSX420C0016) and by a grant from the Affinito-Stewart & President’s Council of
315 Cornell Women, as well as Cornell University start-up funds to MLS.

316 **References**

- 317 1. Gloor GB, Macklaim JM, Pawlowsky-Glahn V, Egoscue JJ. Microbiome Datasets Are
318 Compositional: And This Is Not Optional. *Front Microbiol* 2017;8:2224.
319 <https://doi.org/10.3389/fmicb.2017.02224>
- 320 2. Vandepitte D, Falony G, Vieira-Silva S, Tito RY, Joossens M, Raes J. Stool consistency is
321 strongly associated with gut microbiota richness and composition, enterotypes and bacterial
322 growth rates. *Gut* 2016;65:57–62. <https://doi.org/10.1136/gutjnl-2015-309618>
- 323 3. Barlow JT, Bogatyrev SR, Ismagilov RF. A quantitative sequencing framework for absolute
324 abundance measurements of mucosal and lumenal microbial communities. *Nat Commun*
325 2020;11:2590. <https://doi.org/10.1038/s41467-020-16224-6>
- 326 4. Wang X, How S, Deng F, Zhao J. Current Applications of Absolute Bacterial Quantification
327 in Microbiome Studies and Decision-Making Regarding Different Biological Questions.
328 *Microorganisms* 2021;9:1797. <https://doi.org/10.3390/microorganisms9091797>
- 329 5. Props R, Kerckhof FM, Rubbens P, De Vrieze J, Hernandez-Sanabria E, Waegeman W, et
330 al. Absolute quantification of microbial taxon abundances. *ISME J* 2017;11:584–587.
331 <https://doi.org/10.1038/ismej.2016.117>
- 332 6. Rao C, Coyte KZ, Bainter W, Geha RS, Martin CR, Rakoff-Nahoum S. Multi-kingdom
333 ecological drivers of microbiota assembly in preterm infants. *Nature* 2021;591:633–638.
334 <https://doi.org/10.1038/s41586-021-03241-8>
- 335 7. Bray JR, Curtis JT. An Ordination of the Upland Forest Communities of Southern
336 Wisconsin. *Ecological Monographs* 1957;27:326–349. <https://doi.org/10.2307/1942268>
- 337 8. Lozupone CA, Hamady M, Kelley ST, Knight R. Quantitative and Qualitative β Diversity
338 Measures Lead to Different Insights into Factors That Structure Microbial Communities.
339 *Applied and Environmental Microbiology* 2007;73:1576–1585.
340 <https://doi.org/10.1128/AEM.01996-06>
- 341 9. Pendleton A, Wells M, Schmidt ML. Upwelling periodically disturbs the ecological
342 assembly of microbial communities in the Laurentian Great Lakes. 2025. bioRxiv, 2025.,
343 2025.01.17.633667
- 344 10. Zhang K, Maltais-Landry G, James M, Mendez V, Wright D, George S, et al. Absolute
345 microbiome profiling highlights the links among microbial stability, soil health, and crop

- 346 productivity under long-term sod-based rotation. *Biol Fertil Soils* 2022;58:883–901.
347 <https://doi.org/10.1007/s00374-022-01675-4>
- 348 11. Chen J, Bittinger K, Charlson ES, Hoffmann C, Lewis J, Wu GD, et al. Associating
349 microbiome composition with environmental covariates using generalized UniFrac
350 distances. *Bioinformatics* 2012;28:2106–2113.
351 <https://doi.org/10.1093/bioinformatics/bts342>
- 352 12. Lozupone C, Knight R. UniFrac: a New Phylogenetic Method for Comparing Microbial
353 Communities. *Applied and Environmental Microbiology* 2005;71:8228–8235.
354 <https://doi.org/10.1128/AEM.71.12.8228-8235.2005>
- 355 13. McMurdie PJ, Holmes S. phyloseq: An R package for reproducible interactive analysis and
356 graphics of microbiome census data. *PLoS ONE* 2013;8:e61217.
- 357 14. Bolyen E, Rideout JM, Dillon MR, Bokulich NA, Abnet CC, Al-Ghalith GA, et al.
358 Reproducible, interactive, scalable and extensible microbiome data science using QIIME 2.
359 *Nat Biotechnol* 2019;37:852–857. <https://doi.org/10.1038/s41587-019-0209-9>
- 360 15. Morton JT, Toran L, Edlund A, Metcalf JL, Lauber, C, Knight R. Uncovering the Horseshoe
361 Effect in Microbial Analyses. *mSystems* 2017;2:10.1128/msystems.00166-16.
362 <https://doi.org/10.1128/msystems.00166-16>
- 363 16. Paliy O, Shankar V. Application of multivariate statistical techniques in microbial ecology.
364 *Molecular Ecology* 2016;25:1032–1057. <https://doi.org/10.1111/mec.13536>
- 365 17. Schloss PD. Evaluating different approaches that test whether microbial communities have
366 the same structure. *The ISME Journal* 2008;2:265–275.
367 <https://doi.org/10.1038/ismej.2008.5>
- 368 18. Fukuyama J, McMurdie PJ, Dethlefsen L, Relman DA, Holmes S. Comparisons of distance
369 methods for combining covariates and abundances in microbiome studies. *Biocomputing*
370 2012. WORLD SCIENTIFIC, 2011, 213–224.
- 371 19. McMurdie PJ, Holmes S. Waste Not, Want Not: Why Rarefying Microbiome Data Is
372 Inadmissible. *PLOS Computational Biology* 2014;10:e1003531.
373 <https://doi.org/10.1371/journal.pcbi.1003531>
- 374 20. Wright RJ, Langille MGI. PICRUSt2-SC: an update to the reference database used for
375 functional prediction within PICRUSt2. *Bioinformatics* 2025;41:btaf269.
376 <https://doi.org/10.1093/bioinformatics/btaf269>

- 377 21. Douglas GM, Maffei VJ, Zaneveld JR, Yurgel SN, Brown JR, Taylor CM, et al. PICRUSt2
378 for prediction of metagenome functions. *Nat Biotechnol* 2020;38:685–688.
379 <https://doi.org/10.1038/s41587-020-0548-6>
- 380 22. Griese M, Lange C, Soppa J. Ploidy in cyanobacteria. *FEMS Microbiol Lett* 2011;323:124–
381 131. <https://doi.org/10.1111/j.1574-6968.2011.02368.x>
- 382 23. Mendell JE, Clements KD, Choat JH, Angert ER. Extreme polyploidy in a large bacterium.
383 *Proceedings of the National Academy of Sciences* 2008;105:6730–6734.
384 <https://doi.org/10.1073/pnas.0707522105>
- 385 24. Pecoraro V, Zerulla K, Lange C, Soppa J. Quantification of Ploidy in Proteobacteria
386 Revealed the Existence of Monoploid, (Mero-)Oligoploid and Polyploid Species. *PLOS
387 ONE* 2011;6:e16392. <https://doi.org/10.1371/journal.pone.0016392>
- 388 25. Shapiro OH, Kushmaro A, Brenner A. Bacteriophage predation regulates microbial
389 abundance and diversity in a full-scale bioreactor treating industrial wastewater. *The ISME
390 Journal* 2010;4:327–336. <https://doi.org/10.1038/ismej.2009.118>
- 391 26. Wagner S, Weber M, Paul LS, Grümpel-Schlüter A, Klüss, Neuhaus K, et al. Absolute
392 abundance calculation enhances the significance of microbiome data in antibiotic treatment
393 studies. *Front Microbiol* 2025;16. <https://doi.org/10.3389/fmicb.2025.1481197>
- 394 27. Kers JG, Saccenti E. The Power of Microbiome Studies: Some Considerations on Which
395 Alpha and Beta Metrics to Use and How to Report Results. *Front Microbiol* 2022;12.
396 <https://doi.org/10.3389/fmicb.2021.796025>
- 397
- 398

399 **Figure Legends**

400 **Figure 1. Simulated communities reveal how absolute abundance affects phylogenetic and**
401 **non-phylogenetic β -diversity measures.** (A) We constructed a simple four-ASV community with
402 a known phylogeny and generated all permutations of each ASV having an absolute abundance
403 of 1, 10, or 100, resulting in 81 unique communities and 3,240 pairwise comparisons. (B)
404 Distributions of pairwise differences between weighted UniFrac using absolute abundance (U^A)
405 and three other metrics: Bray-Curtis using relative abundance (BC^R), weighted UniFrac using
406 relative abundance (U^R), and Bray-Curtis using absolute abundance (BC^A). (C) Illustrative
407 sample pairs demonstrate how absolute abundances and phylogenetic structure interact to
408 increase or decrease dissimilarity across metrics. Stars indicate where each scenario falls within
409 the distributions shown in panel B. Actual values for each metric are displayed beneath each
410 scenario.

411 **Figure 2. Absolute UniFrac (U^A) compared with other β -diversity metrics across four real**
412 **microbial datasets.** Each panel shows pairwise sample distances for U^A (x-axis) against another
413 metric (y-axis): Bray-Curtis using relative abundance (BC^R , first column), weighted UniFrac
414 using relative abundances (U^R , second column), and Bray-Curtis using absolute abundances
415 (BC^A , third column). Contours indicate the relative density of pairwise comparisons (n shown for
416 each dataset, left), with darker shading corresponding to more observations. The dashed line
417 marks the 1:1 relationship. Points above the line indicate cases where U^A is smaller than the
418 comparator metric, while points below the line indicate cases where U^A is larger.

419 **Figure 3. Discriminatory performance of U^A and related metrics across four microbial**
420 **systems.** (A) PERMANOVAs were used to quantify the percent variance (R^2) explained by
421 predefined categorical groups (shown in italics beneath each dataset name), with 1,000
422 permutations. PERMANOVA results were evaluated across five metrics and, where applicable,
423 across eleven α values (0-1 in 0.1 increments). For consistency with the original studies, only
424 samples from Reactor cycle 1 were used for the cooling-water dataset, only stool samples for the
425 mouse gut dataset, and only mature rhizosphere samples for the soil dataset (no samples were
426 excluded from the freshwater dataset). (B) Mantel correlation (R) between each distance metric
427 and the pairwise differences in absolute abundance (cell counts or 16S copy number), illustrating
428 the degree to which each metric is driven by biomass differences.

429 **Figure 4. GU^A requires more computational time but remains resilient to quantification error.**
430 (A) Runtime for GU^A (GUniFrac package), U^R (FastUniFrac in the phyloseq package) and BC^A
431 (vegan package) was benchmarked across 50 iterations on a sub-sampled soil dataset (mature
432 samples only) [10], using increasing ASV richness (50, 100, 200, 500, 1,000, 2,000, 5,000,
433 10,000), with 10 samples and one α value per run (unweighted UniFrac is also calculated by
434 default). Error bars represent standard deviation. (B) Quadratic relationship between GU^A
435 computation time and ASV richness. Large center point represents median across 50 iterations,
436 error bars (standard deviation) are too small to be seen. All benchmarks were run on an AMD
437 EPYC 64-core processor with 1014 GB system memory (R v4.3.3, vegan v2.7-1, phyloseq
438 v1.52.0, GUnifrac v1.8.1). (C-D) Sensitivity of GU^A ($\alpha = 1$ and 0.2) and BC^A to measurement
439 error was evaluated by adding random variation ($\pm 1\%$ to $\pm 50\%$; Supporting Methods) to 16S
440 copy number estimates in stool samples from the mouse gut dataset [3]. For each error level, 50
441 replicate matrices were generated and compared to the original values. Panels reflect the (C)
442 mean difference and (D) max difference between the error-added metrics compared to the
443 originals. Error bars represent the standard deviation of the average mean and max difference
444 across 50 iterations.

445

446 **Box 1: β -diversity metrics should reflect the hypothesis being tested**

447 Absolute UniFrac is most informative when variation in microbial load is expected to carry
448 ecological meaning rather than being a nuisance variable. The choice of α determines how
449 strongly abundance differences influence the metric, and should therefore be selected based on
450 the hypothesis, not by convention. In settings where biomass is central to the mechanism under
451 study, higher α values appropriately foreground that signal, whereas in cases where load
452 variation is incidental or confounding, lower α values maintain interpretability. Framing α as a
453 hypothesis-driven choice repositions β -diversity from a default normalization step to an explicit
454 ecological decision.

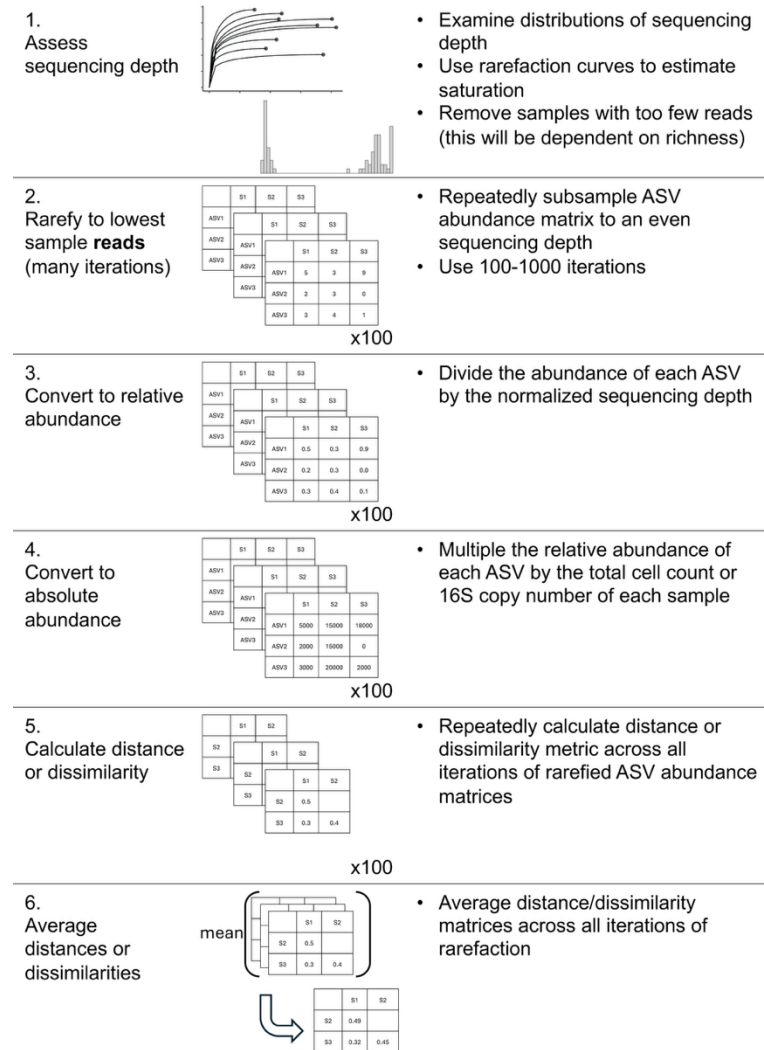
455

456 **Box 1 continued:**

			Metric to Use		Hypothetical Example	
Treat closely related lineages as similar?	Yes	How relevant is microbial load?	Central to hypothesis		$GU^A, \alpha > 0.5$	Cyanobacterial bloom, pathogen proliferation
			Relevant, but associated with other variables of interest		$GU^A, 0.1 < \alpha < 0.5$	Compositional shifts in response to nutrient addition
			Irrelevant	Emphasize rare or dominant taxa?	$GU^R, \alpha > 0.5$	Diet-associated microbiome shifts across hosts
				Rare	$GU^R, \alpha < 0.5$	Tributary inputs of rare taxa
			Unknown		GU^A at multiple α	Random variation in microbial load obscured compositional shifts in soil communities
	No	Microbial load relevant?	Yes		BC^A	Strain turnover and proliferation in the infant gut
	No		BC^R	Temporal succession in chemostat		

458 **Box 2: Rarefaction workflow for incorporating absolute abundance**

459 While we refrain from an in-depth analysis of rarefaction approaches, here we present our
 460 workflow for incorporating
 461 rarefaction alongside absolute
 462 abundance. First, samples were
 463 assessed for anomalously low read
 464 counts and discarded (sequencing
 465 blanks and controls were also
 466 removed). For rarefaction, each
 467 sample in the ASV table was
 468 subsampled to equal *sequencing*
 469 depth (# of reads) across 100
 470 iterations, creating 100 rarefied ASV
 471 tables. These tables were then
 472 converted to relative abundance by
 473 dividing each ASV's count by the
 474 equal sequencing depth (rounding
 475 was not performed). Then, each
 476 ASV's absolute abundance within a
 477 given sample was calculated by
 478 multiplying its relative abundance
 479 by that sample's total cell count or
 480 16S copy number. Methods to predict genomic 16S copy number for a given ASV were not used
 481 unless explicitly stated (Fig. S6) [20, 21]. Each distance/dissimilarity metric was then calculated
 482 across all 100 absolute-normalized ASV tables. The final distance/dissimilarity matrix was
 483 calculated by averaging all 100 iterations of each distance/dissimilarity calculation. Of note for
 484 future users: pruning the phylogenetic tree after rarefaction for each iteration is not necessary –
 485 ASVs removed from the dataset do not contribute nor change the calculated of UniFrac
 486 distances.





1 **Interpreting UniFrac with Absolute Abundance: A Conceptual and Practical Guide**

2 Augustus Pendleton^{1*} & Marian L. Schmidt^{1*}

3 ¹Department of Microbiology, Cornell University, 123 Wing Dr, Ithaca, NY 14850, USA

4 **Corresponding Authors:** Augustus Pendleton: arp277@cornell.edu; Marian L. Schmidt:

5 marschmi@cornell.edu; MarianL.Schmidt@gmail.com

6 **Physical Mailing Address:** Augustus Pendleton or Marian L. Schmidt, Department of

7 Microbiology, Cornell University, 123 Wing Drive, Ithaca, NY, 14853, United States

8 **Running Title:** A Guide to Absolute-Abundance UniFrac

9 **Abstract**

10 β -diversity is central to microbial ecology, yet commonly used metrics overlook changes in
11 microbial load (or “absolute abundance”), limiting their ability to detect ecologically meaningful
12 shifts. Popular for incorporating phylogenetic relationships, UniFrac distances currently default
13 to relative abundance and therefore omit important variation in microbial abundances. As
14 quantifying absolute abundance becomes more accessible, integrating this information into β -
15 diversity analyses is essential. Here, we introduce *Absolute UniFrac* (U^A), a variant of Weighted
16 UniFrac that incorporates absolute abundances. Using simulations and a reanalysis of four 16S
17 rRNA metabarcoding datasets (from a nuclear reactor cooling tank, the mouse gut, a freshwater
18 lake, and the peanut rhizosphere), we demonstrate that Absolute UniFrac captures microbial load,
19 composition, and phylogenetic relationships. While this can improve statistical power to detect
20 ecological shifts, we also find Absolute UniFrac can be strongly correlated to differences in cell
21 abundances alone. To balance these effects, we also incorporate absolute abundance into the
22 generalized extension (GU^A) that has a tunable, continuous ecological parameter (α) that
23 modulates the relative contribution of rare versus abundant lineages to β -diversity calculations.
24 Finally, we benchmark GU^A and show that although computationally slower than conventional
25 alternatives, GU^A is comparably sensitive to noise in load estimates compared to conventional
26 alternatives like Bray-Curtis dissimilarities, particularly at lower α . By coupling phylogeny,
27 composition, and microbial load, Absolute UniFrac integrates three dimensions of ecological
28 change, better equipping microbial ecologists to quantitatively compare microbial communities.

29

30 **Keywords:** Microbial Ecology - Beta Diversity - Absolute Abundance - Bioinformatics -
31 UniFrac

32 **Main Text**

33 Microbial ecologists routinely compare communities using β -diversity metrics derived
34 from relative abundances. Yet this approach overlooks a critical ecological dimension: microbial
35 load. High-throughput sequencing produces compositional data, in which each taxon's
36 abundance is constrained by all others [1]. However, quantitative profiling studies show that cell
37 abundance, not only composition, can drive major community differences [2]. In low-biomass
38 samples, relying on relative abundance can allow contaminants to appear biologically
39 meaningful despite absolute counts too low for concern [3].

40 Sequencing-based microbiome studies therefore rely on relative abundance even when
41 the hypotheses of interest implicitly concern absolute changes in biomass. This creates a
42 mismatch between ecological framing (growth, bloom magnitude, pathogen proliferation,
43 disturbance recovery, or colonization pressure) and the information the β -diversity metric
44 encodes [4]. As a result, β -diversity is often treated as if it includes biomass, even when absolute
45 abundance is either not measured at all or is measured but excluded from the calculation (as in
46 conventional UniFrac). Many studies therefore test biomass-linked hypotheses using a metric
47 that normalizes biomass away [4]. A conceptual correction is needed in which β -diversity is
48 understood as variation along three axes: composition, phylogeny and absolute abundance.

49 Absolute microbial load measurements are now increasingly obtainable through flow
50 cytometry, qPCR, and genomic spike-ins, allowing biomass to be quantified alongside taxonomic
51 composition [4, 5]. These approaches improve detection of functionally relevant taxa and
52 mitigate the compositional constraints imposed by sequencing [1, 2]. Most studies that
53 incorporate absolute abundance counts currently rely on Bray-Curtis dissimilarity, which can
54 capture load but does not consider phylogenetic similarity [5–7]. Unifrac distances provide the
55 opposite strength, incorporating phylogeny but discarding absolute abundance, as they are
56 restricted to relative abundance data by construction [8]. This leaves no phylogenetically
57 informed β -diversity metric that operates on absolute counts, despite the fact that biomass is
58 central to many ecological hypotheses.

59 To evaluate the implications of incorporating absolute abundance into phylogenetic β -
60 diversity, we use both simulations and reanalysis of four 16S rRNA amplicon datasets. The

61 simulations use a simple four-taxon community with controlled abundance shifts to directly
62 compare both Bray-Curtis and UniFrac in their relative and absolute forms, illustrating how each
63 metric responds when abundance, composition, or evolutionary relatedness differ. We then
64 reanalyze four real-world datasets spanning nuclear reactor cooling water [5], the mouse gut [3],
65 a freshwater lake [9], and rhizosphere soil [10]. These differ widely in richness, biomass range,
66 and ecological context, allowing us to test when absolute abundance changes align with or
67 diverge from phylogenetic turnover. Together, these simulations and reanalyses provide the
68 empirical foundation for interpreting Absolute UniFrac relative to existing β -diversity measures
69 across the three axes of ecological difference: abundance, composition, and phylogeny.

70 We also extend Absolute UniFrac as was proposed by [11] to Generalized Absolute
71 UniFrac that incorporates a tunable ecological dimension, α , and evaluate its impact across
72 simulated and real-world datasets. As α increases, β -diversity is increasingly correlated with
73 differences in absolute abundance, allowing researchers to fine tune the relative weight their
74 analyses place on microbial load versus composition.

75 Defining Absolute UniFrac

76 The UniFrac distance was first introduced by Lozupone & Knight (2005) and has since
77 become enormously popular as a measure of β -diversity within the field of microbial ecology
78 [12]. A benefit of the UniFrac distance is that it considers phylogenetic information when
79 estimating the distance between two communities. After first generating a phylogenetic tree
80 representing species (or amplicon sequence variants, “ASVs”) from all samples, the UniFrac
81 distance computes the fraction of branch-lengths which is *shared* between communities, relative
82 to the total branch length represented in the tree. UniFrac can be both unweighted, in which only
83 the incidence of species is considered, or weighted, wherein a branch’s contribution is weighted
84 by the proportional abundance of taxa on that branch [8]. The Weighted UniFrac is derived:

$$85 U^R = \frac{\sum_{i=1}^n b_i |p_i^a - p_i^b|}{\sum_{i=1}^n b_i (p_i^a + p_i^b)}$$

86 where the contribution of each branch length, b_i , is weighted by the difference in the relative
87 abundance of all species (p_i) descended from that branch in sample a or sample b . Here, we
88 denote this distance as U^R , for “Relative UniFrac”. Popular packages which calculate weighted

89 UniFrac—including the diversity-lib QIIME plug-in and the R packages phyloseq and
90 GUniFrac—run this normalization by default [11, 13, 14].

91 Importantly, U^R is most sensitive to changes in abundant lineages, which can sometimes
92 obscure compositional differences driven by rare to moderately-abundant taxa [11]. To address
93 this weakness, Chen et al. (2012) introduced the generalized UniFrac distance (GU^R), in which
94 the impact of abundant lineages can be mitigated by decreasing the parameter α :

$$95 \quad GU^R = \frac{\sum_{i=1}^n b_i (p_i^a + p_i^b)^\alpha \left| \frac{p_i^a - p_i^b}{p_i^a + p_i^b} \right|}{\sum_{i=1}^n b_i (p_i^a + p_i^b)^\alpha}$$

96 where α ranges from 0 (close to Unweighted UniFrac) up to 1 (identical to U^R , above). However,
97 if one wishes to use absolute abundances, both U^R and GU^R can be derived without normalizing
98 to proportions:

$$99 \quad U^A = \frac{\sum_{i=1}^n b_i |c_i^a - c_i^b|}{\sum_{i=1}^n b_i (c_i^a + c_i^b)} \quad GU^A = \frac{\sum_{i=1}^n b_i (c_i^a + c_i^b)^\alpha \left| \frac{c_i^a - c_i^b}{c_i^a + c_i^b} \right|}{\sum_{i=1}^n b_i (c_i^a + c_i^b)^\alpha}$$

100 Where c_i^a and c_i^b denote for the absolute counts of species descending from branch b_i in
101 communities a and b , respectively. We refer to these distances as *Absolute UniFrac* (U^A) and
102 *Generalized Absolute UniFrac* (GU^A). Although substituting absolute for relative abundances is
103 mathematically straightforward, to our knowledge there is no prior work that examines UniFrac
104 in the context of absolute abundance, either conceptually or in application. Incorporating
105 absolute abundances introduces a third axis of ecological variation: beyond differences in
106 composition and phylogenetic similarity, U^A also captures divergence in microbial load. This
107 makes interpretation of U^A nontrivial, particularly in complex microbiomes.

108 **Demonstrating β -diversity metrics' behavior with a simple simulation**

109 To clarify how U^A behaves relative to existing β -diversity metrics, we first constructed a
110 simple four-taxon simulated community arranged in a small phylogeny (Fig. 1A). By varying the
111 absolute abundance of each ASV (1, 10, or 100), we generated 81 samples and 3,240 pairwise
112 comparisons. For each pair, we computed four dissimilarity metrics: Bray-Curtis with relative

113 abundance (BC^R), Bray-Curtis with absolute abundance (BC^A), Weighted UniFrac with relative
114 abundance (U^R), and Weighted UniFrac with absolute abundance (U^A). These comparisons help
115 to illustrate how each axis of ecological difference—abundance, composition, and phylogeny—is
116 expressed by the different metrics.

117 U^A does not consistently yield higher or lower distances compared to other metrics, but
118 instead varies depending on how abundance and phylogeny intersect (Fig. 1B). In the improbable
119 scenario that all branch lengths are equal, U^A is always less than or equal to BC^A (Fig. S1).
120 These comparisons emphasize that once branch lengths differ, incorporating phylogeny and
121 absolute abundance alters the structure of the distance space. The direction and magnitude of that
122 change depend on which branches carry the abundance shifts. U^A is also usually smaller than
123 BC^A and is more strongly correlated with BC^A (Pearson's $r = 0.82$, $p < 0.0001$) than with BC^R (r
124 = 0.41) and U^R ($r = 0.55$).

125 To better understand how these metrics diverge, we examined individual sample pairs
126 (Fig. 1C). Scenario 1 (gold star) illustrates the classic advantage of UniFrac: ASV_1 and ASV_2
127 are phylogenetically close, so U^R and U^A discern greater similarity between samples than BC^R
128 and BC^A , which ignore phylogenetic structure. Scenario 2 (red star) highlights a limitation of
129 relative metrics: two samples with identical relative composition but a 100-fold difference in
130 biomass appear identical to BC^R and U^R , but not to their absolute counterparts. In Scenario 3
131 (green star), incorporating absolute abundance decreases dissimilarity. BC^A and U^A are lower
132 than their relative counterparts because half the community is identical in absolute abundance,
133 even though their proportions differ. In contrast, Scenario 4 (blue star) shows that U^A can exceed
134 BC^A when abundance differences occur on long branches, amplifying phylogenetic dissimilarity.

135 These scenarios demonstrate that U^A integrates variation along three ecologically
136 relevant axes: composition, phylogenetic similarity, and microbial load, rather than isolating any
137 single dimension. Because a given U^A value can reflect multiple drivers of community change,
138 interpreting it requires downstream analyses to disentangle the relative contributions of these
139 three axes. To evaluate how this plays out in real systems we next reanalyzed four previously
140 published datasets spanning diverse microbial environments.

141

142 **Application of Absolute UniFrac to Four Real-World Microbiome Datasets**

143 To illustrate the sensitivity of U^A to both variation in composition and absolute
144 abundance, we re-analyzed four previously published datasets from diverse microbial systems.
145 These datasets included: (i) nuclear reactor cooling water sampled across three reactor cycle
146 phases [5]; (ii) the mouse gut sampled across multiple regions and between two diets [3]; (iii)
147 depth-stratified freshwater communities sampled across two months [9]; and (iv) peanut
148 rhizospheres under two crop rotation schemes (conventional rotation (CR) vs. sod-based rotation
149 (SBR)), plant maturities, and irrigation treatments [10]. Absolute abundance was quantified by
150 flow cytometry for the cooling water and freshwater datasets, droplet digital PCR for the mouse
151 gut, and by qPCR for the rhizosphere dataset. Together these span a wide range of richness—from
152 215 ASVs in the cooling water to 24,000 ASVs in the soil—and microbial load—from as low as
153 4×10^5 cells/ml (cooling water) up to 2×10^{12} 16S rRNA copies/gram (mouse gut). Additional
154 details of the re-analysis workflow, including ASV generation and phylogenetic inference, are
155 provided in the Supporting Methods.

156 We first calculated four β -diversity metrics for all sample pairs in each dataset and
157 compared them to U^A (Fig. 2). The degree of concordance between U^A and other metrics was
158 highly context dependent. In the cooling water dataset, U^A closely tracked all three alternatives,
159 whereas in the remaining systems it diverged substantially. U^A also spanned a similar or wider
160 range of distances than the other metrics. For example, in the soil dataset BC^R and U^R occupied a
161 narrow range relative to the broad separation observed under U^A .

162 U^A generally reported distances that were similar to or greater than U^R , consistent with
163 the simulations shown in Fig. 1B. This reflects the ability of U^A to discern dissimilarity due to
164 differences in microbial load, even when community composition is conserved. In contrast, U^A
165 yielded distances that were similar to or lower than BC^A , again matching the simulated behavior
166 in Fig 1B. In these cases, phylogenetic proximity between abundant, closely-related ASVs leads
167 U^A to register greater similarity than BC^A .

168 Given these differences, we next quantified how well each metric discriminates among
169 categorical sample groups. For each dataset, we ran PERMANOVAs to measure the proportion
170 of variance (R^2) and statistical power (*pseudo-F*, *p*-value) attributable to group structure, using
171 groupings that were determined to be significant in the original publications. To evaluate how

172 strongly absolute abundance contributed to this discrimination, we also calculated GU^A across a
173 range of α values. The resulting R^2 values are displayed in Fig. 3A, with the corresponding
174 *pseudo-F* statistics and *p*-values provided in Fig. S2.

175 As in Fig. 2, the performance of each metric was strongly context dependent (Fig. 3A). In
176 the mouse gut and freshwater datasets, absolute-abundance-aware metrics (BC^A and GU^A)
177 explained the greatest proportion of variance (R^2), and R^2 generally increasing as α increased. In
178 contrast, relative metrics captured more variation in the cooling water dataset (again at higher α),
179 and all metrics explained comparably little variance in the soil dataset. Taken at face value, these
180 trends might suggest that higher α values typically improve group differentiation.

181 However, this comes with a major caveat: at high α values, GU^A becomes strongly
182 correlated with total cell count alone (Fig. 3B). Mantel tests confirmed that absolute-abundance
183 metrics are far more sensitive to differences in microbial load than their relative counterparts.
184 This behavior is intuitive, and to some extent desirable, because these metrics are designed to
185 detect changes in microbial load even when composition remains constant. Yet at $\alpha = 1$, U^A
186 approaches a proxy for sample absolute abundance itself. In ordination space (Fig. S3), this can
187 cause Axis 1 to correlate with absolute abundance and in some cases (freshwater and soil)
188 produces strong horseshoe effects [15], potentially distorting ecological interpretation. Beyond
189 tuning α to modify the influence of abundances, approaches such as NMDS or partial ordination
190 can also be used to modulate the sensitivity of ordinations to microbial load [16].

191 We recommend calibrating α based on research goals, modulating this effect by using
192 GU^A across a range of α rather than relying on U^A ($\alpha = 1$). Researchers should consider how
193 much emphasis they want their dissimilarity metric to place on microbial load (Box 1). When
194 biomass differences are central to the hypothesis being tested (for example, detecting
195 cyanobacterial blooms), high α are recommended. In contrast, if microbial load is irrelevant or
196 independent of the hypothesis in question, low α (or U^R) may be preferred; for example in the
197 soil dataset, fine-scale differences in composition may be obscured by random variation in
198 microbial load.

199 In many systems, microbial biomass is one piece of the story, likely correlated to other
200 variables being tested. If the importance of microbial load in the system is unknown, one

201 potential approach is to calculate correlations as demonstrated in Fig. 3B and select an α prior to
202 any ordinations or statistical testing. Again, correlation to cell count is valuable and is intrinsic to
203 absolute abundance-aware measures, especially when microbial load is relevant to the
204 hypotheses being tested. Correlations to cell count in BC^A , an accepted approach in the literature,
205 ranged from ~0.5 up to ~0.8. As a general recommendation from these analyses, we recommend
206 α values in an intermediate range from 0.1 up to 0.6, wherein GU^A has similar correlation to cell
207 count as BC^A .

208 **Computational and Methodological Considerations**

209 Applying GU^A in practice raises several considerations related to sequencing depth,
210 richness, and computational cost. Both Bray-Curtis and UniFrac can be sensitive to sequencing
211 depth because richness varies with read count [17–19]. To address this, we provide a workflow
212 and accompanying code describing how we incorporated rarefaction into our own analyses (Box
213 2; available code). This approach minimizes sequencing-depth biases while preserving
214 abundance scaling for downstream β -diversity analysis.

215 To explore the sensitivity of GU^A to rarefaction, we calculated GU^A using rarefaction at
216 multiple sequencing depths, and used Mantel tests to assess the correlation between the rarefied
217 GU^A distance matrices the non-rarefied control (Fig. S4; supplemental methods). GU^A was
218 largely insensitive to rarefaction at high α values, even at depths as low as 250 reads per sample,
219 but sensitivity increased as α decreased (Fig. S4). When rarefying to the minimum sequencing
220 depth, as recommended, the effect of rarefaction was negligible (all Mantel's R > 0.95, Fig. S4).

221 GU^A is slower to compute than both BC^A and U^R because it must traverse the phylogenetic
222 tree to calculate branch lengths for each iteration. Computational time of GU^A increases
223 quadratically with ASV number and is 10-20 times slower, though up to 50 times slower, than
224 BC^A (Fig. 4A-B). The number of samples or α values, however, have relatively little effect on
225 runtime (Fig. S5). For a dataset of 24,000 ASVs, computing on a single CPU is still reasonable
226 (1.4 minutes), but repeated rarefaction increases runtime substantially because branch lengths are
227 redundantly calculated with each iteration. Allowing branch-length objects to be cached or
228 incorporated directly into the GUnifrac workflow would considerably improve computational
229 efficiency.

We also evaluated the sensitivity of GU^A to measurement error in absolute abundance due to uncertainty arising from the quantification of cell number or 16S copy number. To assess the sensitivity of GU^A and BC^A to measurement error, we added random error to the 16S copy number measurements from the mouse gut dataset, limiting our analyses to the stool samples where copy numbers varied by an order of magnitude. Across 50 iterations, each copy number could randomly vary by a given percentage of error in either direction. We re-calculated β -diversity (BC^A and GU^A at $\alpha = 1$ and $\alpha = 0.2$) and compared these measurements to the original dataset.

Introducing random variation into measured 16S copy number altered GU^A values only modestly, and the effect was proportional to the magnitude of the added noise (Fig. 4C–D). At $\alpha = 1$, each 1% of quantification error introduced an average difference of 0.0022 in GU^A ; at $\alpha = 0.2$, GU^A was even less sensitive. Thus, moderate α values provide a balance between interpretability and robustness to noise in absolute quantification. The max deviation from true that added error could inflict on a given metric was also proportional (and always less) than the magnitude of the error itself (Fig. 4D). A more rigorous approach to assessing error propagation within these metrics, including mathematical proofs of the relationships estimated above, is outside the scope of this paper but would be helpful.

GU^A was also insensitive to normalization approaches that adjust ASV abundances based on the predicted 16S rRNA gene copy number (Fig. S6; supplemental methods). We used PICRUSt2 (v2.6) to normalize ASV abundances within each dataset based on predicted 16S copy number per genome, and then applied our standard rarefaction pipeline prior to GU^A calculation (Box 2) [20, 21]. Correlations between GU^A distance matrices calculated from 16S copy number-normalized datasets and those from the original, non-normalized datasets were consistently near unity across all datasets (Mantel's R > 0.98, Fig. S6A), demonstrating that 16S copy number-normalization had a negligible effect on GU^A . Sensitivity of GU^A to 16S copy number-normalization generally decreased with increasing values of α in the cooling reactor, freshwater, and soil datasets, but not in the mouse gut dataset (Fig. S6A). In the mouse gut dataset, several highly abundant ASVs belonging to the genus *Faecalibaculum* had predicted 16S copy numbers of seven copies per genome, explaining the relatively greater (though still weak) sensitivity of this dataset to copy number-normalization (Fig. S6B). Finally, we note that 16S copy number-

260 normalization does not account for variation in genome copies per cell (ploidy), which can vary
261 across several orders of magnitude between species and growth phase [22–24].

262 Ecological Interpretation and conceptual significance

263 Absolute UniFrac reframes the interpretation of β -diversity by making biomass an explicit
264 ecological axis rather than an unmeasured or normalized-away quantity. Conventional UniFrac
265 captures composition and shared evolutionary history but implicitly invites interpretation as if it
266 also encodes differences on microbial load. By incorporating absolute abundance directly,
267 Absolute UniFrac helps to resolve this mismatch and restores alignment between ecological
268 hypotheses and the quantities represented in the metric. In this view, β -diversity becomes a three-
269 axis ecological measure, incorporating composition, phylogeny and biomass, rather than a two-
270 axis approximation. That said, the additional dimension of microbial load also increases the
271 complexity of applying and interpreting this metric.

272 There are many cases where the incorporation of absolute abundance allows microbial
273 ecologists to assess more realistic, ecologically-relevant differences in microbial communities,
274 especially when microbial load is mechanistically central. Outside of the datasets re-analyzed
275 here [3, 5, 9, 10]; the temporal development of the infant gut microbiome involves both a rise in
276 absolute abundance and compositional changes [6]; bacteriophage predation in wastewater
277 bioreactors can be understood only when microbial load is considered [25]; and antibiotic-driven
278 declines in specific swine gut taxa were missed using relative abundance approaches [26]. As β -
279 diversity metrics (and UniFrac specifically) remain central to microbial ecology, these findings
280 highlight how interpretation changes once biomass is incorporated. Broader adoption of absolute
281 abundance profiling will also depend on data availability. Few studies currently make absolute
282 quantification data publicly accessible, underscoring the need to deposit absolute measurements
283 alongside sequencing reads for reproducibility, ideally as metadata within SRA submissions.

284 While demonstrated here with 16S rRNA data, the approach should extend to other marker
285 genes or (meta)genomic features, provided absolute abundance estimates are available. In this
286 sense, GU^A offers a more ecologically grounded view of lineage turnover by jointly reflecting
287 variation in biomass and phylogenetic structure.

288 No single metric (or α in GU^A), however, is universally “best”. Each β -diversity metric
289 emphasizes a different dimension of community change. Researchers should therefore select
290 metrics based on the ecological quantity that is hypothesized to matter most (Box 1). Here, we
291 demonstrate not that GU^A outperforms other measures, but that it faithfully incorporates the three
292 axes of variation it was designed to incorporate: composition, phylogenetic similarity, and
293 absolute abundance (Fig. 1 and Fig. 2). As with any β -diversity analysis, interpretation requires
294 matching the metric to the ecological question at hand, and exploring sensitivity across different
295 metrics where appropriate [27]. By providing demonstrations and code for the application and
296 interpretation of U^A/GU^A , we hope to encourage the use of these metrics as a tool of microbial
297 ecology.

298 **Conclusion**

299 By explicitly incorporating absolute abundance, Absolute UniFrac shifts phylogenetic β -
300 diversity from a two-axis approximation to a three-axis ecological measure. This reframing
301 connects the metric to the underlying biological questions that motivate many microbiome
302 studies. As methods for quantifying microbial load continue to expand, the ability to interpret β -
303 diversity in a biomass-aware framework will become increasingly important for distinguishing
304 true ecological turnover from proportional change alone. In this way, Absolute UniFrac is not
305 simply an alternative distance metric but a tool for aligning statistical representation with
306 ecological mechanism.

307 **Author Contribution Statement:** Both authors contributed equally to the manuscript.

308 **Preprint servers:** This article was submitted to *bioRxiv* (doi: 10.1101/2025.07.18.665540) under
309 a CC-BY-NC-ND 4.0 International license.

310 **Data Availability:** All data and code used to produce the manuscript are available at
311 https://github.com/MarschmiLab/Pendleton_2025_Absolute_Unifrac_Paper, in addition to a
312 reproducible renv environment. All packages used for analysis are listed in Table S1.

313 **Funding Statement:** This work was supported by a NOAA Margaret A. Davidson Fellowship to
314 AP (NA24NOSX420C0016) and by a grant from the Affinito-Stewart & President’s Council of
315 Cornell Women, as well as Cornell University start-up funds to MLS.

316 **References**

- 317 1. Gloor GB, Macklaim JM, Pawlowsky-Glahn V, Egoscue JJ. Microbiome Datasets Are
318 Compositional: And This Is Not Optional. *Front Microbiol* 2017;8:2224.
319 <https://doi.org/10.3389/fmicb.2017.02224>
- 320 2. Vandepitte D, Falony G, Vieira-Silva S, Tito RY, Joossens M, Raes J. Stool consistency is
321 strongly associated with gut microbiota richness and composition, enterotypes and bacterial
322 growth rates. *Gut* 2016;65:57–62. <https://doi.org/10.1136/gutjnl-2015-309618>
- 323 3. Barlow JT, Bogatyrev SR, Ismagilov RF. A quantitative sequencing framework for absolute
324 abundance measurements of mucosal and luminal microbial communities. *Nat Commun*
325 2020;11:2590. <https://doi.org/10.1038/s41467-020-16224-6>
- 326 4. Wang X, How S, Deng F, Zhao J. Current Applications of Absolute Bacterial Quantification
327 in Microbiome Studies and Decision-Making Regarding Different Biological Questions.
328 *Microorganisms* 2021;9:1797. <https://doi.org/10.3390/microorganisms9091797>
- 329 5. Props R, Kerckhof FM, Rubbens P, De Vrieze J, Hernandez-Sanabria E, Waegeman W, et
330 al. Absolute quantification of microbial taxon abundances. *ISME J* 2017;11:584–587.
331 <https://doi.org/10.1038/ismej.2016.117>
- 332 6. Rao C, Coyte KZ, Bainter W, Geha RS, Martin CR, Rakoff-Nahoum S. Multi-kingdom
333 ecological drivers of microbiota assembly in preterm infants. *Nature* 2021;591:633–638.
334 <https://doi.org/10.1038/s41586-021-03241-8>
- 335 7. Bray JR, Curtis JT. An Ordination of the Upland Forest Communities of Southern
336 Wisconsin. *Ecological Monographs* 1957;27:326–349. <https://doi.org/10.2307/1942268>
- 337 8. Lozupone CA, Hamady M, Kelley ST, Knight R. Quantitative and Qualitative β Diversity
338 Measures Lead to Different Insights into Factors That Structure Microbial Communities.
339 *Applied and Environmental Microbiology* 2007;73:1576–1585.
340 <https://doi.org/10.1128/AEM.01996-06>
- 341 9. Pendleton A, Wells M, Schmidt ML. Upwelling periodically disturbs the ecological
342 assembly of microbial communities in the Laurentian Great Lakes. 2025. bioRxiv, 2025.,
343 2025.01.17.633667
- 344 10. Zhang K, Maltais-Landry G, James M, Mendez V, Wright D, George S, et al. Absolute
345 microbiome profiling highlights the links among microbial stability, soil health, and crop

- 346 productivity under long-term sod-based rotation. *Biol Fertil Soils* 2022;58:883–901.
347 <https://doi.org/10.1007/s00374-022-01675-4>
- 348 11. Chen J, Bittinger K, Charlson ES, Hoffmann C, Lewis J, Wu GD, et al. Associating
349 microbiome composition with environmental covariates using generalized UniFrac
350 distances. *Bioinformatics* 2012;28:2106–2113.
351 <https://doi.org/10.1093/bioinformatics/bts342>
- 352 12. Lozupone C, Knight R. UniFrac: a New Phylogenetic Method for Comparing Microbial
353 Communities. *Applied and Environmental Microbiology* 2005;71:8228–8235.
354 <https://doi.org/10.1128/AEM.71.12.8228-8235.2005>
- 355 13. McMurdie PJ, Holmes S. phyloseq: An R package for reproducible interactive analysis and
356 graphics of microbiome census data. *PLoS ONE* 2013;8:e61217.
- 357 14. Bolyen E, Rideout JM, Dillon MR, Bokulich NA, Abnet CC, Al-Ghalith GA, et al.
358 Reproducible, interactive, scalable and extensible microbiome data science using QIIME 2.
359 *Nat Biotechnol* 2019;37:852–857. <https://doi.org/10.1038/s41587-019-0209-9>
- 360 15. Morton JT, Toran L, Edlund A, Metcalf JL, Lauber, C, Knight R. Uncovering the Horseshoe
361 Effect in Microbial Analyses. *mSystems* 2017;2:10.1128/msystems.00166-16.
362 <https://doi.org/10.1128/msystems.00166-16>
- 363 16. Paliy O, Shankar V. Application of multivariate statistical techniques in microbial ecology.
364 *Molecular Ecology* 2016;25:1032–1057. <https://doi.org/10.1111/mec.13536>
- 365 17. Schloss PD. Evaluating different approaches that test whether microbial communities have
366 the same structure. *The ISME Journal* 2008;2:265–275.
367 <https://doi.org/10.1038/ismej.2008.5>
- 368 18. Fukuyama J, McMurdie PJ, Dethlefsen L, Relman DA, Holmes S. Comparisons of distance
369 methods for combining covariates and abundances in microbiome studies. *Biocomputing*
370 2012. WORLD SCIENTIFIC, 2011, 213–224.
- 371 19. McMurdie PJ, Holmes S. Waste Not, Want Not: Why Rarefying Microbiome Data Is
372 Inadmissible. *PLOS Computational Biology* 2014;10:e1003531.
373 <https://doi.org/10.1371/journal.pcbi.1003531>
- 374 20. Wright RJ, Langille MGI. PICRUSt2-SC: an update to the reference database used for
375 functional prediction within PICRUSt2. *Bioinformatics* 2025;41:btaf269.
376 <https://doi.org/10.1093/bioinformatics/btaf269>

- 377 21. Douglas GM, Maffei VJ, Zaneveld JR, Yurgel SN, Brown JR, Taylor CM, et al. PICRUSt2
378 for prediction of metagenome functions. *Nat Biotechnol* 2020;38:685–688.
379 <https://doi.org/10.1038/s41587-020-0548-6>
- 380 22. Griese M, Lange C, Soppa J. Ploidy in cyanobacteria. *FEMS Microbiol Lett* 2011;323:124–
381 131. <https://doi.org/10.1111/j.1574-6968.2011.02368.x>
- 382 23. Mendell JE, Clements KD, Choat JH, Angert ER. Extreme polyploidy in a large bacterium.
383 *Proceedings of the National Academy of Sciences* 2008;105:6730–6734.
384 <https://doi.org/10.1073/pnas.0707522105>
- 385 24. Pecoraro V, Zerulla K, Lange C, Soppa J. Quantification of Ploidy in Proteobacteria
386 Revealed the Existence of Monoploid, (Mero-)Oligoploid and Polyploid Species. *PLOS
387 ONE* 2011;6:e16392. <https://doi.org/10.1371/journal.pone.0016392>
- 388 25. Shapiro OH, Kushmaro A, Brenner A. Bacteriophage predation regulates microbial
389 abundance and diversity in a full-scale bioreactor treating industrial wastewater. *The ISME
390 Journal* 2010;4:327–336. <https://doi.org/10.1038/ismej.2009.118>
- 391 26. Wagner S, Weber M, Paul LS, Grümpel-Schlüter A, Klüss, Neuhaus K, et al. Absolute
392 abundance calculation enhances the significance of microbiome data in antibiotic treatment
393 studies. *Front Microbiol* 2025;16. <https://doi.org/10.3389/fmicb.2025.1481197>
- 394 27. Kers JG, Saccenti E. The Power of Microbiome Studies: Some Considerations on Which
395 Alpha and Beta Metrics to Use and How to Report Results. *Front Microbiol* 2022;12.
396 <https://doi.org/10.3389/fmicb.2021.796025>
- 397
- 398

399 **Figure Legends**

400 **Figure 1. Simulated communities reveal how absolute abundance affects phylogenetic and**
401 **non-phylogenetic β -diversity measures.** (A) We constructed a simple four-ASV community with
402 a known phylogeny and generated all permutations of each ASV having an absolute abundance
403 of 1, 10, or 100, resulting in 81 unique communities and 3,240 pairwise comparisons. (B)
404 Distributions of pairwise differences between weighted UniFrac using absolute abundance (U^A)
405 and three other metrics: Bray-Curtis using relative abundance (BC^R), weighted UniFrac using
406 relative abundance (U^R), and Bray-Curtis using absolute abundance (BC^A). (C) Illustrative
407 sample pairs demonstrate how absolute abundances and phylogenetic structure interact to
408 increase or decrease dissimilarity across metrics. Stars indicate where each scenario falls within
409 the distributions shown in panel B. Actual values for each metric are displayed beneath each
410 scenario.

411 **Figure 2. Absolute UniFrac (U^A) compared with other β -diversity metrics across four real**
412 **microbial datasets.** Each panel shows pairwise sample distances for U^A (x-axis) against another
413 metric (y-axis): Bray-Curtis using relative abundance (BC^R , first column), weighted UniFrac
414 using relative abundances (U^R , second column), and Bray-Curtis using absolute abundances
415 (BC^A , third column). Contours indicate the relative density of pairwise comparisons (n shown for
416 each dataset, left), with darker shading corresponding to more observations. The dashed line
417 marks the 1:1 relationship. Points above the line indicate cases where U^A is smaller than the
418 comparator metric, while points below the line indicate cases where U^A is larger.

419 **Figure 3. Discriminatory performance of U^A and related metrics across four microbial**
420 **systems.** (A) PERMANOVAs were used to quantify the percent variance (R^2) explained by
421 predefined categorical groups (shown in italics beneath each dataset name), with 1,000
422 permutations. PERMANOVA results were evaluated across five metrics and, where applicable,
423 across eleven α values (0-1 in 0.1 increments). For consistency with the original studies, only
424 samples from Reactor cycle 1 were used for the cooling-water dataset, only stool samples for the
425 mouse gut dataset, and only mature rhizosphere samples for the soil dataset (no samples were
426 excluded from the freshwater dataset). (B) Mantel correlation (R) between each distance metric
427 and the pairwise differences in absolute abundance (cell counts or 16S copy number), illustrating
428 the degree to which each metric is driven by biomass differences.

429 **Figure 4. GU^A requires more computational time but remains resilient to quantification error.**
430 (A) Runtime for GU^A (GUniFrac package), U^R (FastUniFrac in the phyloseq package) and BC^A
431 (vegan package) was benchmarked across 50 iterations on a sub-sampled soil dataset (mature
432 samples only) [10], using increasing ASV richness (50, 100, 200, 500, 1,000, 2,000, 5,000,
433 10,000), with 10 samples and one α value per run (unweighted UniFrac is also calculated by
434 default). Error bars represent standard deviation. (B) Quadratic relationship between GU^A
435 computation time and ASV richness. Large center point represents median across 50 iterations,
436 error bars (standard deviation) are too small to be seen. All benchmarks were run on an AMD
437 EPYC 64-core processor with 1014 GB system memory (R v4.3.3, vegan v2.7-1, phyloseq
438 v1.52.0, GUnifrac v1.8.1). (C-D) Sensitivity of GU^A ($\alpha = 1$ and 0.2) and BC^A to measurement
439 error was evaluated by adding random variation ($\pm 1\%$ to $\pm 50\%$; Supporting Methods) to 16S
440 copy number estimates in stool samples from the mouse gut dataset [3]. For each error level, 50
441 replicate matrices were generated and compared to the original values. Panels reflect the (C)
442 mean difference and (D) max difference between the error-added metrics compared to the
443 originals. Error bars represent the standard deviation of the average mean and max difference
444 across 50 iterations.

445

446 **Box 1: β -diversity metrics should reflect the hypothesis being tested**

447 Absolute UniFrac is most informative when variation in microbial load is expected to carry
448 ecological meaning rather than being a nuisance variable. The choice of α determines how
449 strongly abundance differences influence the metric, and should therefore be selected based on
450 the hypothesis, not by convention. In settings where biomass is central to the mechanism under
451 study, higher α values appropriately foreground that signal, whereas in cases where load
452 variation is incidental or confounding, lower α values maintain interpretability. Framing α as a
453 hypothesis-driven choice repositions β -diversity from a default normalization step to an explicit
454 ecological decision.

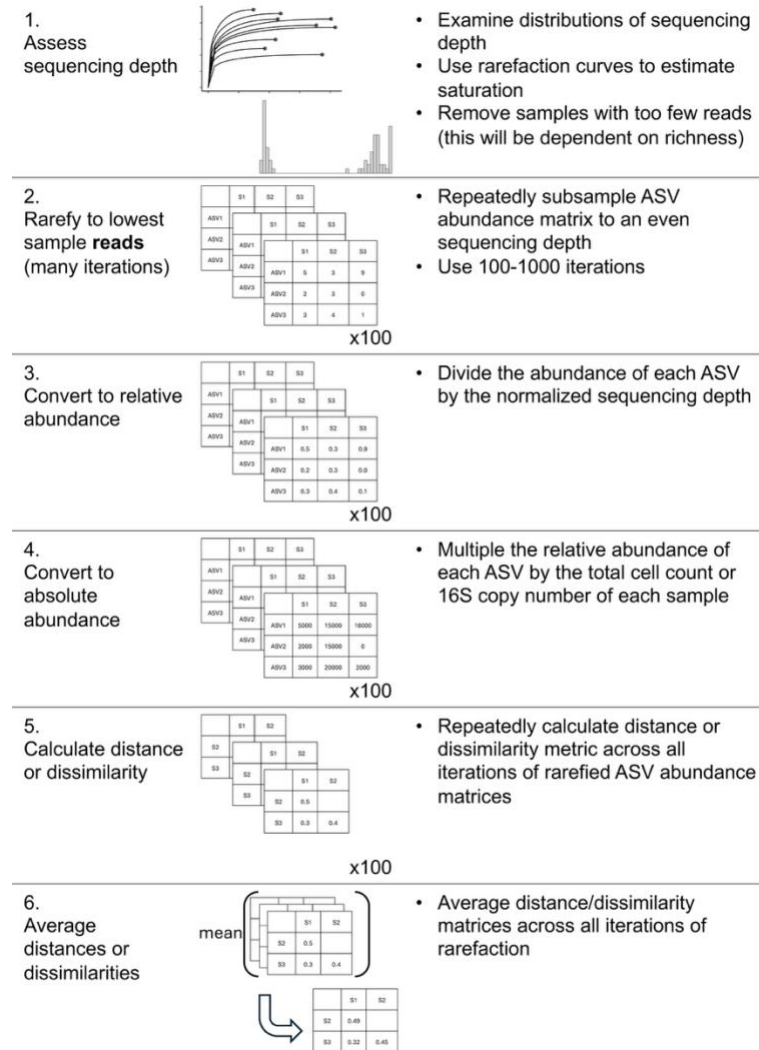
455

456 **Box 1 continued:**

			Metric to Use		Hypothetical Example	
Treat closely related lineages as similar?	Yes	How relevant is microbial load?	Central to hypothesis		$GU^A, \alpha > 0.5$	Cyanobacterial bloom, pathogen proliferation
			Relevant, but associated with other variables of interest		$GU^A, 0.1 < \alpha < 0.5$	Compositional shifts in response to nutrient addition
			Irrelevant	Emphasize rare or dominant taxa?	$GU^R, \alpha > 0.5$	Diet-associated microbiome shifts across hosts
				Rare	$GU^R, \alpha < 0.5$	Tributary inputs of rare taxa
	No	Microbial load relevant?	Unknown		GU^A at multiple α	Random variation in microbial load obscured compositional shifts in soil communities
	Yes		BC^A	Strain turnover and proliferation in the infant gut		
	No		BC^R	Temporal succession in chemostat		

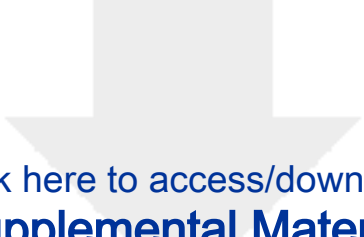
458 **Box 2: Rarefaction workflow for incorporating absolute abundance**

459 While we refrain from an in-depth analysis of rarefaction approaches, here we present our
 460 workflow for incorporating
 461 rarefaction alongside absolute
 462 abundance. First, samples were
 463 assessed for anomalously low read
 464 counts and discarded (sequencing
 465 blanks and controls were also
 466 removed). For rarefaction, each
 467 sample in the ASV table was
 468 subsampled to equal *sequencing*
 469 depth (# of reads) across 100
 470 iterations, creating 100 rarefied ASV
 471 tables. These tables were then
 472 converted to relative abundance by
 473 dividing each ASV's count by the
 474 equal sequencing depth (rounding
 475 was not performed). Then, each
 476 ASV's absolute abundance within a
 477 given sample was calculated by
 478 multiplying its relative abundance
 479 by that sample's total cell count or
 480 16S copy number. Methods to predict genomic 16S copy number for a given ASV were not used
 481 unless explicitly stated (Fig. S6) [20, 21]. Each distance/dissimilarity metric was then calculated
 482 across all 100 absolute-normalized ASV tables. The final distance/dissimilarity matrix was
 483 calculated by averaging all 100 iterations of each distance/dissimilarity calculation. Of note for
 484 future users: pruning the phylogenetic tree after rarefaction for each iteration is not necessary –
 485 ASVs removed from the dataset do not contribute nor change the calculated UniFrac
 486 distances.





Click here to access/download
Supplemental Material
03_Pendleton_Supplement_FINAL.docx

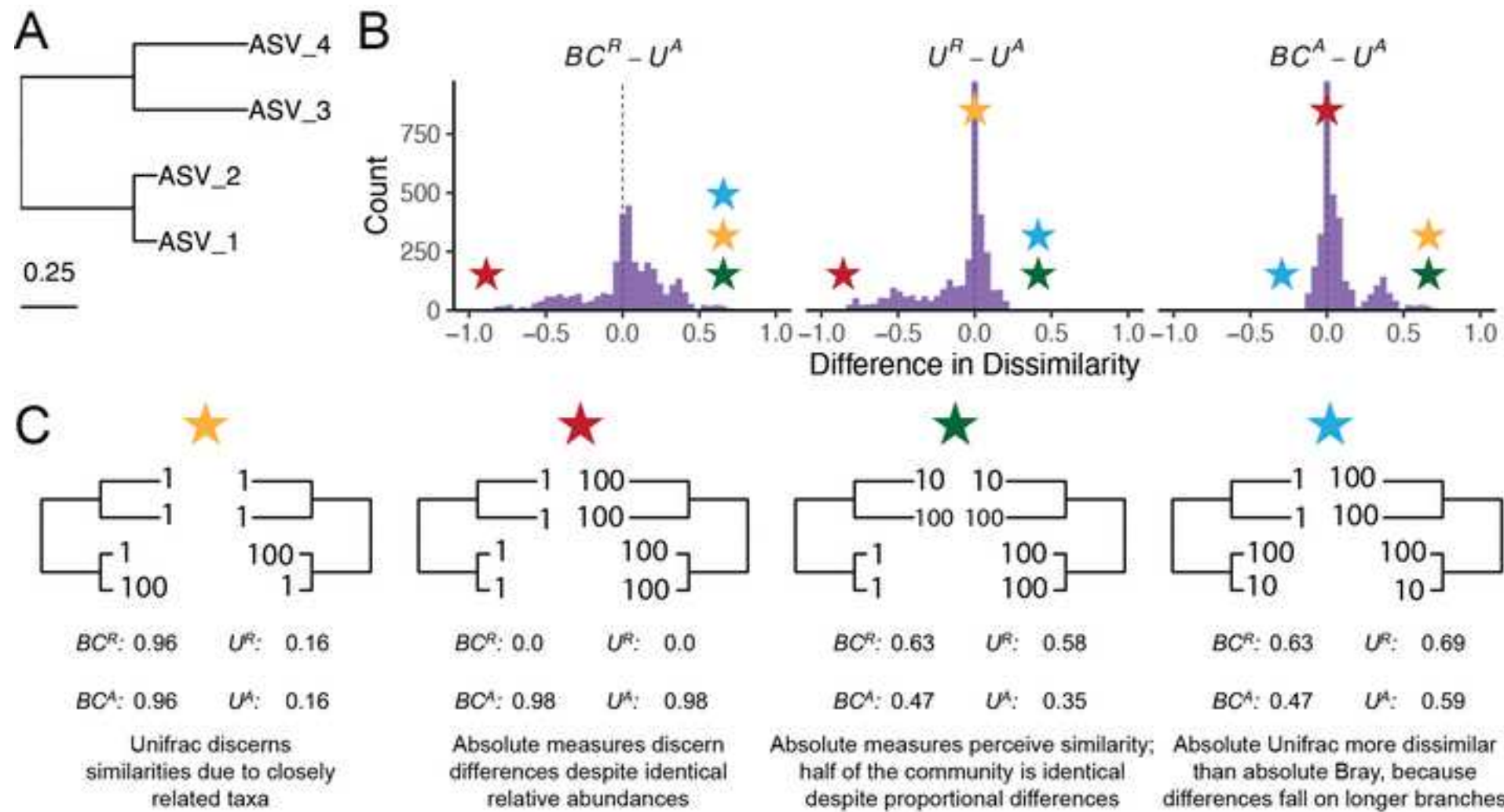


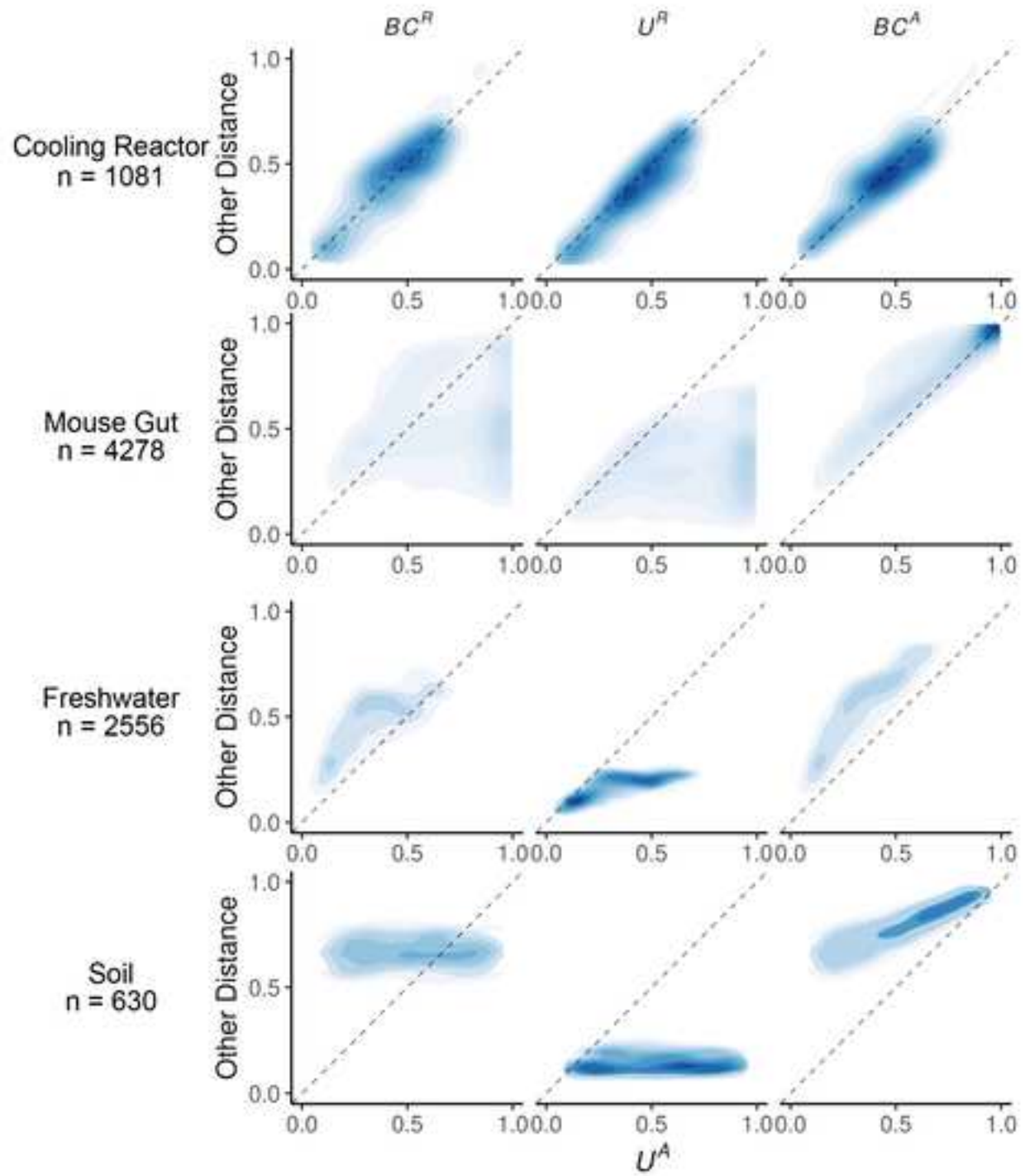
Click here to access/download

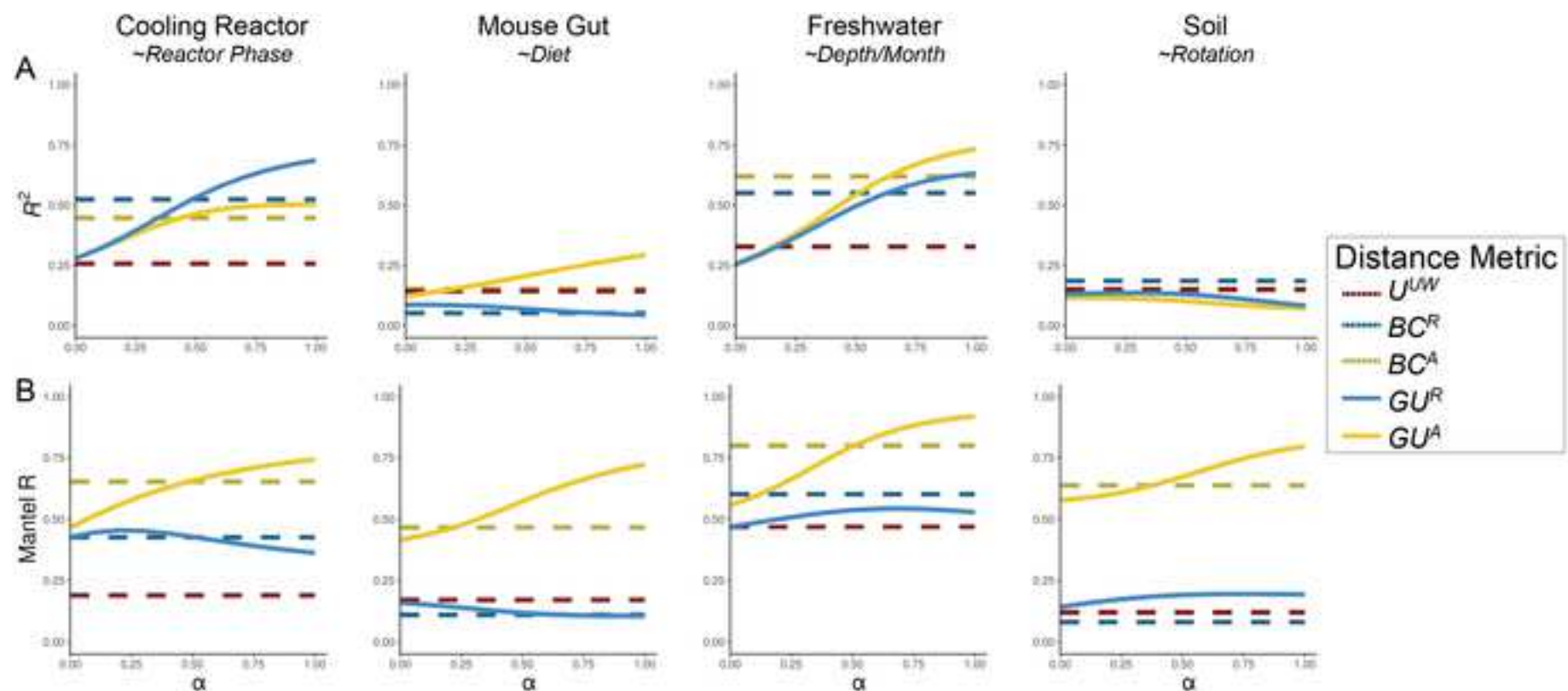
Supplemental Material

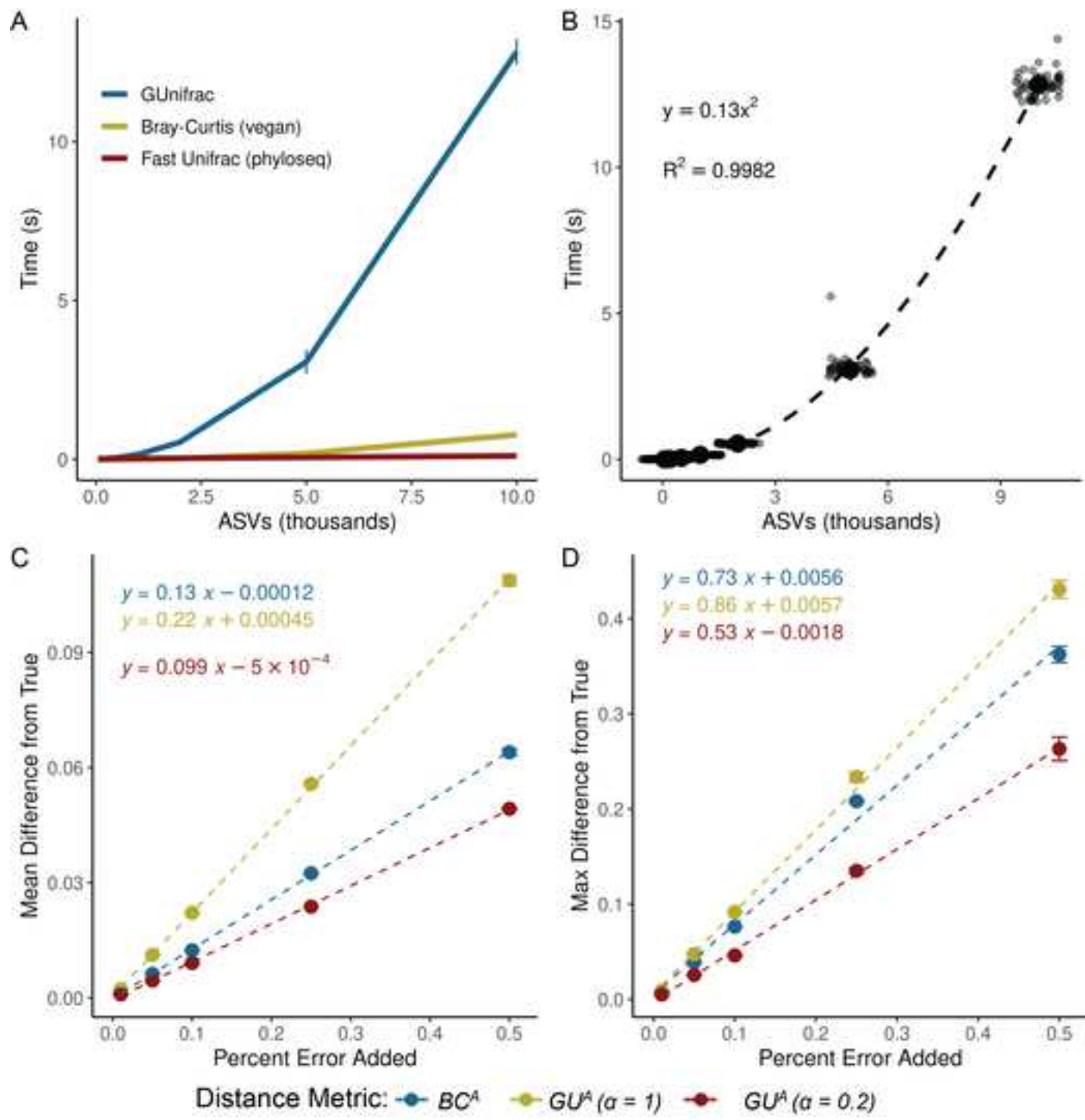
03_Pendleton_Supplement_FINAL.pdf



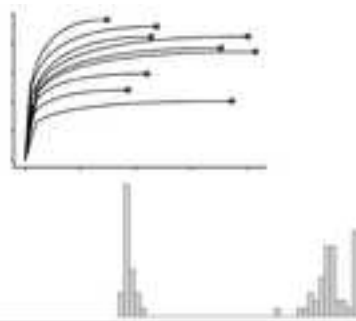








1.
Assess sequencing depth



- Examine distributions of sequencing depth
- Use rarefaction curves to estimate saturation
- Remove samples with too few reads (this will be dependent on richness)

2.
Rarefy to lowest sample **reads** (many iterations)

	S1	S2	S3
ASV1	100	100	100
ASV2	100	100	100
ASV3	100	100	100
ASV4	100	100	100
ASV5	100	100	100

x100

- Repeatedly subsample ASV abundance matrix to an even sequencing depth
- Use 100-1000 iterations

3.
Convert to relative abundance

	S1	S2	S3
ASV1	100	100	100
ASV2	100	100	100
ASV3	100	100	100
ASV4	100	100	100
ASV5	100	100	100

x100

- Divide the abundance of each ASV by the normalized sequencing depth

4.
Convert to absolute abundance

	S1	S2	S3
ASV1	100	100	100
ASV2	100	100	100
ASV3	100	100	100
ASV4	100	100	100
ASV5	100	100	100

x100

- Multiple the relative abundance of each ASV by the total cell count or 16S copy number of each sample

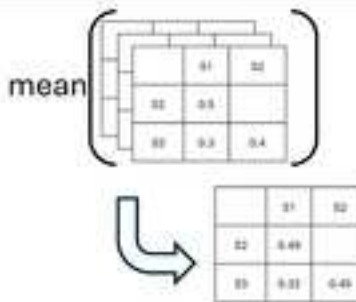
5.
Calculate distance or dissimilarity

	S1	S2
S1	100	100
S2	100	100
S3	100	100
S4	100	100

x100

- Repeatedly calculate distance or dissimilarity metric across all iterations of rarefied ASV abundance matrices

6.
Average distances or dissimilarities



- Average distance/dissimilarity matrices across all iterations of rarefaction

We thank both the reviewers for their comments, which have greatly improved our manuscript. Note that line numbers correspond to the “TrackedChanges” version of the manuscript.

Reviewer #1

1. The authors have done a great job revising this manuscript. They have addressed all my comments, and I especially appreciate the addition of distance metric comparisons across four real-world data sets, which I find very helpful.
 - a. Thank you! We agree the addition of the real-world datasets greatly improved the manuscript.
2. I am happy to recommend the manuscript for publication, and I only have one minor comment: In the abstract, I interpret your formulation as a general claim that your new metric is less sensitive to noise than other metrics such as Bray-Curtis. However, as you show in the new Fig. 4, Bray-Curtis is in fact less sensitive to noise than the new metric at high alpha values. Perhaps this can be clarified before publication.
 - a. After reflection, we see how the phrase “comparably insensitive” is confusing – it sounds like GUA is always less sensitive, when it can be more sensitive than BC (at high alpha) or less sensitive (at lower alpha). We’ve edited the sentence:
 - b. Line 31: “...GUA is comparably **sensitive** to realistic noise in load estimates compared to conventional alternatives like Bray-Curtis dissimilarities, particularly at lower α .”

Reviewer #2

1. Pendleton and Schmidt present Absolute UniFrac, a modification of Weighted UniFrac that uses absolute abundances from qPCR, dPCR, flow cytometry, or spike-in standards to capture the joint effects of phylogeny and biomass. The revision expands the evidence beyond the original Lake Ontario case and adds practical guidance. You retain the four-taxon toy simulation and add four 16S rRNA datasets spanning a nuclear reactor cooling system, the mouse gut, a stratified freshwater lake, and peanut rhizosphere soil, with absolute load quantified by flow cytometry for the cooling water and lake, droplet digital PCR for the gut, and quantitative PCR (qPCR) for the soil. The datasets span roughly 215 to 24,000 ASVs and loads from approximately 4×10^5 cells per milliliter to 2×10^{12} 16S copies per gram. Code, data, and an R environment are provided. The goal is to present guidance on a new, practical, abundance-aware phylogenetic dissimilarity for studies that already measure absolute counts. Overall, the revision resolves the main first-round requests. The remaining items are clarity tweaks and two small robustness checks. Note, at over 2700 words, not including figure legends, this is on the long end for a Brief Communication (expected word count ~1000)

- a. We thank the reviewer for the thorough consideration of our manuscript, and feel the paper has greatly improved due to their suggestions. We recognize the manuscript has also grown significantly in size due to these additions, but still feel that it retains the character of a Brief Communication (communicating a new idea), less than an original article presenting a full research project. We will defer these considerations to the editor for their decision.
2. Dataset breadth: Addressed. You added three datasets beyond the original lake analysis and compared UA to BCR, UR, and BCA for each system. See Fig. 2 and the surrounding text in the tracked or clean manuscript.
- a. Thank you for noting that the expanded analyses across systems addressed this point.
3. Alpha guidance: Addressed. You move from coarse choices to α in 0.1 steps, report PERMANOVA R² across α , and give practical selection advice. See Fig. 3, its caption, and Box 1.
- a. We appreciate the reviewer's acknowledgment that the revised analyses and guidance adequality addressed this concern.
4. Rarefaction guidance: Addressed in a practical sense. Box 2 provides a concrete workflow and code pointers for incorporating rarefaction while preserving absolute scaling. Please also include a minimal sensitivity check against a no-rarefaction pipeline for one dataset in the supplement, using a Mantel R test to compare the two distance matrices. This will preempt common questions associated with understanding if rarefying your data actually changes the results.
- a. This is a great suggestion, and we're grateful for the encouragement to run these experiments. We tested the impact of rarefaction on GUA values for all four datasets and have included an additional figure in the supplement showing these analyses (Fig. S4). We've also added additional information within the main text describing our findings:
 - b. Line 245: "Applying GU^A in practice raises several considerations related to sequencing depth, richness, and computational cost. Both Bray-Curtis and UniFrac can be sensitive to sequencing depth because richness varies with read count [17–19]. To address this, we provide a workflow and accompanying code describing how we incorporated rarefaction into our own analyses (Box 2; available code). This approach minimizes sequencing-depth biases while preserving abundance scaling for downstream β -diversity analysis."

To explore the sensitivity of GU^A to rarefaction, we calculated GU^A using rarefaction at multiple sequencing depths, and used Mantel tests to assess the correlation between the rarefied GU^A distance matrices the non-rarefied control (Fig. S4; supplemental methods). GU^A was largely insensitive to rarefaction at

high α values, even at depths as low as 250 reads per sample, but sensitivity increased as α decreased (Fig. S4). When rarefying to the minimum sequencing depth, as recommended, the effect of rarefaction was negligible (all Mantel's R > 0.95, Fig. S4)."

5. Computational scaling: Addressed. You benchmark GUA against Fast UniFrac and Bray-Curtis, showing quadratic growth with richness, and note caching opportunities. Please add the CPU model, RAM, R version, and package versions directly in the Fig. 4 caption or Methods so the timing is contextualized without following external links.
 - a. We are grateful for the suggestion. We've added:
 - b. Line 277: "All benchmarks were run on an AMD EPYC 64-core processor with 1014 GB system memory (R v4.3.3, vegan v2.7-1, phyloseq v1.52.0, GUnifrac v1.8.1)."
6. Copy-number assumptions: Partially addressed. Because readers will wonder, add a sentence justifying your choice not to apply per-taxon 16S copy-number correction, and, if possible, include a brief sensitivity check for one dataset in the supplement. This will preempt another common question set associated with multicopy 16S genes, which can be: 1) divergent within a single genome and 2) number >15 in some lineages (e.g., Proteobacteria).
 - a. We also enjoyed following up on this suggestion. We tested the effect of copy-number normalization (using PICRUSt2) on GUA, and have incorporated these analyses into a new supporting figure (Fig. S6). We also included results text discussing these findings:
 - b. Line 310: " GU^A was also insensitive to normalization approaches that adjust ASV abundances based on the predicted 16S rRNA gene copy number (Fig. S6; supplemental methods). We used PICRUSt2 (v2.6) to normalize ASV abundances within each dataset based on predicted 16S copy number per genome, and then applied our standard rarefaction pipeline prior to GU^A calculation (Box 2) [20, 21]. Correlations between GU^A distance matrices calculated from 16S copy number-normalized datasets and those from the original, non-normalized datasets were consistently near unity across all datasets (Mantel's R > 0.98, Fig. S6A), demonstrating that 16S copy number-normalization had a negligible effect on GU^A . Sensitivity of GU^A to 16S copy number-normalization generally decreased with increasing values of α in the cooling reactor, freshwater, and soil datasets, but not in the mouse gut dataset (Fig. S6A). In the mouse gut dataset, several highly abundant ASVs belonging to the genus *Faecalibaculum* had predicted 16S copy numbers of seven copies per genome, explaining the relatively greater (though still weak) sensitivity of this dataset to copy number-normalization (Fig. S6B). Finally, we note that 16S copy number-normalization does not account for variation in genome copies per cell (ploidy), which can vary across several orders of magnitude between species and growth phase [22–24]."

Minor Comments

7. Abstract: Early in the abstract, it might be useful to indicate clearly that "load" and "abundance" are synonymous. This recommendation is based on the fact that "load" tends to be more of a medical-focused term, whereas the new metric is useful for other microbial environments (e.g., soils, oceans) where the term "load" is less frequently used compared to "abundance".
 - a. The first sentence now reads:
 - b. Line 16: " β -diversity is central to microbial ecology, yet commonly used metrics overlook changes in microbial load (or "absolute abundance")..."
8. Abstract line 31: if using alpha in the abstract, need to define as "tunable ecological dimension" or similar.
 - a. We've edited this sentence to make this clearer:
 - b. Line 28: "To balance these effects, we also incorporate absolute abundance into the generalized extension (GU^A) that has a tunable, continuous ecological parameter (α) that modulates the relative contribution of rare versus abundant lineages to β -diversity calculations."
9. Novelty statement is clearer. Add cautious "to our knowledge" phrasing on line 152.
 - a. This is a fair point. We've reworded:
 - b. Line 109: "Although substituting absolute for relative abundances is mathematically straightforward, to our knowledge there is no prior work that examines UniFrac in the context of absolute abundance..."
10. Box 1 is useful. Add a one-line note in the text that high α may produce biomass-dominated ordinations and that NMDS or partial ordinations can help when Axis 1 tracks load. Aligns Box 1 advice with lines 198-200.
 - a. We are glad that Box 1 is useful! And the recommendation for NMDS or partial ordination is an excellent idea. We've added a sentence (after discussing the ordinations) to provide this option:
 - b. Line 214: "Beyond tuning α to modify the influence of abundances, approaches such as NMDS or partial ordination can also be used to modulate the sensitivity of ordinations to microbial load [16]."

11. Line 268: Possible word error: "cell number of 16S copy number" to "cell number or 16S copy number"
 - a. This typo has been corrected.
12. Figure 3 Legend Line 331: Is the Freshwater dataset needing to be mentioned in this sentence?
 - a. It was originally unmentioned as no samples were subsetted from this dataset; to clarify this, we've added:
 - b. Line 224: "...and only mature rhizosphere samples for the soil dataset (no samples were excluded from the freshwater dataset)."
13. Figure S3: Define CR and SBR in the figure legend.
 - a. This suggestion has been incorporated, by defining conventional and sod-based rotation strategies directly in the legend of Fig. S3.

1 **Interpreting UniFrac with Absolute Abundance: A Conceptual and Practical Guide**

2 Augustus Pendleton^{1*} & Marian L. Schmidt^{1*}

3 ¹Department of Microbiology, Cornell University, 123 Wing Dr, Ithaca, NY 14850, USA

4 **Corresponding Authors:** Augustus Pendleton: arp277@cornell.edu; Marian L. Schmidt:
5 marschmi@cornell.edu

6 **Author Contribution Statement:** Both authors contributed equally to the manuscript.

7 **Preprint servers:** This article was submitted to *bioRxiv* (doi: 10.1101/2025.07.18.665540) under
8 a CC-BY-NC-ND 4.0 International license.

9 **Keywords:** Microbial Ecology - Beta Diversity - Absolute Abundance - Bioinformatics -
10 UniFrac

11 **Data Availability:** All data and code used to produce the manuscript are available at
12 https://github.com/MarschmiLab/Pendleton_2025_Absolute_Unifrac_Paper, in addition to a
13 reproducible renv environment. All packages used for analysis are listed in Table S1.

14

15 **Abstract**

16 β -diversity is central to microbial ecology, yet commonly used metrics overlook changes in
17 microbial load (or “absolute abundance”), limiting their ability to detect ecologically meaningful
18 shifts. Popular for incorporating phylogenetic relationships, UniFrac distances currently default
19 to relative abundance and therefore omit important variation in microbial abundances. As
20 quantifying absolute abundance becomes more accessible, integrating this information into β -
21 diversity analyses is essential. Here, we introduce *Absolute UniFrac* (U^A), a variant of Weighted
22 UniFrac that incorporates absolute abundances. Using simulations and a reanalysis of four 16S
23 rRNA metabarcoding datasets (from a nuclear reactor cooling tank, the mouse gut, a freshwater
24 lake, and the peanut rhizosphere), we demonstrate that Absolute UniFrac captures microbial load,
25 composition, and phylogenetic relationships. While this can improve statistical power to detect
26 ecological shifts, we also find Absolute UniFrac can be strongly correlated to differences in cell
27 abundances alone. To balance these effects, we also incorporate absolute abundance into the
28 generalized extension (GU^A) that has a tunable, continuous ecological parameter (α) that
29 modulates the relative contribution of rare versus abundant lineages to β -diversity calculations.
30 Finally, we benchmark GU^A and show that although computationally slower than conventional
31 alternatives, GU^A is comparably sensitive to noise in load estimates compared to conventional
32 alternatives like Bray-Curtis dissimilarities, particularly at lower α . By coupling phylogeny,
33 composition, and microbial load, Absolute UniFrac integrates three dimensions of ecological
34 change, better equipping microbial ecologists to quantitatively compare microbial communities.

35 **Main Text**

36 Microbial ecologists routinely compare communities using β -diversity metrics derived
37 from relative abundances. Yet this approach overlooks a critical ecological dimension: microbial
38 load. High-throughput sequencing produces compositional data, in which each taxon's
39 abundance is constrained by all others [1]. However, quantitative profiling studies show that cell
40 abundance, not only composition, can drive major community differences [2]. In low-biomass
41 samples, relying on relative abundance can allow contaminants to appear biologically
42 meaningful despite absolute counts too low for concern [3].

43 Sequencing-based microbiome studies therefore rely on relative abundance even when
44 the hypotheses of interest implicitly concern absolute changes in biomass. This creates a
45 mismatch between ecological framing (growth, bloom magnitude, pathogen proliferation,
46 disturbance recovery, or colonization pressure) and the information the β -diversity metric
47 encodes [4]. As a result, β -diversity is often treated as if it includes biomass, even when absolute
48 abundance is either not measured at all or is measured but excluded from the calculation (as in
49 conventional UniFrac). Many studies therefore test biomass-linked hypotheses using a metric
50 that normalizes biomass away [4]. A conceptual correction is needed in which β -diversity is
51 understood as variation along three axes: composition, phylogeny and absolute abundance.

52 Absolute microbial load measurements are now increasingly obtainable through flow
53 cytometry, qPCR, and genomic spike-ins, allowing biomass to be quantified alongside taxonomic
54 composition [4, 5]. These approaches improve detection of functionally relevant taxa and
55 mitigate the compositional constraints imposed by sequencing [1, 2]. Most studies that
56 incorporate absolute abundance counts currently rely on Bray-Curtis dissimilarity, which can
57 capture load but does not consider phylogenetic similarity [5–7]. Unifrac distances provide the
58 opposite strength, incorporating phylogeny but discarding absolute abundance, as they are
59 restricted to relative abundance data by construction [8]. This leaves no phylogenetically
60 informed β -diversity metric that operates on absolute counts, despite the fact that biomass is
61 central to many ecological hypotheses.

62 To evaluate the implications of incorporating absolute abundance into phylogenetic β -
63 diversity, we use both simulations and reanalysis of four 16S rRNA amplicon datasets. The
64 simulations use a simple four-taxon community with controlled abundance shifts to directly
65 compare both Bray-Curtis and UniFrac in their relative and absolute forms, illustrating how each
66 metric responds when abundance, composition, or evolutionary relatedness differ. We then
67 reanalyze four real-world datasets spanning nuclear reactor cooling water [5], the mouse gut [3],
68 a freshwater lake [9], and rhizosphere soil [10]. These differ widely in richness, biomass range,
69 and ecological context, allowing us to test when absolute abundance changes align with or
70 diverge from phylogenetic turnover. Together, these simulations and reanalyses provide the
71 empirical foundation for interpreting Absolute UniFrac relative to existing β -diversity measures
72 across the three axes of ecological difference: abundance, composition, and phylogeny.

73 We also extend Absolute UniFrac as was proposed by [11] to Generalized Absolute
74 UniFrac that incorporates a tunable ecological dimension, α , and evaluate its impact across
75 simulated and real-world datasets. As α increases, β -diversity is increasingly correlated with
76 differences in absolute abundance, allowing researchers to fine tune the relative weight their
77 analyses place on microbial load versus composition.

78 **Defining Absolute UniFrac**

79 The UniFrac distance was first introduced by Lozupone & Knight (2005) and has since
 80 become enormously popular as a measure of β -diversity within the field of microbial ecology
 81 [12]. A benefit of the UniFrac distance is that it considers phylogenetic information when
 82 estimating the distance between two communities. After first generating a phylogenetic tree
 83 representing species (or amplicon sequence variants, “ASVs”) from all samples, the UniFrac
 84 distance computes the fraction of branch-lengths which is *shared* between communities, relative
 85 to the total branch length represented in the tree. UniFrac can be both unweighted, in which only
 86 the incidence of species is considered, or weighted, wherein a branch’s contribution is weighted
 87 by the proportional abundance of taxa on that branch [8]. The Weighted UniFrac is derived:

$$88 \quad U^R = \frac{\sum_{i=1}^n b_i |p_i^a - p_i^b|}{\sum_{i=1}^n b_i (p_i^a + p_i^b)}$$

89 where the contribution of each branch length, b_i , is weighted by the difference in the relative
 90 abundance of all species (p_i) descended from that branch in sample a or sample b . Here, we
 91 denote this distance as U^R , for “Relative UniFrac”. Popular packages which calculate weighted
 92 UniFrac—including the diversity-lib QIIME plug-in and the R packages phyloseq and
 93 GUniFrac—run this normalization by default [11, 13, 14].

94 Importantly, U^R is most sensitive to changes in abundant lineages, which can sometimes
 95 obscure compositional differences driven by rare to moderately-abundant taxa [11]. To address
 96 this weakness, Chen et al. (2012) introduced the generalized UniFrac distance (GU^R), in which
 97 the impact of abundant lineages can be mitigated by decreasing the parameter α :

$$98 \quad GU^R = \frac{\sum_{i=1}^n b_i (p_i^a + p_i^b)^\alpha \left| \frac{p_i^a - p_i^b}{p_i^a + p_i^b} \right|}{\sum_{i=1}^n b_i (p_i^a + p_i^b)^\alpha}$$

99 where α ranges from 0 (close to Unweighted UniFrac) up to 1 (identical to U^R , above). However,
 100 if one wishes to use absolute abundances, both U^R and GU^R can be derived without normalizing
 101 to proportions:

$$102 \quad U^A = \frac{\sum_{i=1}^n b_i |c_i^a - c_i^b|}{\sum_{i=1}^n b_i (c_i^a + c_i^b)} \quad GU^A = \frac{\sum_{i=1}^n b_i (c_i^a + c_i^b)^\alpha \left| \frac{c_i^a - c_i^b}{c_i^a + c_i^b} \right|}{\sum_{i=1}^n b_i (c_i^a + c_i^b)^\alpha}$$

103 Where c_i^a and c_i^b denote for the absolute counts of species descending from branch b_i in
 104 communities a and b , respectively. We refer to these distances as *Absolute UniFrac* (U^A) and
 105 *Generalized Absolute UniFrac* (GU^A). Although substituting absolute for relative abundances is
 106 mathematically straightforward, to our knowledge there is no prior work that examines UniFrac
 107 in the context of absolute abundance, either conceptually or in application. Incorporating
 108 absolute abundances introduces a third axis of ecological variation: beyond differences in
 109 composition and phylogenetic similarity, U^A also captures divergence in microbial load. This
 110 makes interpretation of U^A nontrivial, particularly in complex microbiomes.

111 **Demonstrating β -diversity metrics’ behavior with a simple simulation**

To clarify how U^A behaves relative to existing β -diversity metrics, we first constructed a simple four-taxon simulated community arranged in a small phylogeny (Fig. 1A). By varying the absolute abundance of each ASV (1, 10, or 100), we generated 81 samples and 3,240 pairwise comparisons. For each pair, we computed four dissimilarity metrics: Bray-Curtis with relative abundance (BC^R), Bray-Curtis with absolute abundance (BC^A), Weighted UniFrac with relative abundance (U^R), and Weighted UniFrac with absolute abundance (U^A). These comparisons help to illustrate how each axis of ecological difference—abundance, composition, and phylogeny—is expressed by the different metrics.

U^A does not consistently yield higher or lower distances compared to other metrics, but instead varies depending on how abundance and phylogeny intersect (Fig. 1B). In the improbable scenario that all branch lengths are equal, U^A is always less than or equal to BC^A (Fig. S1). These comparisons emphasize that once branch lengths differ, incorporating phylogeny and absolute abundance alters the structure of the distance space. The direction and magnitude of that change depend on which branches carry the abundance shifts. U^A is also usually smaller than BC^A and is more strongly correlated with BC^A (Pearson's $r = 0.82$, $p < 0.0001$) than with BC^R ($r = 0.41$) and U^R ($r = 0.55$).

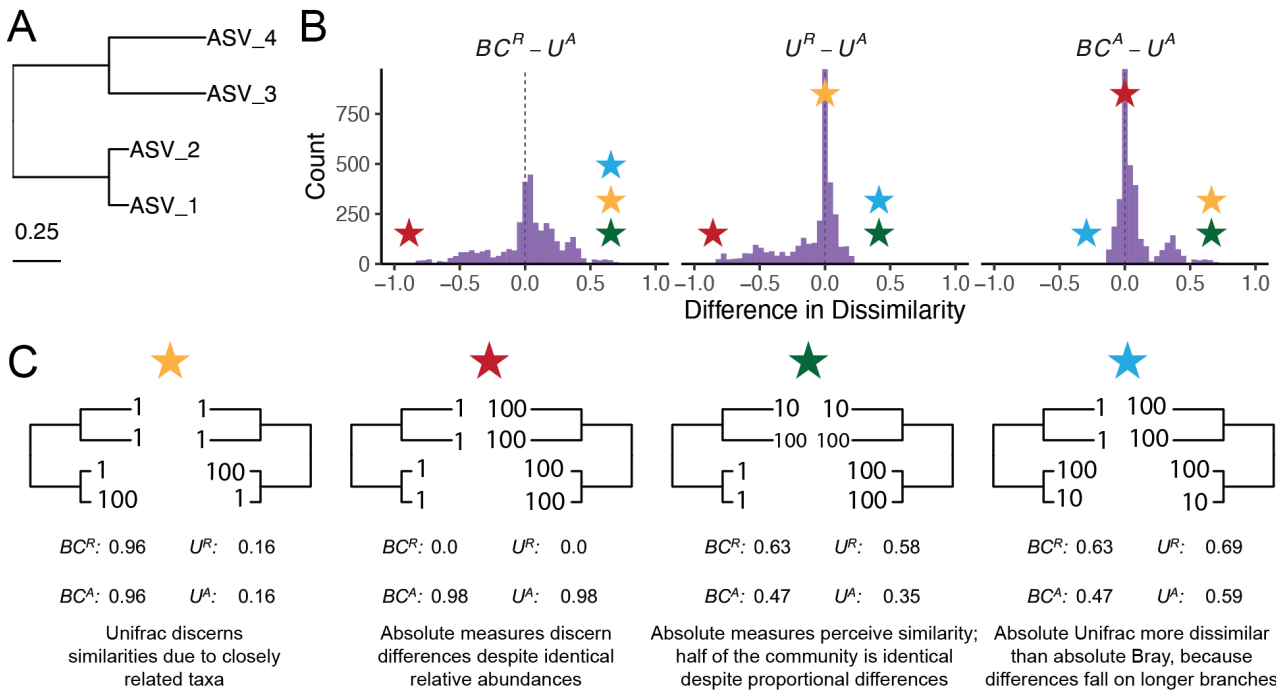
To better understand how these metrics diverge, we examined individual sample pairs (Fig. 1C). Scenario 1 (gold star) illustrates the classic advantage of UniFrac: ASV_1 and ASV_2 are phylogenetically close, so U^R and U^A discern greater similarity between samples than BC^R and BC^A , which ignore phylogenetic structure. Scenario 2 (red star) highlights a limitation of relative metrics: two samples with identical relative composition but a 100-fold difference in biomass appear identical to BC^R and U^R , but not to their absolute counterparts. In Scenario 3 (green star), incorporating absolute abundance decreases dissimilarity. BC^A and U^A are lower than their relative counterparts because half the community is identical in absolute abundance, even though their proportions differ. In contrast, Scenario 4 (blue star) shows that U^A can exceed BC^A when abundance differences occur on long branches, amplifying phylogenetic dissimilarity.

These scenarios demonstrate that U^A integrates variation along three ecologically relevant axes: composition, phylogenetic similarity, and microbial load, rather than isolating any single dimension. Because a given U^A value can reflect multiple drivers of community change, interpreting it requires downstream analyses to disentangle the relative contributions of these three axes. To evaluate how this plays out in real systems we next reanalyzed four previously published datasets spanning diverse microbial environments.

144

145

146

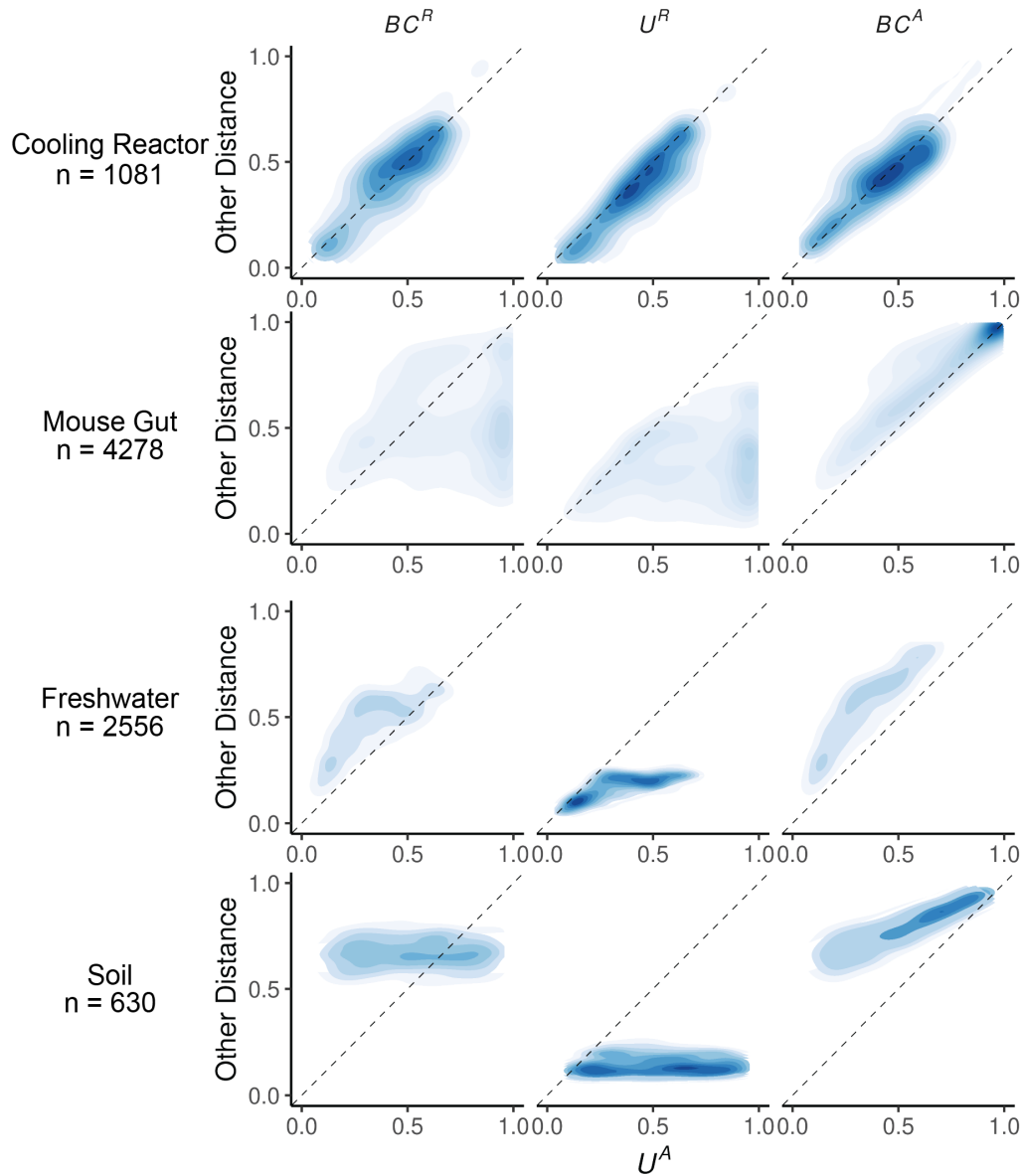


147 *Figure 1. Simulated communities reveal how absolute abundance affects phylogenetic and non-phylogenetic β -*
148 *diversity measures.* (A) We constructed a simple four-ASV community with a known phylogeny and generated all
149 permutations of each ASV having an absolute abundance of 1, 10, or 100, resulting in 81 unique communities and
150 3,240 pairwise comparisons. (B) Distributions of pairwise differences between weighted UniFrac using absolute
151 abundance (U^A) and three other metrics: Bray-Curtis using relative abundance (BC^R), weighted UniFrac using
152 relative abundance (UR), and Bray-Curtis using absolute abundance (BC^A). (C) Illustrative sample pairs demonstrate
153 how absolute abundances and phylogenetic structure interact to increase or decrease dissimilarity across metrics.
154 Stars indicate where each scenario falls within the distributions shown in panel B. Actual values for each metric are
155 displayed beneath each scenario.

156 Application of Absolute UniFrac to Four Real-World Microbiome Datasets

157 To illustrate the sensitivity of U^A to both variation in composition and absolute
158 abundance, we re-analyzed four previously published datasets from diverse microbial systems.
159 These datasets included: (i) nuclear reactor cooling water sampled across three reactor cycle
160 phases [5]; (ii) the mouse gut sampled across multiple regions and between two diets [3]; (iii)
161 depth-stratified freshwater communities sampled across two months [9]; and (iv) peanut
162 rhizospheres under two crop rotation schemes (conventional rotation (CR) vs. sod-based rotation
163 (SBR)), plant maturities, and irrigation treatments [10]. Absolute abundance was quantified by
164 flow cytometry for the cooling water and freshwater datasets, droplet digital PCR for the mouse
165 gut, and by qPCR for the rhizosphere dataset. Together these span a wide range of richness—from
166 215 ASVs in the cooling water to 24,000 ASVs in the soil—and microbial load—from as low as
167 4×10^5 cells/ml (cooling water) up to 2×10^{12} 16S rRNA copies/gram (mouse gut). Additional

168 details of the re-analysis workflow, including ASV generation and phylogenetic inference, are
169 provided in the Supporting Methods.



170 *Figure 2. Absolute UniFrac (U^A) compared with other β -diversity metrics across four real microbial datasets.* Each
171 panel shows pairwise sample distances for U^A (x-axis) against another metric (y-axis): Bray-Curtis using relative
172 abundance (BC^R , first column), weighted UniFrac using relative abundances (U^R , second column), and Bray-curtis
173 using absolute abundances (BC^A , third column). Contours indicate the relative density of pairwise comparisons (n
174 shown for each dataset, left), with darker shading corresponding to more observations. The dashed line marks the
175 1:1 relationship. Points above the line indicate cases where U^A is smaller than the comparator metric, while points
176 below the line indicate cases where U^A is larger.

177 We first calculated four β -diversity metrics for all sample pairs in each dataset and
178 compared them to U^A (Fig. 2). The degree of concordance between U^A and other metrics was
179 highly context dependent. In the cooling water dataset, U^A closely tracked all three alternatives,
180 whereas in the remaining systems it diverged substantially. U^A also spanned a similar or wider

181 range of distances than the other metrics. For example, in the soil dataset BC^R and U^R occupied a
182 narrow range relative to the broad separation observed under U^A .

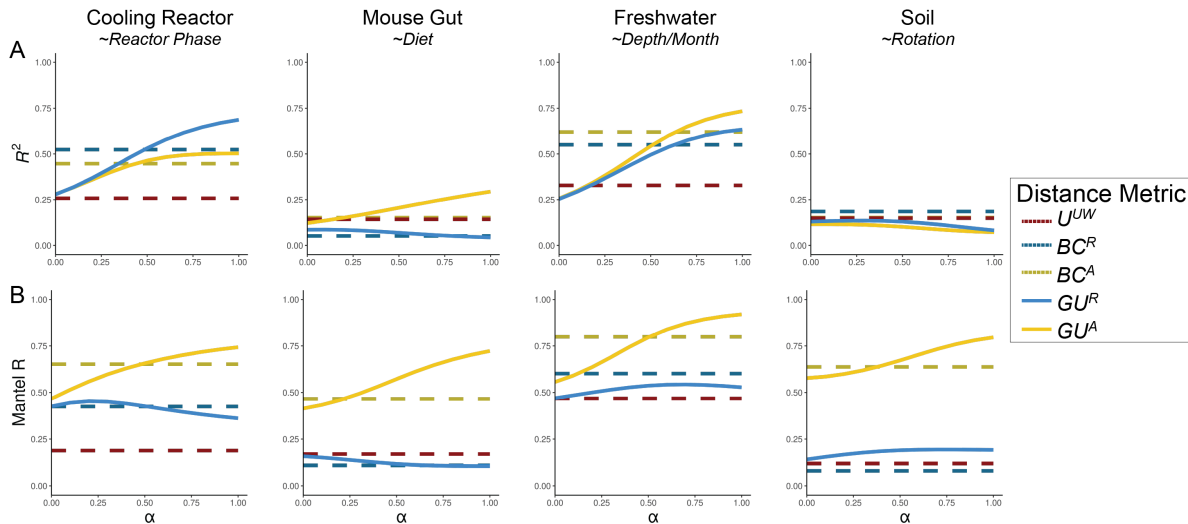
183 U^A generally reported distances that were similar to or greater than U^R , consistent with
184 the simulations shown in Fig. 1B. This reflects the ability of U^A to discern dissimilarity due to
185 differences in microbial load, even when community composition is conserved. In contrast, U^A
186 yielded distances that were similar to or lower than BC^A , again matching the simulated behavior
187 in Fig 1B. In these cases, phylogenetic proximity between abundant, closely-related ASVs leads
188 U^A to register greater similarity than BC^A .

189 Given these differences, we next quantified how well each metric discriminates among
190 categorical sample groups. For each dataset, we ran PERMANOVAs to measure the proportion
191 of variance (R^2) and statistical power (*pseudo-F*, *p*-value) attributable to group structure, using
192 groupings that were determined to be significant in the original publications. To evaluate how
193 strongly absolute abundance contributed to this discrimination, we also calculated GU^A across a
194 range of α values. The resulting R^2 values are displayed in Fig. 3A, with the corresponding
195 *pseudo-F* statistics and *p*-values provided in Fig. S2.

196 As in Fig. 2, the performance of each metric was strongly context dependent (Fig. 3A). In the
197 mouse gut and freshwater datasets, absolute-abundance-aware metrics (BC^A and GU^A) explained
198 the greatest proportion of variance (R^2), and R^2 generally increasing as α increased. In contrast,
199 relative metrics captured more variation in the cooling water dataset (again at higher α), and all
200 metrics explained comparably little variance in the soil dataset. Taken at face value, these trends
201 might suggest that higher α values typically improve group differentiation.

202 However, this comes with a major caveat: at high α values, GU^A becomes strongly
203 correlated with total cell count alone (Fig. 3B). Mantel tests confirmed that absolute-abundance
204 metrics are far more sensitive to differences in microbial load than their relative counterparts.
205 This behavior is intuitive, and to some extent desirable, because these metrics are designed to
206 detect changes in microbial load even when composition remains constant. Yet at $\alpha = 1$, U^A
207 approaches a proxy for sample absolute abundance itself. In ordination space (Fig. S3), this can
208 cause Axis 1 to correlate with absolute abundance and in some cases (freshwater and soil)
209 produces strong horseshoe effects [15], potentially distorting ecological interpretation. Beyond
210 tuning α to modify the influence of abundances, approaches such as NMDS or partial ordination
211 can also be used to modulate the sensitivity of ordinations to microbial load [16].

212



213 *Figure 3. Discriminatory performance of U^A and related metrics across four microbial systems.* (A) PERMANOVAs
 214 were used to quantify the percent variance (R^2) explained by predefined categorical groups (shown in italics beneath
 215 each dataset name), with 1,000 permutations. PERMANOVA results were evaluated across five metrics and, where
 216 applicable, across eleven α values (0-1 in 0.1 increments). For consistency with the original studies, only samples
 217 from Reactor cycle 1 were used for the cooling-water dataset, only stool samples for the mouse gut dataset, and only
 218 mature rhizosphere samples for the soil dataset (no samples were excluded from the freshwater dataset). (B) Mantel
 219 correlation (R) between each distance metric and the pairwise differences in absolute abundance (cell counts or 16S
 220 copy number), illustrating the degree to which each metric is driven by biomass differences.

221 We recommend calibrating α based on research goals, modulating this effect by using
 222 GU^A across a range of α rather than relying on U^A ($\alpha = 1$). Researchers should consider how
 223 much emphasis they want their dissimilarity metric to place on microbial load (Box 1). When
 224 biomass differences are central to the hypothesis being tested (for example, detecting
 225 cyanobacterial blooms), high α are recommended. In contrast, if microbial load is irrelevant or
 226 independent of the hypothesis in question, low α (or U^R) may be preferred; for example in the
 227 soil dataset, fine-scale differences in composition may be obscured by random variation in
 228 microbial load.

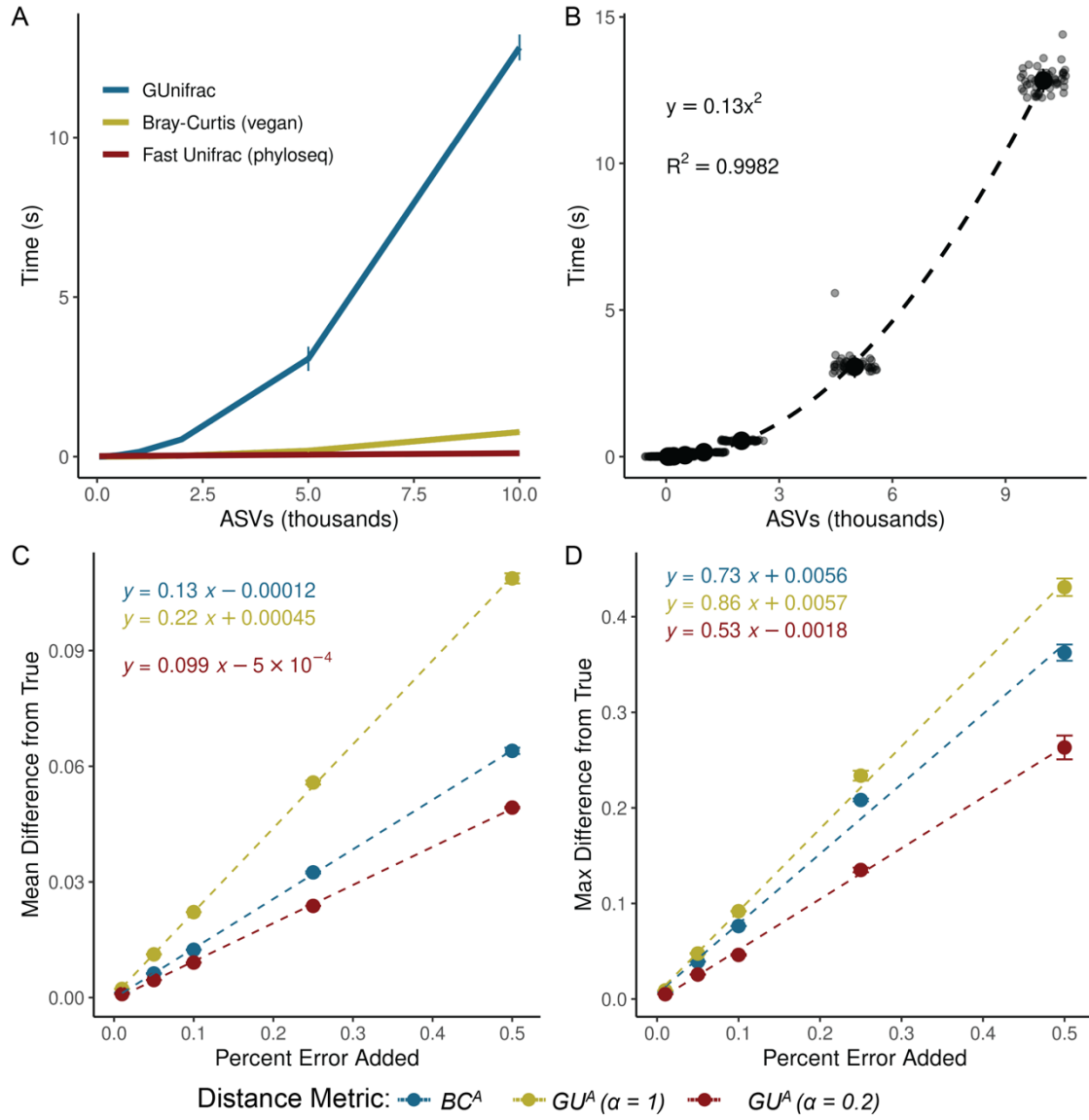
229 In many systems, microbial biomass is one piece of the story, likely correlated to other
 230 variables being tested. If the importance of microbial load in the system is unknown, one
 231 potential approach is to calculate correlations as demonstrated in Fig. 3B and select an α prior to
 232 any ordinations or statistical testing. Again, correlation to cell count is valuable and is intrinsic to
 233 absolute abundance-aware measures, especially when microbial load is relevant to the
 234 hypotheses being tested. Correlations to cell count in BC^A , an accepted approach in the literature,
 235 ranged from ~0.5 up to ~0.8. As a general recommendation from these analyses, we recommend
 236 α values in an intermediate range from 0.1 up to 0.6, wherein GU^A has similar correlation to cell
 237 count as BC^A .

238 Computational and Methodological Considerations

239 Applying GU^A in practice raises several considerations related to sequencing depth,
 240 richness, and computational cost. Both Bray-Curtis and UniFrac can be sensitive to sequencing
 241 depth because richness varies with read count [17–19]. To address this, we provide a workflow
 242 and accompanying code describing how we incorporated rarefaction into our own analyses (Box

243 2; available code). This approach minimizes sequencing-depth biases while preserving
 244 abundance scaling for downstream β -diversity analysis.

245 To explore the sensitivity of GU^A to rarefaction, we calculated GU^A using rarefaction at
 246 multiple sequencing depths, and used Mantel tests to assess the correlation between the rarefied
 247 GU^A distance matrices the non-rarefied control (Fig. S4; supplemental methods). GU^A was
 248 largely insensitive to rarefaction at high α values, even at depths as low as 250 reads per sample,
 249 but sensitivity increased as α decreased (Fig. S4). When rarefying to the minimum sequencing
 250 depth, as recommended, the effect of rarefaction was negligible (all Mantel's R > 0.95, Fig. S4).



251
 252 *Figure 4. GU^A requires more computational time but remains resilient to quantification error.* (A) Runtime for GU^A
 253 (GUniFrac package), U^R (FastUniFrac in the phyloseq package) and BC^A (vegan package) was benchmarked across
 254 50 iterations on a sub-sampled soil dataset (mature samples only) [10], using increasing ASV richness (50, 100, 200,
 255 500, 1,000, 2,000, 5,000, 10,000), with 10 samples and one α value per run (unweighted UniFrac is also calculated
 256 by default). Error bars represent standard deviation. (B) Quadratic relationship between GU^A computation time and
 257 ASV richness. Large center point represents median across 50 iterations, error bars (standard deviation) are too

258 small to be seen. All benchmarks were run on an AMD EPYC 64-core processor with 1014 GB system memory (R
259 v4.3.3, vegan v2.7-1, phyloseq v1.52.0, GUnifrac v1.8.1). (C-D) Sensitivity of GU^A ($\alpha = 1$ and 0.2) and BC^A to
260 measurement error was evaluated by adding random variation ($\pm 1\%$ to $\pm 50\%$; Supporting Methods) to 16S copy
261 number estimates in stool samples from the mouse gut dataset [3]. For each error level, 50 replicate matrices were
262 generated and compared to the original values. Panels reflect the (C) mean difference and (D) max difference
263 between the error-added metrics compared to the originals. Error bars represent the standard deviation of the average
264 mean and max difference across 50 iterations.

265 GU^A is slower to compute than both BC^A and U^R because it must traverse the phylogenetic
266 tree to calculate branch lengths for each iteration. Computational time of GU^A increases
267 quadratically with ASV number and is 10-20 times slower, though up to 50 times slower, than
268 BC^A (Fig. 4A-B). The number of samples or α values, however, have relatively little effect on
269 runtime (Fig. S5). For a dataset of 24,000 ASVs, computing on a single CPU is still reasonable
270 (1.4 minutes), but repeated rarefaction increases runtime substantially because branch lengths are
271 redundantly calculated with each iteration. Allowing branch-length objects to be cached or
272 incorporated directly into the GUnifrac workflow would considerably improve computational
273 efficiency.

274 We also evaluated the sensitivity of GU^A to measurement error in absolute abundance due
275 to uncertainty arising from the quantification of cell number or 16S copy number. To assess the
276 sensitivity of GU^A and BC^A to measurement error, we added random error to the 16S copy
277 number measurements from the mouse gut dataset, limiting our analyses to the stool samples
278 where copy numbers varied by an order of magnitude. Across 50 iterations, each copy number
279 could randomly vary by a given percentage of error in either direction. We re-calculated β -
280 diversity (BC^A and GU^A at $\alpha = 1$ and $\alpha = 0.2$) and compared these measurements to the original
281 dataset.

282 Introducing random variation into measured 16S copy number altered GU^A values only
283 modestly, and the effect was proportional to the magnitude of the added noise (Fig. 4C-D). At α
284 = 1, each 1% of quantification error introduced an average difference of 0.0022 in GU^A ; at $\alpha =$
285 0.2, GU^A was even less sensitive. Thus, moderate α values provide a balance between
286 interpretability and robustness to noise in absolute quantification. The max deviation from true
287 that added error could inflict on a given metric was also proportional (and always less) than the
288 magnitude of the error itself (Fig. 4D). A more rigorous approach to assessing error propagation
289 within these metrics, including mathematical proofs of the relationships estimated above, is
290 outside the scope of this paper but would be helpful.

291 GU^A was also insensitive to normalization approaches that adjust ASV abundances based
292 on the predicted 16S rRNA gene copy number (Fig. S6; supplemental methods). We used
293 PICRUSt2 (v2.6) to normalize ASV abundances within each dataset based on predicted 16S copy
294 number per genome, and then applied our standard rarefaction pipeline prior to GU^A calculation
295 (Box 2) [20, 21]. Correlations between GU^A distance matrices calculated from 16S copy number-
296 normalized datasets and those from the original, non-normalized datasets were consistently near
297 unity across all datasets (Mantel's R > 0.98, Fig. S6A), demonstrating that 16S copy number-
298 normalization had a negligible effect on GU^A . Sensitivity of GU^A to 16S copy number-
299 normalization generally decreased with increasing values of α in the cooling reactor, freshwater,
300 and soil datasets, but not in the mouse gut dataset (Fig. S6A). In the mouse gut dataset, several
301 highly abundant ASVs belonging to the genus *Faecalibaculum* had predicted 16S copy numbers
302 of seven copies per genome, explaining the relatively greater (though still weak) sensitivity of

303 this dataset to copy number-normalization (Fig. S6B). Finally, we note that 16S copy number-
304 normalization does not account for variation in genome copies per cell (ploidy), which can vary
305 across several orders of magnitude between species and growth phase [22–24].

306 Ecological Interpretation and conceptual significance

307 Absolute UniFrac reframes the interpretation of β -diversity by making biomass an explicit
308 ecological axis rather than an unmeasured or normalized-away quantity. Conventional UniFrac
309 captures composition and shared evolutionary history but implicitly invites interpretation as if it
310 also encodes differences on microbial load. By incorporating absolute abundance directly,
311 Absolute UniFrac helps to resolve this mismatch and restores alignment between ecological
312 hypotheses and the quantities represented in the metric. In this view, β -diversity becomes a three-
313 axis ecological measure, incorporating composition, phylogeny and biomass, rather than a two-
314 axis approximation. That said, the additional dimension of microbial load also increases the
315 complexity of applying and interpreting this metric.

316 There are many cases where the incorporation of absolute abundance allows microbial
317 ecologists to assess more realistic, ecologically-relevant differences in microbial communities,
318 especially when microbial load is mechanistically central. Outside of the datasets re-analyzed
319 here [3, 5, 9, 10]; the temporal development of the infant gut microbiome involves both a rise in
320 absolute abundance and compositional changes [6]; bacteriophage predation in wastewater
321 bioreactors can be understood only when microbial load is considered [25]; and antibiotic-driven
322 declines in specific swine gut taxa were missed using relative abundance approaches [26]. As β -
323 diversity metrics (and UniFrac specifically) remain central to microbial ecology, these findings
324 highlight how interpretation changes once biomass is incorporated. Broader adoption of absolute
325 abundance profiling will also depend on data availability. Few studies currently make absolute
326 quantification data publicly accessible, underscoring the need to deposit absolute measurements
327 alongside sequencing reads for reproducibility, ideally as metadata within SRA submissions.

328 While demonstrated here with 16S rRNA data, the approach should extend to other marker
329 genes or (meta)genomic features, provided absolute abundance estimates are available. In this
330 sense, GU^A offers a more ecologically grounded view of lineage turnover by jointly reflecting
331 variation in biomass and phylogenetic structure.

332 No single metric (or α in GU^A), however, is universally “best”. Each β -diversity metric
333 emphasizes a different dimension of community change. Researchers should therefore select
334 metrics based on the ecological quantity that is hypothesized to matter most (Box 1). Here, we
335 demonstrate not that GU^A outperforms other measures, but that it faithfully incorporates the three
336 axes of variation it was designed to incorporate: composition, phylogenetic similarity, and
337 absolute abundance (Fig. 1 and Fig. 2). As with any β -diversity analysis, interpretation requires
338 matching the metric to the ecological question at hand, and exploring sensitivity across different
339 metrics where appropriate [27]. By providing demonstrations and code for the application and
340 interpretation of U^A/GU^A , we hope to encourage the use of these metrics as a tool of microbial
341 ecology.

342 Conclusion

343 By explicitly incorporating absolute abundance, Absolute UniFrac shifts phylogenetic β -
344 diversity from a two-axis approximation to a three-axis ecological measure. This reframing

345 connects the metric to the underlying biological questions that motivate many microbiome
346 studies. As methods for quantifying microbial load continue to expand, the ability to interpret β -
347 diversity in a biomass-aware framework will become increasingly important for distinguishing
348 true ecological turnover from proportional change alone. In this way, Absolute UniFrac is not
349 simply an alternative distance metric but a tool for aligning statistical representation with
350 ecological mechanism.

351

352

353 **Box 1: β -diversity metrics should reflect the hypothesis being tested**

354 Absolute UniFrac is most informative when variation in microbial load is expected to carry
 355 ecological meaning rather than being a nuisance variable. The choice of α determines how
 356 strongly abundance differences influence the metric, and should therefore be selected based on
 357 the hypothesis, not by convention. In settings where biomass is central to the mechanism under
 358 study, higher α values appropriately foreground that signal, whereas in cases where load
 359 variation is incidental or confounding, lower α values maintain interpretability. Framing α as a
 360 hypothesis-driven choice repositions β -diversity from a default normalization step to an explicit
 361 ecological decision.

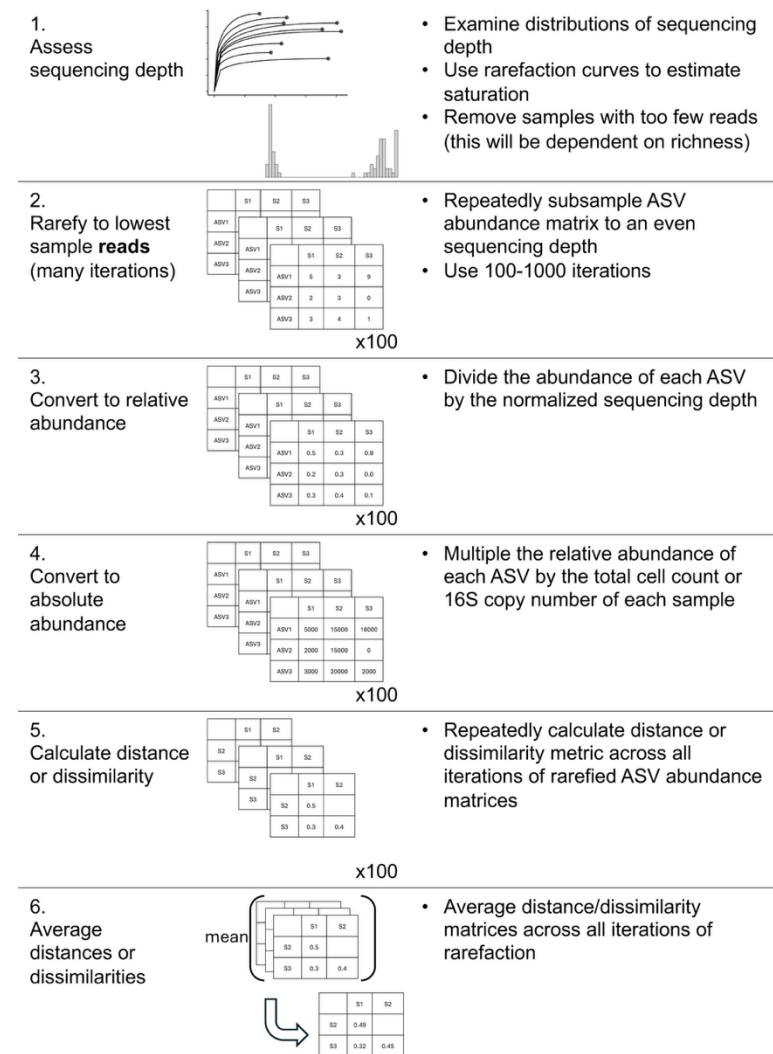
				Metric to Use	Hypothetical Example
Treat closely related lineages as similar?	Yes	How relevant is microbial load?	Central to hypothesis	$GU^A, \alpha > 0.5$	Cyanobacterial bloom, pathogen proliferation
			Relevant, but associated with other variables of interest	$GU^A, 0.1 < \alpha < 0.5$	Compositional shifts in response to nutrient addition
			Irrelevant	Dominant	$GU^R, \alpha > 0.5$
				Rare	$GU^R, \alpha < 0.5$
	No	Microbial load relevant?	Unknown	GU^A at multiple α	Random variation in microbial load obscured compositional shifts in soil communities
			Yes	BC^A	Strain turnover and proliferation in the infant gut
			No	BC^R	Temporal succession in chemostat

362

363

365 **Box 2: Rarefaction workflow for incorporating absolute abundance**

366 While we refrain from an in-depth
 367 analysis of rarefaction approaches,
 368 here we present our workflow for
 369 incorporating rarefaction alongside
 370 absolute abundance. First, samples
 371 were assessed for anomalously low
 372 read counts and discarded
 373 (sequencing blanks and controls
 374 were also removed). For rarefaction,
 375 each sample in the ASV table was
 376 subsampled to equal *sequencing*
 377 depth (# of reads) across 100
 378 iterations, creating 100 rarefied ASV
 379 tables. These tables were then
 380 converted to relative abundance by
 381 dividing each ASV's count by the
 382 equal sequencing depth (rounding
 383 was not performed). Then, each
 384 ASV's absolute abundance within a
 385 given sample was calculated by
 386 multiplying its relative abundance
 387 by that sample's total cell count or
 388 16S copy number. Methods to
 389 predict genomic 16S copy number
 390 for a given ASV were not used
 391 unless explicitly stated (Fig. S6) [20, 21]. Each distance/dissimilarity metric was then calculated
 392 across all 100 absolute-normalized ASV tables. The final distance/dissimilarity matrix was
 393 calculated by averaging all 100 iterations of each distance/dissimilarity calculation. Of note for
 394 future users: pruning the phylogenetic tree after rarefaction for each iteration is not necessary –
 395 ASVs removed from the dataset do not contribute nor change the calculated of UniFrac
 396 distances.



398

399

400 **References**

- 401 1. Gloor GB et al. Microbiome Datasets Are Compositional: And This Is Not Optional. *Front
Microbiol* 2017;8:2224. <https://doi.org/10.3389/fmicb.2017.02224>
- 402 2. Vandepitte D et al. Stool consistency is strongly associated with gut microbiota richness
403 and composition, enterotypes and bacterial growth rates. *Gut* 2016;65:57–62.
<https://doi.org/10.1136/gutjnl-2015-309618>
- 404 3. Barlow JT, Bogatyrev SR, Ismagilov RF. A quantitative sequencing framework for absolute
405 abundance measurements of mucosal and luminal microbial communities. *Nat Commun*
406 2020;11:2590. <https://doi.org/10.1038/s41467-020-16224-6>
- 407 4. Wang X et al. Current Applications of Absolute Bacterial Quantification in Microbiome
408 Studies and Decision-Making Regarding Different Biological Questions. *Microorganisms*
409 2021;9:1797. <https://doi.org/10.3390/microorganisms9091797>
- 410 5. Props R et al. Absolute quantification of microbial taxon abundances. *ISME J* 2017;11:584–
411 587. <https://doi.org/10.1038/ismej.2016.117>
- 412 6. Rao C et al. Multi-kingdom ecological drivers of microbiota assembly in preterm infants.
413 *Nature* 2021;591:633–638. <https://doi.org/10.1038/s41586-021-03241-8>
- 414 7. Bray JR, Curtis JT. An Ordination of the Upland Forest Communities of Southern
415 Wisconsin. *Ecological Monographs* 1957;27:326–349. <https://doi.org/10.2307/1942268>
- 416 8. Lozupone CA et al. Quantitative and Qualitative β Diversity Measures Lead to Different
417 Insights into Factors That Structure Microbial Communities. *Applied and Environmental
418 Microbiology* 2007;73:1576–1585. <https://doi.org/10.1128/AEM.01996-06>

- 421 9. Pendleton A, Wells M, Schmidt ML. Upwelling periodically disturbs the ecological
422 assembly of microbial communities in the Laurentian Great Lakes. 2025. bioRxiv, 2025. ,
423 2025.01.17.633667
- 424 10. Zhang K et al. Absolute microbiome profiling highlights the links among microbial
425 stability, soil health, and crop productivity under long-term sod-based rotation. *Biol Fertil
426 Soils* 2022;58:883–901. <https://doi.org/10.1007/s00374-022-01675-4>
- 427 11. Chen J et al. Associating microbiome composition with environmental covariates using
428 generalized UniFrac distances. *Bioinformatics* 2012;28:2106–2113.
429 <https://doi.org/10.1093/bioinformatics/bts342>
- 430 12. Lozupone C, Knight R. UniFrac: a New Phylogenetic Method for Comparing Microbial
431 Communities. *Applied and Environmental Microbiology* 2005;71:8228–8235.
432 <https://doi.org/10.1128/AEM.71.12.8228-8235.2005>
- 433 13. McMurdie PJ, Holmes S. phyloseq: An R package for reproducible interactive analysis and
434 graphics of microbiome census data. *PLoS ONE* 2013;8:e61217.
- 435 14. Bolyen E et al. Reproducible, interactive, scalable and extensible microbiome data science
436 using QIIME 2. *Nat Biotechnol* 2019;37:852–857. [https://doi.org/10.1038/s41587-019-0209-9](https://doi.org/10.1038/s41587-019-
437 0209-9)
- 438 15. Morton JT et al. Uncovering the Horseshoe Effect in Microbial Analyses. *mSystems*
439 2017;2:10.1128/msystems.00166-16. <https://doi.org/10.1128/msystems.00166-16>
- 440 16. Paliy O, Shankar V. Application of multivariate statistical techniques in microbial ecology.
441 *Molecular Ecology* 2016;25:1032–1057. <https://doi.org/10.1111/mec.13536>

- 442 17. Schloss PD. Evaluating different approaches that test whether microbial communities have
443 the same structure. *The ISME Journal* 2008;2:265–275.
444 <https://doi.org/10.1038/ismej.2008.5>
- 445 18. Fukuyama J et al. Comparisons of distance methods for combining covariates and
446 abundances in microbiome studies. Biocomputing 2012. WORLD SCIENTIFIC, 2011,
447 213–224.
- 448 19. McMurdie PJ, Holmes S. Waste Not, Want Not: Why Rarefying Microbiome Data Is
449 Inadmissible. *PLOS Computational Biology* 2014;10:e1003531.
450 <https://doi.org/10.1371/journal.pcbi.1003531>
- 451 20. Wright RJ, Langille MGI. PICRUSt2-SC: an update to the reference database used for
452 functional prediction within PICRUSt2. *Bioinformatics* 2025;41:btaf269.
453 <https://doi.org/10.1093/bioinformatics/btaf269>
- 454 21. Douglas GM et al. PICRUSt2 for prediction of metagenome functions. *Nat Biotechnol*
455 2020;38:685–688. <https://doi.org/10.1038/s41587-020-0548-6>
- 456 22. Griesse M, Lange C, Soppa J. Ploidy in cyanobacteria. *FEMS Microbiol Lett* 2011;323:124–
457 131. <https://doi.org/10.1111/j.1574-6968.2011.02368.x>
- 458 23. Mendell JE et al. Extreme polyploidy in a large bacterium. *Proceedings of the National
459 Academy of Sciences* 2008;105:6730–6734. <https://doi.org/10.1073/pnas.0707522105>
- 460 24. Pecoraro V et al. Quantification of Ploidy in Proteobacteria Revealed the Existence of
461 Monoploid, (Mero-)Oligoploid and Polyploid Species. *PLOS ONE* 2011;6:e16392.
462 <https://doi.org/10.1371/journal.pone.0016392>

- 463 25. Shapiro OH, Kushmaro A, Brenner A. Bacteriophage predation regulates microbial
464 abundance and diversity in a full-scale bioreactor treating industrial wastewater. *The ISME*
465 *Journal* 2010;4:327–336. <https://doi.org/10.1038/ismej.2009.118>
- 466 26. Wagner S et al. Absolute abundance calculation enhances the significance of microbiome
467 data in antibiotic treatment studies. *Front Microbiol* 2025;**16**.
468 <https://doi.org/10.3389/fmicb.2025.1481197>
- 469 27. Kers JG, Saccenti E. The Power of Microbiome Studies: Some Considerations on Which
470 Alpha and Beta Metrics to Use and How to Report Results. *Front Microbiol* 2022;**12**.
471 <https://doi.org/10.3389/fmicb.2021.796025>
- 472



1 **Interpreting UniFrac with Absolute Abundance: A Conceptual and Practical Guide**

2 Augustus Pendleton^{1*} & Marian L. Schmidt^{1*}

3 ¹Department of Microbiology, Cornell University, 123 Wing Dr, Ithaca, NY 14850, USA

4 **Corresponding Authors:** Augustus Pendleton: arp277@cornell.edu; Marian L. Schmidt:
5 marschmi@cornell.edu

6 **Author Contribution Statement:** Both authors contributed equally to the manuscript.

7 **Preprint servers:** This article was submitted to *bioRxiv* (doi: 10.1101/2025.07.18.665540) under
8 a CC-BY-NC-ND 4.0 International license.

9 **Keywords:** Microbial Ecology - Beta Diversity - Absolute Abundance - Bioinformatics -
10 UniFrac

11 **Data Availability:** All data and code used to produce the manuscript are available at
12 https://github.com/MarschmiLab/Pendleton_2025_Absolute_Unifrac_Paper, in addition to a
13 reproducible renv environment. All packages used for analysis are listed in Table S1.

14

15 **Abstract**

16 β -diversity is central to microbial ecology, yet commonly used metrics overlook changes in
17 microbial load (or “absolute abundance”), limiting their ability to detect ecologically meaningful
18 shifts. Popular for incorporating phylogenetic relationships, UniFrac distances currently default
19 to relative abundance and therefore omit important variation in microbial abundances. As
20 quantifying absolute abundance becomes more accessible, integrating this information into β -
21 diversity analyses is essential. Here, we introduce *Absolute UniFrac* (U^A), a variant of Weighted
22 UniFrac that incorporates absolute abundances. Using simulations and a reanalysis of four 16S
23 rRNA metabarcoding datasets (from a nuclear reactor cooling tank, the mouse gut, a freshwater
24 lake, and the peanut rhizosphere), we demonstrate that Absolute UniFrac captures microbial load,
25 composition, and phylogenetic relationships. While this can improve statistical power to detect
26 ecological shifts, we also find Absolute UniFrac can be strongly correlated to differences in cell
27 abundances alone. To balance these effects, we also incorporate absolute abundance into the
28 generalized extension (GU^A) that has a tunable, continuous ecological parameter (α) that
29 modulates the relative contribution of rare versus abundant lineages to β -diversity calculations.
30 Finally, we benchmark GU^A and show that although computationally slower than conventional
31 alternatives, GU^A is comparably sensitive to noise in load estimates compared to conventional
32 alternatives like Bray-Curtis dissimilarities, particularly at lower α . By coupling phylogeny,
33 composition, and microbial load, Absolute UniFrac integrates three dimensions of ecological
34 change, better equipping microbial ecologists to quantitatively compare microbial communities.

Deleted: that has a tunable α parameter to adjust the influence of abundance and composition.

Deleted: in

Deleted: realistic

39 **Main Text**

40 Microbial ecologists routinely compare communities using β -diversity metrics derived
41 from relative abundances. Yet this approach overlooks a critical ecological dimension: microbial
42 load. High-throughput sequencing produces compositional data, in which each taxon's
43 abundance is constrained by all others [1]. However, quantitative profiling studies show that cell
44 abundance, not only composition, can drive major community differences [2]. In low-biomass
45 samples, relying on relative abundance can allow contaminants to appear biologically
46 meaningful despite absolute counts too low for concern [3].

47 Sequencing-based microbiome studies therefore rely on relative abundance even when
48 the hypotheses of interest implicitly concern absolute changes in biomass. This creates a
49 mismatch between ecological framing (growth, bloom magnitude, pathogen proliferation,
50 disturbance recovery, or colonization pressure) and the information the β -diversity metric
51 encodes [4]. As a result, β -diversity is often treated as if it includes biomass, even when absolute
52 abundance is either not measured at all or is measured but excluded from the calculation (as in
53 conventional UniFrac). Many studies therefore test biomass-linked hypotheses using a metric
54 that normalizes biomass away [4]. A conceptual correction is needed in which β -diversity is
55 understood as variation along three axes: composition, phylogeny and absolute abundance.

56 Absolute microbial load measurements are now increasingly obtainable through flow
57 cytometry, qPCR, and genomic spike-ins, allowing biomass to be quantified alongside taxonomic
58 composition [4, 5]. These approaches improve detection of functionally relevant taxa and
59 mitigate the compositional constraints imposed by sequencing [1, 2]. Most studies that
60 incorporate absolute abundance counts currently rely on Bray-Curtis dissimilarity, which can
61 capture load but does not consider phylogenetic similarity [5–7]. Unifrac distances provide the
62 opposite strength, incorporating phylogeny but discarding absolute abundance, as they are
63 restricted to relative abundance data by construction [8]. This leaves no phylogenetically
64 informed β -diversity metric that operates on absolute counts, despite the fact that biomass is
65 central to many ecological hypotheses.

66 To evaluate the implications of incorporating absolute abundance into phylogenetic β -
67 diversity, we use both simulations and reanalysis of four 16S rRNA amplicon datasets. The
68 simulations use a simple four-taxon community with controlled abundance shifts to directly
69 compare both Bray-Curtis and UniFrac in their relative and absolute forms, illustrating how each
70 metric responds when abundance, composition, or evolutionary relatedness differ. We then
71 reanalyze four real-world datasets spanning nuclear reactor cooling water [5], the mouse gut [3],
72 a freshwater lake [9], and rhizosphere soil [10]. These differ widely in richness, biomass range,
73 and ecological context, allowing us to test when absolute abundance changes align with or
74 diverge from phylogenetic turnover. Together, these simulations and reanalyses provide the
75 empirical foundation for interpreting Absolute UniFrac relative to existing β -diversity measures
76 across the three axes of ecological difference: abundance, composition, and phylogeny.

77 We also extend Absolute UniFrac as was proposed by [11] to Generalized Absolute
78 UniFrac that incorporates a tunable ecological dimension, α , and evaluate its impact across
79 simulated and real-world datasets. As α increases, β -diversity is increasingly correlated with
80 differences in absolute abundance, allowing researchers to fine tune the relative weight their
81 analyses place on microbial load versus composition.

82 **Defining Absolute UniFrac**

83 The UniFrac distance was first introduced by Lozupone & Knight (2005) and has since
 84 become enormously popular as a measure of β -diversity within the field of microbial ecology
 85 [12]. A benefit of the UniFrac distance is that it considers phylogenetic information when
 86 estimating the distance between two communities. After first generating a phylogenetic tree
 87 representing species (or amplicon sequence variants, “ASVs”) from all samples, the UniFrac
 88 distance computes the fraction of branch-lengths which is *shared* between communities, relative
 89 to the total branch length represented in the tree. UniFrac can be both unweighted, in which only
 90 the incidence of species is considered, or weighted, wherein a branch’s contribution is weighted
 91 by the proportional abundance of taxa on that branch [8]. The Weighted UniFrac is derived:

$$92 \quad U^R = \frac{\sum_{i=1}^n b_i |p_i^a - p_i^b|}{\sum_{i=1}^n b_i (p_i^a + p_i^b)}$$

93 where the contribution of each branch length, b_i , is weighted by the difference in the relative
 94 abundance of all species (p_i) descended from that branch in sample a or sample b . Here, we
 95 denote this distance as U^R , for “Relative UniFrac”. Popular packages which calculate weighted
 96 UniFrac—including the diversity-lib QIIME plug-in and the R packages phyloseq and
 97 GUniFrac—run this normalization by default [11, 13, 14].

98 Importantly, U^R is most sensitive to changes in abundant lineages, which can sometimes
 99 obscure compositional differences driven by rare to moderately-abundant taxa [11]. To address
 100 this weakness, Chen et al. (2012) introduced the generalized UniFrac distance (GU^R), in which
 101 the impact of abundant lineages can be mitigated by decreasing the parameter α :

$$102 \quad GU^R = \frac{\sum_{i=1}^n b_i (p_i^a + p_i^b)^\alpha |p_i^a - p_i^b|}{\sum_{i=1}^n b_i (p_i^a + p_i^b)^\alpha}$$

103 where α ranges from 0 (close to Unweighted UniFrac) up to 1 (identical to U^R , above). However,
 104 if one wishes to use absolute abundances, both U^R and GU^R can be derived without normalizing
 105 to proportions:

$$106 \quad U^A = \frac{\sum_{i=1}^n b_i |c_i^a - c_i^b|}{\sum_{i=1}^n b_i (c_i^a + c_i^b)} \quad GU^A = \frac{\sum_{i=1}^n b_i (c_i^a + c_i^b)^\alpha |c_i^a - c_i^b|}{\sum_{i=1}^n b_i (c_i^a + c_i^b)^\alpha}$$

107 Where c_i^a and c_i^b denote for the absolute counts of species descending from branch b_i in
 108 communities a and b , respectively. We refer to these distances as *Absolute UniFrac* (U^A) and
 109 *Generalized Absolute UniFrac* (GU^A). Although substituting absolute for relative abundances is
 110 mathematically straightforward, to our knowledge there is no prior work that examines UniFrac
 111 in the context of absolute abundance, either conceptually or in application. Incorporating
 112 absolute abundances introduces a third axis of ecological variation: beyond differences in
 113 composition and phylogenetic similarity, U^A also captures divergence in microbial load. This
 114 makes interpretation of U^A nontrivial, particularly in complex microbiomes.

Deleted: we found

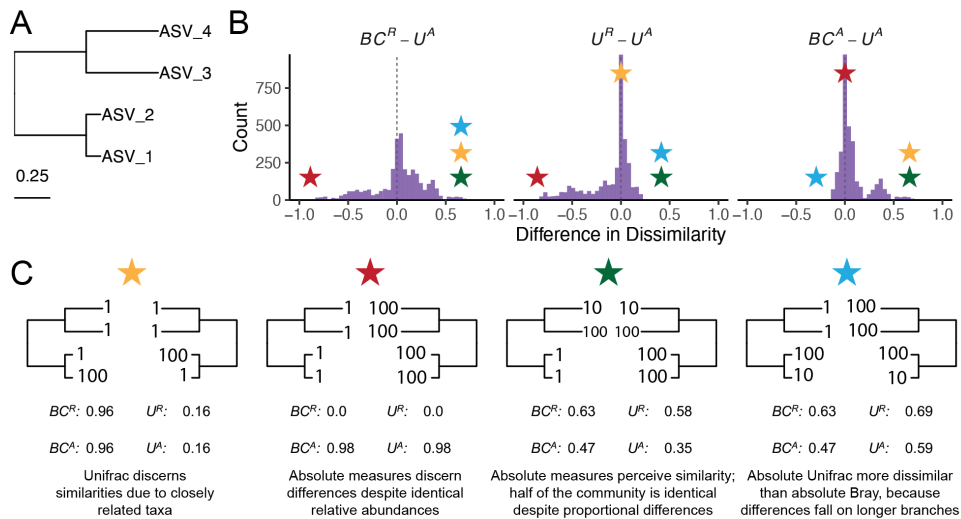
115 **Demonstrating β -diversity metrics’ behavior with a simple simulation**

117 To clarify how U^A behaves relative to existing β -diversity metrics, we first constructed a
118 simple four-taxon simulated community arranged in a small phylogeny (Fig. 1A). By varying the
119 absolute abundance of each ASV (1, 10, or 100), we generated 81 samples and 3,240 pairwise
120 comparisons. For each pair, we computed four dissimilarity metrics: Bray-Curtis with relative
121 abundance (BC^R), Bray-Curtis with absolute abundance (BC^A), Weighted UniFrac with relative
122 abundance (U^R), and Weighted UniFrac with absolute abundance (U^A). These comparisons help
123 to illustrate how each axis of ecological difference—abundance, composition, and phylogeny—is
124 expressed by the different metrics.

125 U^A does not consistently yield higher or lower distances compared to other metrics, but
126 instead varies depending on how abundance and phylogeny intersect (Fig. 1B). In the improbable
127 scenario that all branch lengths are equal, U^A is always less than or equal to BC^A (Fig. S1).
128 These comparisons emphasize that once branch lengths differ, incorporating phylogeny and
129 absolute abundance alters the structure of the distance space. The direction and magnitude of that
130 change depend on which branches carry the abundance shifts. U^A is also usually smaller than
131 BC^A and is more strongly correlated with BC^A (Pearson's $r = 0.82$, $p < 0.0001$) than with BC^R (r
132 = 0.41) and U^R ($r = 0.55$).

133 To better understand how these metrics diverge, we examined individual sample pairs
134 (Fig. 1C). Scenario 1 (gold star) illustrates the classic advantage of UniFrac: ASV_1 and ASV_2
135 are phylogenetically close, so U^R and U^A discern greater similarity between samples than BC^R
136 and BC^A , which ignore phylogenetic structure. Scenario 2 (red star) highlights a limitation of
137 relative metrics: two samples with identical relative composition but a 100-fold difference in
138 biomass appear identical to BC^R and U^R , but not to their absolute counterparts. In Scenario 3
139 (green star), incorporating absolute abundance decreases dissimilarity. BC^A and U^A are lower
140 than their relative counterparts because half the community is identical in absolute abundance,
141 even though their proportions differ. In contrast, Scenario 4 (blue star) shows that U^A can exceed
142 BC^A when abundance differences occur on long branches, amplifying phylogenetic dissimilarity.

143 These scenarios demonstrate that U^A integrates variation along three ecologically
144 relevant axes: composition, phylogenetic similarity, and microbial load, rather than isolating any
145 single dimension. Because a given U^A value can reflect multiple drivers of community change,
146 interpreting it requires downstream analyses to disentangle the relative contributions of these
147 three axes. To evaluate how this plays out in real systems we next reanalyzed four previously
148 published datasets spanning diverse microbial environments.

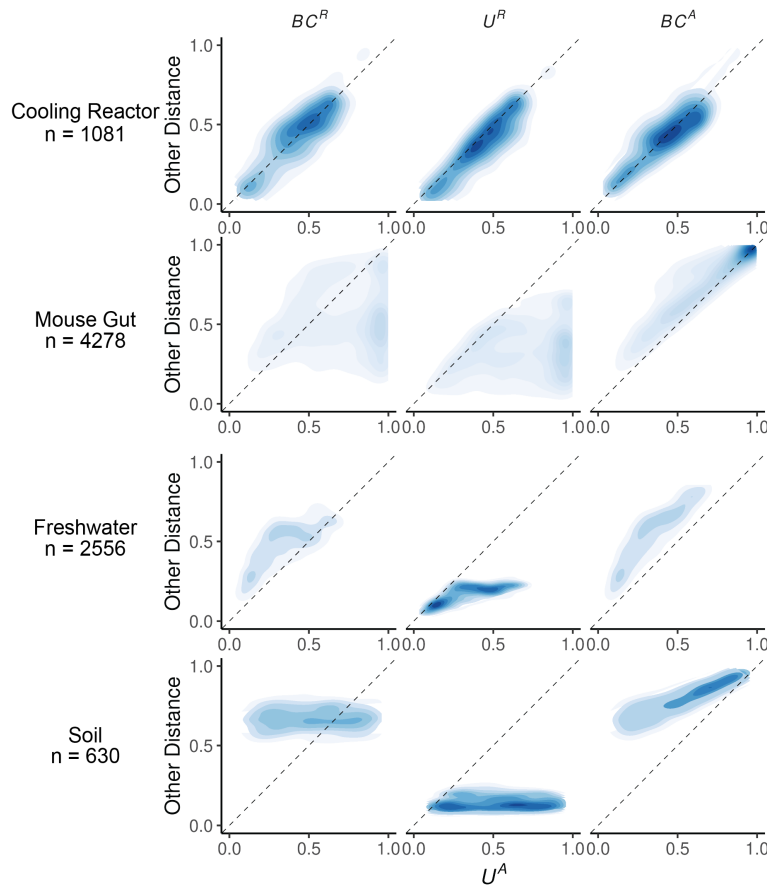


152 *Figure 1. Simulated communities reveal how absolute abundance affects phylogenetic and non-phylogenetic β -*
153 *diversity measures.* (A) We constructed a simple four-ASV community with a known phylogeny and generated all
154 permutations of each ASV having an absolute abundance of 1, 10, or 100, resulting in 81 unique communities and
155 3,240 pairwise comparisons. (B) Distributions of pairwise differences between weighted UniFrac using absolute
156 abundance (U^A) and three other metrics: Bray-Curtis using relative abundance (BC^R), weighted UniFrac using
157 relative abundance (U^R), and Bray-Curtis using absolute abundance (BC^A). (C) Illustrative sample pairs demonstrate
158 how absolute abundances and phylogenetic structure interact to increase or decrease dissimilarity across metrics.
159 Stars indicate where each scenario falls within the distributions shown in panel B. Actual values for each metric are
160 displayed beneath each scenario.

161 Application of Absolute UniFrac to Four Real-World Microbiome Datasets

162 To illustrate the sensitivity of U^A to both variation in composition and absolute
163 abundance, we re-analyzed four previously published datasets from diverse microbial systems.
164 These datasets included: (i) nuclear reactor cooling water sampled across three reactor cycle
165 phases [5]; (ii) the mouse gut sampled across multiple regions and between two diets [3]; (iii)
166 depth-stratified freshwater communities sampled across two months [9]; and (iv) peanut
167 rhizospheres under two crop rotation schemes (conventional rotation (CR) vs. sod-based rotation
168 (SBR)), plant maturities, and irrigation treatments [10]. Absolute abundance was quantified by
169 flow cytometry for the cooling water and freshwater datasets, droplet digital PCR for the mouse
170 gut, and by qPCR for the rhizosphere dataset. Together these span a wide range of richness—from as low as
171 215 ASVs in the cooling water to 24,000 ASVs in the soil—and microbial load—from as low as
172 4×10^5 cells/ml (cooling water) up to 2×10^{12} 16S rRNA copies/gram (mouse gut). Additional

173 details of the re-analysis workflow, including ASV generation and phylogenetic inference, are
 174 provided in the Supporting Methods.



175 *Figure 2. Absolute UniFrac (U^A) compared with other β -diversity metrics across four real microbial datasets.* Each
 176 panel shows pairwise sample distances for U^A (x-axis) against another metric (y-axis): Bray-Curtis using relative
 177 abundance (BC^R , first column), weighted UniFrac using relative abundances (U^R , second column), and Bray-Curtis
 178 using absolute abundances (BC^A , third column). Contours indicate the relative density of pairwise comparisons (n
 179 shown for each dataset, left), with darker shading corresponding to more observations. The dashed line marks the
 180 1:1 relationship. Points above the line indicate cases where U^A is smaller than the comparator metric, while points
 181 below the line indicate cases where U^A is larger.

182 We first calculated four β -diversity metrics for all sample pairs in each dataset and
 183 compared them to U^A (Fig. 2). The degree of concordance between U^A and other metrics was
 184 highly context dependent. In the cooling water dataset, U^A closely tracked all three alternatives,
 185 whereas in the remaining systems it diverged substantially. U^A also spanned a similar or wider

186 range of distances than the other metrics. For example, in the soil dataset BC^R and U^R occupied a
187 narrow range relative to the broad separation observed under U^A .

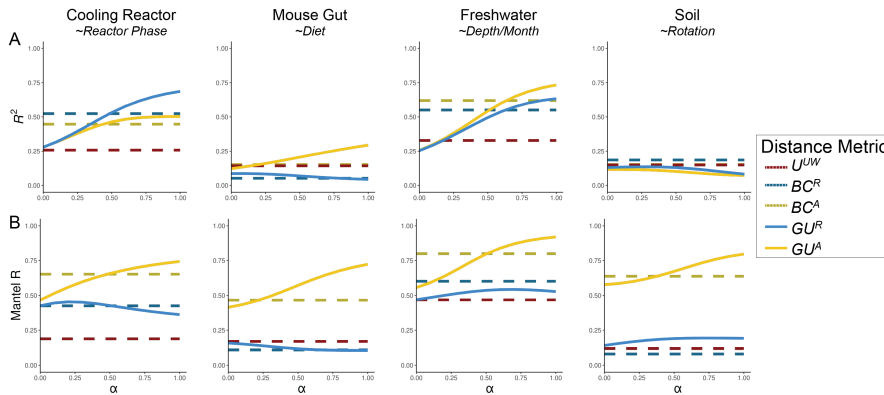
188 U^A generally reported distances that were similar to or greater than U^R , consistent with
189 the simulations shown in Fig. 1B. This reflects the ability of U^A to discern dissimilarity due to
190 differences in microbial load, even when community composition is conserved. In contrast, U^A
191 yielded distances that were similar to or lower than BC^A , again matching the simulated behavior
192 in Fig 1B. In these cases, phylogenetic proximity between abundant, closely-related ASVs leads
193 to register greater similarity than BC^A .

194 Given these differences, we next quantified how well each metric discriminates among
195 categorical sample groups. For each dataset, we ran PERMANOVAs to measure the proportion
196 of variance (R^2) and statistical power (*pseudo-F*, *p*-value) attributable to group structure, using
197 groupings that were determined to be significant in the original publications. To evaluate how
198 strongly absolute abundance contributed to this discrimination, we also calculated GU^A across a
199 range of α values. The resulting R^2 values are displayed in Fig. 3A, with the corresponding
200 *pseudo-F* statistics and *p*-values provided in Fig. S2.

201 As in Fig. 2, the performance of each metric was strongly context dependent (Fig. 3A). In the
202 mouse gut and freshwater datasets, absolute-abundance-aware metrics (BC^A and GU^A) explained
203 the greatest proportion of variance (R^2), and R^2 generally increasing as α increased. In contrast,
204 relative metrics captured more variation in the cooling water dataset (again at higher α), and all
205 metrics explained comparably little variance in the soil dataset. Taken at face value, these trends
206 might suggest that higher α values typically improve group differentiation.

207 However, this comes with a major caveat: at high α values, GU^A becomes strongly
208 correlated with total cell count alone (Fig. 3B). Mantel tests confirmed that absolute-abundance
209 metrics are far more sensitive to differences in microbial load than their relative counterparts.
210 This behavior is intuitive, and to some extent desirable, because these metrics are designed to
211 detect changes in microbial load even when composition remains constant. Yet at $\alpha = 1$, U^A
212 approaches a proxy for sample absolute abundance itself. In ordination space (Fig. S3), this can
213 cause Axis 1 to correlate with absolute abundance and in some cases (freshwater and soil)
214 produces strong horseshoe effects [15], potentially distorting ecological interpretation. Beyond
215 tuning α to modify the influence of abundances, approaches such as NMDS or partial ordination
216 can also be used to modulate the sensitivity of ordinations to microbial load [16].

Deleted: [16]



219 *Figure 3. Discriminatory performance of U^A and related metrics across four microbial systems.* (A) PERMANOVAs
 220 were used to quantify the percent variance (R^2) explained by predefined categorical groups (shown in italics beneath
 221 each dataset name), with 1,000 permutations. PERMANOVA results were evaluated across five metrics and, where
 222 applicable, across eleven α values (0-1 in 0.1 increments). For consistency with the original studies, only samples
 223 from Reactor cycle 1 were used for the cooling-water dataset, only stool samples for the mouse gut dataset, and only
 224 mature rhizosphere samples for the [soil dataset](#) ([no samples were excluded from the freshwater dataset](#)). (B) Mantel
 225 correlation (R) between each distance metric and the pairwise differences in absolute abundance (cell counts or 16S
 226 copy number), illustrating the degree to which each metric is driven by biomass differences.

227 We recommend calibrating α based on research goals, modulating this effect by using
 228 GU^A across a range of α rather than relying on U^A ($\alpha = 1$). Researchers should consider how
 229 much emphasis they want their dissimilarity metric to place on microbial load (Box 1). When
 230 biomass differences are central to the hypothesis being tested (for example, detecting
 231 cyanobacterial blooms), high α are recommended. In contrast, if microbial load is irrelevant or
 232 independent of the hypothesis in question, low α (or U^R) may be preferred; for example in the
 233 soil dataset, fine-scale differences in composition may be obscured by random variation in
 234 microbial load.

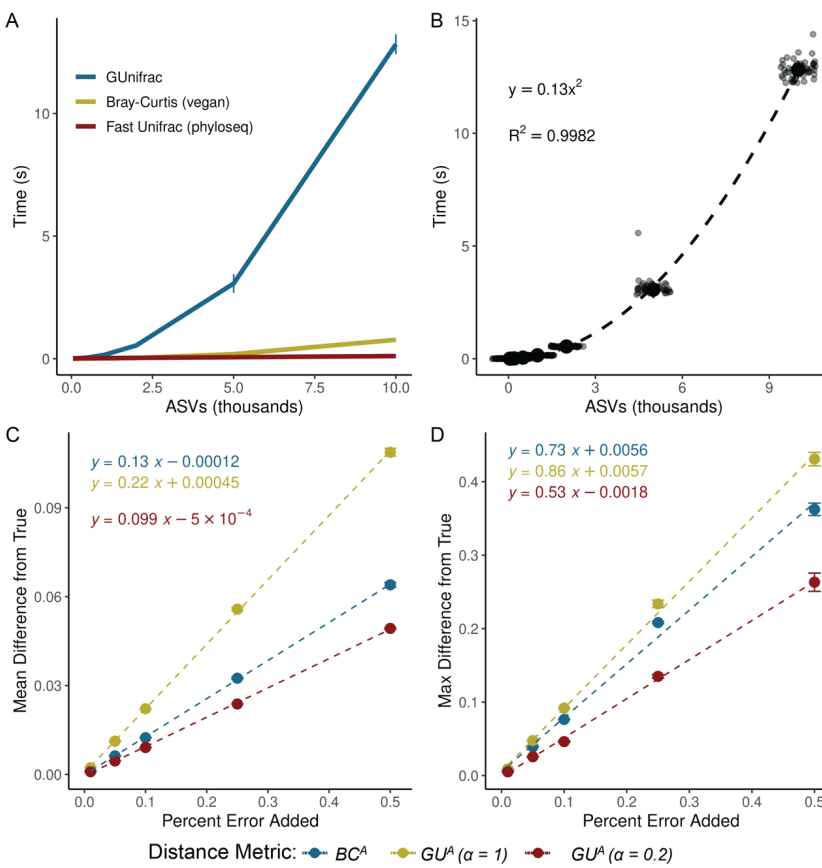
235 In many systems, microbial biomass is one piece of the story, likely correlated to other
 236 variables being tested. If the importance of microbial load in the system is unknown, one
 237 potential approach is to calculate correlations as demonstrated in Fig. 3B and select an α prior to
 238 any ordinations or statistical testing. Again, correlation to cell count is valuable and is intrinsic to
 239 absolute abundance-aware measures, especially when microbial load is relevant to the
 240 hypotheses being tested. Correlations to cell count in BC^A , an accepted approach in the literature,
 241 ranged from ~0.5 up to ~0.8. As a general recommendation from these analyses, we recommend
 242 α values in an intermediate range from 0.1 up to 0.6, wherein GU^A has similar correlation to cell
 243 count as BC^A .

244 Computational and Methodological Considerations

245 [Applying \$GU^A\$ in practice raises several considerations related to sequencing depth,](#)
 246 [richness, and computational cost. Both Bray-Curtis and UniFrac can be sensitive to sequencing](#)
 247 [depth because richness varies with read count \[17–19\]. To address this, we provide a workflow](#)
 248 [and accompanying code describing how we incorporated rarefaction into our own analyses \(Box](#)

249
250 2; available code). This approach minimizes sequencing-depth biases while preserving
abundance scaling for downstream β -diversity analysis.

251 To explore the sensitivity of GU^A to rarefaction, we calculated GU^A using rarefaction at
252 multiple sequencing depths, and used Mantel tests to assess the correlation between the rarefied
253 GU^A distance matrices the non-rarefied control (Fig. S4; supplemental methods). GU^A was
254 largely insensitive to rarefaction at high α values, even at depths as low as 250 reads per sample,
255 but sensitivity increased as α decreased (Fig. S4). When rarefying to the minimum sequencing
256 depth, as recommended, the effect of rarefaction was negligible (all Mantel's R > 0.95, Fig. S4).



257
258 *Figure 4. GU^A requires more computational time but remains resilient to quantification error. (A) Runtime for GU^A*
259 *(GUUnifrac package), U^R (FastUniFrac in the phyloseq package) and BC^A (vegan package) was benchmarked across*
260 *50 iterations on a sub-sampled soil dataset (mature samples only) [10], using increasing ASV richness (50, 100, 200,*
261 *500, 1,000, 2,000, 5,000, 10,000), with 10 samples and one α value per run (unweighted UniFrac is also calculated*
262 *by default). Error bars represent standard deviation. (B) Quadratic relationship between GU^A computation time and*
263 *ASV richness. Large center point represents median across 50 iterations, error bars (standard deviation) are too*

Deleted: Applying GU^A in practice raises several considerations related to sequencing depth, richness, and computational cost. Both Bray-Curtis and UniFrac can be sensitive to sequencing depth because richness varies with read count [17–19]. Methods to address these concerns, including rarefaction, remain debated and are challenging to benchmark rigorously [19]. We do not evaluate the sensitivity of U^A or GU^A to different rarefaction strategies here, but we do provide a workflow and code for how we incorporated rarefaction into our own analyses (Box 2 and available code). This approach minimizes sequencing-depth biases while preserving abundance scaling for downstream β -diversity analysis.

277 small to be seen. All benchmarks were run on an AMD EPYC 64-core processor with 1014 GB system memory (R
278 v4.3.3, vegan v2.7-1, phyloseq v1.52.0, GUnifrac v1.8.1). (C-D) Sensitivity of GU^A ($\alpha = 1$ and 0.2) and BC^A to
279 measurement error was evaluated by adding random variation ($\pm 1\%$ to $\pm 50\%$; Supporting Methods) to 16S copy
280 number estimates in stool samples from the mouse gut dataset [3]. For each error level, 50 replicate matrices were
281 generated and compared to the original values. Panels reflect the (C) mean difference and (D) max difference
282 between the error-added metrics compared to the originals. Error bars represent the standard deviation of the average
283 mean and max difference across 50 iterations.

Deleted:

284 GU^A is slower to compute than both BC^A and U^R because it must traverse the phylogenetic
285 tree to calculate branch lengths for each iteration. Computational time of GU^A increases
286 quadratically with ASV number and is 10-20 times slower, though up to 50 times slower, than
287 BC^A (Fig. 4A-B). The number of samples or α values, however, have relatively little effect on
288 runtime (Fig. S5). For a dataset of 24,000 ASVs, computing on a single CPU is still reasonable
289 (1.4 minutes), but repeated rarefaction increases runtime substantially because branch lengths are
290 redundantly calculated with each iteration. Allowing branch-length objects to be cached or
291 incorporated directly into the GUnifrac workflow would considerably improve computational
292 efficiency.

Deleted: Fig. S4

293 We also evaluated the sensitivity of GU^A to measurement error in absolute abundance due
294 to uncertainty arising from the quantification of cell number or 16S copy number. To assess the
295 sensitivity of GU^A and BC^A to measurement error, we added random error to the 16S copy
296 number measurements from the mouse gut dataset, limiting our analyses to the stool samples
297 where copy numbers varied by an order of magnitude. Across 50 iterations, each copy number
298 could randomly vary by a given percentage of error in either direction. We re-calculated β -
299 diversity (BC^A and GU^A at $\alpha = 1$ and $\alpha = 0.2$) and compared these measurements to the original
300 dataset.

Deleted: f

301 Introducing random variation into measured 16S copy number altered GU^A values only
302 modestly, and the effect was proportional to the magnitude of the added noise (Fig. 4C-D). At α
303 = 1, each 1% of quantification error introduced an average difference of 0.0022 in GU^A ; at $\alpha =$
304 0.2, GU^A was even less sensitive. Thus, moderate α values provide a balance between
305 interpretability and robustness to noise in absolute quantification. The max deviation from true
306 that added error could inflict on a given metric was also proportional (and always less) than the
307 magnitude of the error itself (Fig. 4D). A more rigorous approach to assessing error propagation
308 within these metrics, including mathematical proofs of the relationships estimated above, is
309 outside the scope of this paper but would be helpful.

310 GU^A was also insensitive to normalization approaches that adjust ASV abundances based
311 on the predicted 16S rRNA gene copy number (Fig. S6; supplemental methods). We used
312 PICRUSt2 (v2.6) to normalize ASV abundances within each dataset based on predicted 16S copy
313 number per genome, and then applied our standard rarefaction pipeline prior to GU^A calculation
314 (Box 2) [20, 21]. Correlations between GU^A distance matrices calculated from 16S copy number-
315 normalized datasets and those from the original, non-normalized datasets were consistently near
316 unity across all datasets (Mantel's R > 0.98, Fig. S6A), demonstrating that 16S copy number-
317 normalization had a negligible effect on GU^A . Sensitivity of GU^A to 16S copy number-
318 normalization generally decreased with increasing values of α in the cooling reactor, freshwater,
319 and soil datasets, but not in the mouse gut dataset (Fig. S6A). In the mouse gut dataset, several
320 highly abundant ASVs belonging to the genus *Faecalibaculum* had predicted 16S copy numbers
321 of seven copies per genome, explaining the relatively greater (though still weak) sensitivity of

325 this dataset to copy number-normalization (Fig. S6B). Finally, we note that 16S copy number-
326 normalization does not account for variation in genome copies per cell (ploidy), which can vary
327 across several orders of magnitude between species and growth phase [22–24].

328 Ecological Interpretation and conceptual significance

Deleted: [20, 21][22–24]

329 Absolute UniFrac reframes the interpretation of β -diversity by making biomass an explicit
330 ecological axis rather than an unmeasured or normalized-away quantity. Conventional UniFrac
331 captures composition and shared evolutionary history, but implicitly invites interpretation as if it
332 also encodes differences on microbial load. By incorporating absolute abundance directly,
333 Absolute UniFrac helps to resolve this mismatch and restores alignment between ecological
334 hypotheses and the quantities represented in the metric. In this view, β -diversity becomes a three-
335 axis ecological measure, incorporating composition, phylogeny and biomass, rather than a two-
336 axis approximation. That said, the additional dimension of microbial load also increases the
337 complexity of applying and interpreting this metric.

Deleted: ,

338 There are many cases where the incorporation of absolute abundance allows microbial
339 ecologists to assess more realistic, ecologically-relevant differences in microbial communities,
340 especially when microbial load is mechanistically central. Outside of the datasets re-analyzed
341 here [3, 5, 9, 10]; the temporal development of the infant gut microbiome involves both a rise in
342 absolute abundance and compositional changes [6]; bacteriophage predation in wastewater
343 bioreactors can be understood only when microbial load is considered [25]; and antibiotic-driven
344 declines in specific swine gut taxa were missed using relative abundance approaches [26]. As β -
345 diversity metrics (and UniFrac specifically) remain central to microbial ecology, these findings
346 highlight how interpretation changes once biomass is incorporated. Broader adoption of absolute
347 abundance profiling will also depend on data availability. Few studies currently make absolute
348 quantification data publicly accessible, underscoring the need to deposit absolute measurements
349 alongside sequencing reads for reproducibility, ideally as metadata within SRA submissions.

350 While demonstrated here with 16S rRNA data, the approach should extend to other marker
351 genes or (meta)genomic features, provided absolute abundance estimates are available. In this
352 sense, GU^A offers a more ecologically grounded view of lineage turnover by jointly reflecting
353 variation in biomass and phylogenetic structure.

354 No single metric (or α in GU^A), however, is universally “best”. Each β -diversity metric
355 emphasizes a different dimension of community change. Researchers should therefore select
356 metrics based on the ecological quantity that is hypothesized to matter most (Box 1). Here, we
357 demonstrate not that GU^A outperforms other measures, but that it faithfully incorporates the three
358 axes of variation it was designed to incorporate: composition, phylogenetic similarity, and
359 absolute abundance (Fig. 1 and Fig. 2). As with any β -diversity analysis, interpretation requires
360 matching the metric to the ecological question at hand, and exploring sensitivity across different
361 metrics where appropriate [27]. By providing demonstrations and code for the application and
362 interpretation of U^A/GU^A , we hope to encourage the use of these metrics as a tool of microbial
363 ecology.

364 Conclusion

365 By explicitly incorporating absolute abundance, Absolute UniFrac shifts phylogenetic β -
366 diversity from a two-axis approximation to a three-axis ecological measure. This reframing

369 connects the metric to the underlying biological questions that motivate many microbiome
370 studies. As methods for quantifying microbial load continue to expand, the ability to interpret β -
371 diversity in a biomass-aware framework will become increasingly important for distinguishing
372 true ecological turnover from proportional change alone. In this way, Absolute UniFrac is not
373 simply an alternative distance metric but a tool for aligning statistical representation with
374 ecological mechanism.

375

377 **Box 1: β -diversity metrics should reflect the hypothesis being tested**

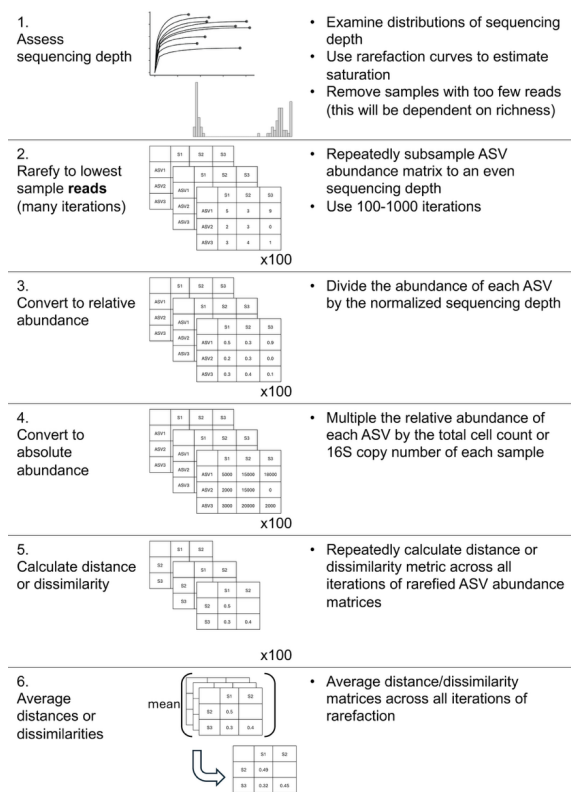
378 Absolute UniFrac is most informative when variation in microbial load is expected to carry
 379 ecological meaning rather than being a nuisance variable. The choice of α determines how
 380 strongly abundance differences influence the metric, and should therefore be selected based on
 381 the hypothesis, not by convention. In settings where biomass is central to the mechanism under
 382 study, higher α values appropriately foreground that signal, whereas in cases where load
 383 variation is incidental or confounding, lower α values maintain interpretability. Framing α as a
 384 hypothesis-driven choice repositions β -diversity from a default normalization step to an explicit
 385 ecological decision.

			Central to hypothesis			Metric to Use	Hypothetical Example	
Treat closely related lineages as similar?	Yes	How relevant is microbial load?	Relevant, but associated with other variables of interest			$GU^A, \alpha > 0.5$	Cyanobacterial bloom, pathogen proliferation	
			Irrelevant	Emphasize rare or dominant taxa?	Dominant	$GU^A, 0.1 < \alpha < 0.5$	Compositional shifts in response to nutrient addition	
					Rare	$GU^R, \alpha < 0.5$	Diet-associated microbiome shifts across hosts	
			Unknown			GU^A at multiple α	Tributary inputs of rare taxa	
	No	Microbial load relevant?	Yes			BC^A	Random variation in microbial load obscured compositional shifts in soil communities	
			No			BC^R	Strain turnover and proliferation in the infant gut	
						Temporal succession in chemostat		

389 Box 2: Rarefaction workflow for incorporating absolute abundance

While we refrain from an in-depth analysis of rarefaction approaches, here we present our workflow for incorporating rarefaction alongside absolute abundance. First, samples were assessed for anomalously low read counts and discarded (sequencing blanks and controls were also removed). For rarefaction, each sample in the ASV table was subsampled to equal *sequencing* depth (# of reads) across 100 iterations, creating 100 rarefied ASV tables. These tables were then converted to relative abundance by dividing each ASV's count by the equal sequencing depth (rounding was not performed). Then, each ASV's absolute abundance within a given sample was calculated by multiplying its relative abundance by that sample's total cell count or 16S copy number. Methods to predict genomic 16S copy number for a given ASV were not used unless explicitly stated (Fig. S6) [20].

415 unless explicitly stated (Fig. S6) [20, 21]. Each distance/dissimilarity metric was then calculated
416 across all 100 absolute-normalized ASV tables. The final distance/dissimilarity matrix was
417 calculated by averaging all 100 iterations of each distance/dissimilarity calculation. Of note for
418 future users: pruning the phylogenetic tree after rarefaction for each iteration is not necessary –
419 ASVs removed from the dataset do not contribute nor change the calculated UniFrac
420 distances.



422
423
424 **References**
425 1. Gloor GB et al. Microbiome Datasets Are Compositional: And This Is Not Optional. *Front*
426 *Microbiol* 2017;8:2224. <https://doi.org/10.3389/fmicb.2017.02224>
427 2. Vandeputte D et al. Stool consistency is strongly associated with gut microbiota richness
428 and composition, enterotypes and bacterial growth rates. *Gut* 2016;65:57–62.
429 <https://doi.org/10.1136/gutjnl-2015-309618>
430 3. Barlow JT, Bogatyrev SR, Ismagilov RF. A quantitative sequencing framework for absolute
431 abundance measurements of mucosal and luminal microbial communities. *Nat Commun*
432 2020;11:2590. <https://doi.org/10.1038/s41467-020-16224-6>
433 4. Wang X et al. Current Applications of Absolute Bacterial Quantification in Microbiome
434 Studies and Decision-Making Regarding Different Biological Questions. *Microorganisms*
435 2021;9:1797. <https://doi.org/10.3390/microorganisms9091797>
436 5. Props R et al. Absolute quantification of microbial taxon abundances. *ISME J* 2017;11:584–
437 587. <https://doi.org/10.1038/ismej.2016.117>
438 6. Rao C et al. Multi-kingdom ecological drivers of microbiota assembly in preterm infants.
439 *Nature* 2021;591:633–638. <https://doi.org/10.1038/s41586-021-03241-8>
440 7. Bray JR, Curtis JT. An Ordination of the Upland Forest Communities of Southern
441 Wisconsin. *Ecological Monographs* 1957;27:326–349. <https://doi.org/10.2307/1942268>
442 8. Lozupone CA et al. Quantitative and Qualitative β Diversity Measures Lead to Different
443 Insights into Factors That Structure Microbial Communities. *Applied and Environmental*
444 *Microbiology* 2007;73:1576–1585. <https://doi.org/10.1128/AEM.01996-06>

- 445 9. Pendleton A, Wells M, Schmidt ML. Upwelling periodically disturbs the ecological
446 assembly of microbial communities in the Laurentian Great Lakes. 2025. bioRxiv, 2025. ,
447 2025.01.17.633667
- 448 10. Zhang K et al. Absolute microbiome profiling highlights the links among microbial
449 stability, soil health, and crop productivity under long-term sod-based rotation. *Biol Fertil
450 Soils* 2022;58:883–901. <https://doi.org/10.1007/s00374-022-01675-4>
- 451 11. Chen J et al. Associating microbiome composition with environmental covariates using
452 generalized UniFrac distances. *Bioinformatics* 2012;28:2106–2113.
453 <https://doi.org/10.1093/bioinformatics/bts342>
- 454 12. Lozupone C, Knight R. UniFrac: a New Phylogenetic Method for Comparing Microbial
455 Communities. *Applied and Environmental Microbiology* 2005;71:8228–8235.
456 <https://doi.org/10.1128/AEM.71.12.8228-8235.2005>
- 457 13. McMurdie PJ, Holmes S. phyloseq: An R package for reproducible interactive analysis and
458 graphics of microbiome census data. *PLoS ONE* 2013;8:e61217.
- 459 14. Bolyen E et al. Reproducible, interactive, scalable and extensible microbiome data science
460 using QIIME 2. *Nat Biotechnol* 2019;37:852–857. [https://doi.org/10.1038/s41587-019-0209-9](https://doi.org/10.1038/s41587-019-
461 0209-9)
- 462 15. Morton JT et al. Uncovering the Horseshoe Effect in Microbial Analyses. *mSystems*
463 2017;2:10.1128/msystems.00166-16. <https://doi.org/10.1128/msystems.00166-16>
- 464 16. Paliy O, Shankar V. Application of multivariate statistical techniques in microbial ecology.
465 *Molecular Ecology* 2016;25:1032–1057. <https://doi.org/10.1111/mec.13536>

- 466 17. Schloss PD. Evaluating different approaches that test whether microbial communities have
467 the same structure. *The ISME Journal* 2008;2:265–275.
468 <https://doi.org/10.1038/ismej.2008.5>
- 469 18. Fukuyama J et al. Comparisons of distance methods for combining covariates and
470 abundances in microbiome studies. *Biocomputing 2012*. WORLD SCIENTIFIC, 2011,
471 213–224.
- 472 19. McMurdie PJ, Holmes S. Waste Not, Want Not: Why Rarefying Microbiome Data Is
473 Inadmissible. *PLOS Computational Biology* 2014;10:e1003531.
474 <https://doi.org/10.1371/journal.pcbi.1003531>
- 475 20. Wright RJ, Langille MGI. PICRUSt2-SC: an update to the reference database used for
476 functional prediction within PICRUSt2. *Bioinformatics* 2025;41:btaf269.
477 <https://doi.org/10.1093/bioinformatics/btaf269>
- 478 21. Douglas GM et al. PICRUSt2 for prediction of metagenome functions. *Nat Biotechnol*
479 2020;38:685–688. <https://doi.org/10.1038/s41587-020-0548-6>
- 480 22. Griesse M, Lange C, Soppa J. Ploidy in cyanobacteria. *FEMS Microbiol Lett* 2011;323:124–
481 131. <https://doi.org/10.1111/j.1574-6968.2011.02368.x>
- 482 23. Mendell JE et al. Extreme polyploidy in a large bacterium. *Proceedings of the National
483 Academy of Sciences* 2008;105:6730–6734. <https://doi.org/10.1073/pnas.0707522105>
- 484 24. Pecoraro V et al. Quantification of Ploidy in Proteobacteria Revealed the Existence of
485 Monoploid, (Mero-)Oligoploid and Polyploid Species. *PLOS ONE* 2011;6:e16392.
486 <https://doi.org/10.1371/journal.pone.0016392>

- 487 25. Shapiro OH, Kushmaro A, Brenner A. Bacteriophage predation regulates microbial
488 abundance and diversity in a full-scale bioreactor treating industrial wastewater. *The ISME
489 Journal* 2010;4:327–336. <https://doi.org/10.1038/ismej.2009.118>
- 490 26. Wagner S et al. Absolute abundance calculation enhances the significance of microbiome
491 data in antibiotic treatment studies. *Front Microbiol* 2025;**16**.
492 <https://doi.org/10.3389/fmicb.2025.1481197>
- 493 27. Kers JG, Saccenti E. The Power of Microbiome Studies: Some Considerations on Which
494 Alpha and Beta Metrics to Use and How to Report Results. *Front Microbiol* 2022;**12**.
495 <https://doi.org/10.3389/fmicb.2021.796025>
- 496

Click here to access/download

Supplemental Material

[**02_Pendleton_ISME_PostReview_SupportingInformation_Clean.pdf**](#)

We thank both the reviewers for their comments, which have greatly improved our manuscript. Note that line numbers correspond to the “TrackedChanges” version of the manuscript.

Reviewer #1:

I thank the authors for their simple but useful generalization of weighted UniFrac distances from relative to absolute abundances. The key concepts are explained well and the properties and utility of the metrics are demonstrated and compared to others through toy examples as well as a real-world dataset. In general, it would be interesting to see comparison of metrics for more than one example, but I guess there are strict limitations for a brief communication.

We thank the reviewer for their interest and encouragement. We have added substantially to the paper, including three additional data sets within our analysis, and an extended discussion (moving outside the constraints of the brief communication).

My only major comment is as follows:

To me, it seems trivial to replace relative abundance by absolute counts. Is this the first time this has been suggested or tried? Why isn't this already commonly used, given that suitable absolute abundance data is available?

This is a useful comment, and reflects what was to us as a surprising gap in the literature. We added additional information (line 172) to emphasize that these metrics have (to our knowledge) not been used, and that while its derivation and application are simple, the resulting interpretation is nontrivial:

“Although substituting absolute for relative abundances is mathematically straightforward, we found no prior work that examines UniFrac in the context of absolute abundance, either conceptually or in application. Incorporating absolute abundances introduces a third axis of ecological variation: beyond differences in composition and phylogenetic similarity, *UA* also captures divergence in microbial load. This makes interpretation of *UA* nontrivial, particularly in complex microbiomes.”

In addition to this, I have some minor comments that should be addressed before publication:

99: It's informative to see how UA relates to the other metrics for specific examples, but I find it hard to draw the conclusion that it "integrates ecological realism" just from the numbers that are provided. Could you substantiate this claim more? I am also curious about how interpretable UA is compared to other metrics?

We agree additional nuance is warranted. We've revised the text to reflect that UA is able to integrate multiple axes of important ecological variation, but that this integrative nature makes its interpretation more complex (line 176). We also think the addition of Box 1 helps connect a given distance metric to ecologically meaningful hypotheses. This revision provides a natural transition to the new analyses presented in our study, as follows:

Line 217: “These scenarios demonstrate that UA integrates variation along three ecologically relevant axes: composition, phylogenetic similarity, and microbial load, rather than isolating any single dimension. Because a given UA value can reflect multiple drivers of community change, interpreting it requires downstream analyses to disentangle the relative contributions of these three axes. To evaluate how this plays out in real systems we next reanalyzed four previously

published datasets spanning diverse microbial environments.”

Fig. 1B: Why aren't all the colored stars indicated in all the distributions in B?

We had originally added stars to the histograms sparingly, to draw attention to specific comparisons. However, stars have been added to all panels now.

Fig. 1C: Maybe I'm misunderstanding something, but aren't the first two trees in C (gold star) exactly the same, including the absolute abundances? In that case, shouldn't distances and dissimilarities be zero? Is there an error in the labels of one of the trees?

Thank you so much for catching this. We have corrected this mistake.

108: "UA yields greater or smaller dissimilarity than other metrics". UA and UR are the same in the first example.

We've clarified this sentence, so that it's not declarative of UA's relation to all other metrics, but reflects that these scenarios were chosen to illustrate specific cases where UA differs from at least one other metric in a conceptually important way. The new sentence reads:

Line 241: “Illustrative sample pairs demonstrate how absolute abundances and phylogenetic structure interact to increase or decrease dissimilarity across metrics.

142: "In this dataset, we recommend an intermediate of 0.5". This seems a bit arbitrary, and isn't the horseshoe still discernible for alpha = 0.5? Why do you recommend this value and how do you recommend choosing alpha in general?

Thank you for this question. We've updated our analyses to include a finer range of alphas (in steps of 0.1, rather than in 0.5), and included a new guidance for choosing an alpha, including Box 1 and lines 356-372, where we recommend tailoring alpha to better match the hypothesis being tested, exploring multiple levels of alpha, or choosing alpha *a priori* to modulate the impact of cell abundance on your diversity estimation using Mantel correlations.

158: "For example, the temporal development of the infant microbiome". It would have been interesting to see the different metrics applied to data for this example.

Unfortunately we were unable to access the necessary absolute abundance metadata to reanalyze that study. However, (as discussed elsewhere) we've incorporated analyses from three other datasets across a broad range of environments, richness, and evenness.

Reviewer #2

Pendleton and Schmidt introduce Absolute UniFrac, which is a modification of the Weighted UniFrac that replaces relative sequence values with microbial abundances derivable by, for example, qPCR, flow cytometry, or spike-in standards. As a result, the new metric varies depending on the intersection of abundance and phylogeny, so it stands to reason that a range of simulated and actual communities, combined with their known abundance values, should be used to demonstrate the value of this new metric. In this work, the authors use simulation data (four-ASVs with three different abundance values) and a re-analysis of a 66-sample Lake Ontario 16S rRNA ASV-clustered data set to demonstrate that this new metric can detect changes in biomass when composition remains constant. Code, data, and an R environment are provided for reproducibility. The study is attempting to fill a methodological gap for researchers who now routinely measure absolute counts yet still rely on relative β -diversity metrics.

We thank the reviewer for their thoughtful comments, which we feel have greatly improved the breadth and nuance of our paper.

Major Comments:

As indicated by your own words on lines 81-83, "These comparisons emphasize that incorporating phylogeny and absolute abundance reshapes distance estimates in nontrivial ways.", there are novel properties associated with the newly proposed Absolute Unifrac and Generalized Absolute Unifrac metrics. These need to be understood through more than a toy four-ASV phylogeny and one freshwater 16S data set. It would be ideal to at least test:

- 1) data derived from multiple environments (e.g. soils, human gut) that represent a range of species diversity and abundances,**

Thank you for this thoughtful suggestion. We agree and have now incorporated three additional datasets from a nuclear cooling reactor, mouse guts, and soils, which range widely in richness and abundances, which we feel has greatly improved the manuscript. While analyzing even more datasets would be preferable, we struggled to find many studies that (1) used modern sequencing strategies appropriate for ASV generation via dada2, (2) quantified absolute abundance and provided that data publicly, and (3) provided sequencing data via the SRA with sufficient metadata to link samples to experimental treatments.

- 2) data derived from other marker genes (e.g. 18S, cytochrome oxidase, etc.),**

We agree that more analyses would be useful to the field. Even though there is a cultural sense in the field that absolute abundance data is commonplace, it was already difficult to find studies with publicly available sequencing data, absolute abundance measurements, and high-quality metadata that were acceptable for reanalysis (see above). Studies incorporating absolute abundance are few and far between; studies with well-reported data are also unfortunately not as common as they should be, a point we now bring up in the manuscript itself. While one dataset we accessed (Zhang et al., peanut rhizosphere) did include fungal ITS sequences, we felt it wasn't additive to compare these results to the bacterial 16S results, without other ITS or 18S studies with which to compare it. That said, we found many examples where Weighted UniFrac was used on ITS or 18S datasets, reinforcing that the application of UniFrac distances is conceptually valid outside of 16S metabarcoding, specifically.

- 3) how the metric's validity is impacted by precision and error at the qPCR or flow-cytometry steps that could propagate into Absolute UniFrac distances,**

Great suggestion. We agree this is an important point. While a mathematical analysis of error propagation in UA vs. BCA is outside our expertise, we include simple simulations wherein error was added to absolute abundance measurements and GUA/BCA were re-calculated (Fig. 4C/D and corresponding results text, lines 485-501), demonstrating the general resilience of these methods to quantification error.

4) how this metric is impacted by rarefaction decisions.

On the last point re: rarefaction but also related to other points, the authors note on line 171 that "We also do not address...how sequencing depth influences richness estimates or whether rarefaction should be applied before calculating GUA.", but given that this is the paper introducing this new metric, and given that the metric directly relies on the abundance values which are the target of rarefaction efforts, it seems reasonable to expect guidance for readers on these steps. Likely, more testing is required to assess the impact of rarefaction on various data sets employing GUA, but this key effort would lead to the creation of the guide readers require to apply this new computation tool.

A thoughtful question! We agree that the effects of rarefaction are an important consideration, especially given that GUA directly incorporates abundance information. While a comprehensive evaluation of rarefaction strategies is beyond the scope of this paper, we have expanded the manuscript to provide conceptual guidance for readers. Specifically, we now include an overview of our rarefaction approach (Box 2) and publicly available implementation code (Github link). We hope this addition will help readers apply GUA in a consistent and transparent way and will motivate future studies explicitly evaluating how rarefaction influences this and related β -diversity metrics.

If such a guide could be produced to highlight the use cases for this new metric, it should be published. Ideally, everyone understands the conditions under which this metric outperforms other abundance-aware distances, of which there are many.

This was a thought-provoking comment that influenced how we frame our results. We now emphasize that no single metric necessarily “outperforms” another, as each metric captures distinct yet valid axes of variation among microbial communities. In the revised discussion (lines 529-538) and Box 1, we highlight that the choice and interpretation of a metric should be guided by the specific hypotheses being tested and whether they concern compositional similarity, phylogenetic relatedness, or absolute abundance differences. Taken together, the manuscript demonstrates that UA integrates all three dimensions and provides concrete examples of how its results can be interpreted in ecological context.

Minor Comments:

The simulation data used for the phylogeny is far too simple and does not demonstrate ecological realism. Related to the comments about testing more data sets, the in-silico data can certainly be more complex and robust as a test data set.

We appreciate this comment and agree that more complex simulations can be valuable for testing new metrics. However, the purpose of Fig. 1 is illustrative rather than analytical. The four-ASV community was intentionally designed as the simplest possible system to demonstrate, in a transparent way, how these metrics can respond to changes in composition, abundance, and phylogenetic relatedness. Increasing the complexity of this simulation would obscure these

conceptual contrasts. We believe the inclusion of multiple new empirical datasets now addresses this concern more directly, as they capture the same patterns observed in Fig. 1 while providing the ecological realism the reviewer highlights.

The data and code available to produce the manuscript are all seemingly shared in a public Github. Kudos to the authors for this important step in providing a reproducible analysis.

Thank you! We greatly appreciate this recognition, as ensuring full reproducibility is both deeply important and time-intensive. We have maintained this degree of reproducibility throughout all subsequent reanalyses as well.

If possible, for when data exists for a range of diverse data sets, it would be valuable to add any statements about computational efficiency relative to existing metrics (e.g. Bray-Curtis, Unifrac, Weighted Unifrac, etc.).

We appreciate this suggestion and have added new analyses to address it. Specifically, Fig. 4 and Fig. S4 now compare computational performances across metrics, showing that GUnifrac is slower than Bray-Curtis (vegan package) and Fast Unifrac (phyloseq package). We also provide recommendations for how future implementations of GUA, particularly across repeated rarefaction, could improve computational efficiency (line 482).

Figure S2 could indicate the sample labels, or at least a key for the labels, to aid in interpretability.

Thank you for this suggestion. As the manuscript now includes multiple datasets, we have restructured the figures and no longer include the original Fig. S2 and S3. The ordination based on UR (formerly Fig. S3) is now presented as a sub-panel in the new Fig. S3, which compares ordinations using UR and UA across all four datasets.

1 **Interpreting UniFrac with Absolute Abundance: A Conceptual and Practical Guide**

2 Augustus Pendleton^{1*} & Marian L. Schmidt^{1*}

3 ¹Department of Microbiology, Cornell University, 123 Wing Dr, Ithaca, NY 14850, USA

4 **Corresponding Authors:** Augustus Pendleton: arp277@cornell.edu; Marian L. Schmidt:
5 marschmi@cornell.edu

6 **Author Contribution Statement:** Both authors contributed equally to the manuscript.

7 **Preprint servers:** This article was submitted to *bioRxiv* (doi: 10.1101/2025.07.18.665540) under
8 a CC-BY-NC-ND 4.0 International license.

9 **Keywords:** Microbial Ecology - Beta Diversity - Absolute Abundance - Bioinformatics -
10 UniFrac

11 **Data Availability:** All data and code used to produce the manuscript are available at
12 https://github.com/MarschmiLab/Pendleton_2025_Absolute_Unifrac_Paper, in addition to a
13 reproducible renv environment. All packages used for analysis are listed in Table S1.

14

15 **Abstract**

16 β -diversity is central to microbial ecology, yet commonly used metrics overlook changes in
17 microbial load, limiting their ability to detect ecologically meaningful shifts. Popular for
18 incorporating phylogenetic relationships, UniFrac distances currently default to relative
19 abundance and therefore omit important variation in microbial abundances. As quantifying
20 absolute abundance becomes more accessible, integrating this information into β -diversity
21 analyses is essential. Here, we introduce *Absolute UniFrac* (U^A), a variant of Weighted UniFrac
22 that incorporates absolute abundances. Using simulations and a reanalysis of four 16S rRNA
23 metabarcoding datasets (from a nuclear reactor cooling tank, the mouse gut, a freshwater lake,
24 and the peanut rhizosphere), we demonstrate that Absolute UniFrac captures microbial load,
25 composition, and phylogenetic relationships. While this can improve statistical power to detect
26 ecological shifts, we also find Absolute UniFrac can be strongly correlated to differences in cell
27 abundances alone. To balance these effects, we also incorporate absolute abundance into the
28 generalized extension (GU^A) that has a tunable α parameter to adjust the influence of abundance
29 and composition. Finally, we benchmark GU^A and show that although computationally slower
30 than conventional alternatives, GU^A is comparably insensitive to realistic noise in load estimates
31 compared to conventional alternatives like Bray-Curtis dissimilarities, particularly at lower α . By
32 coupling phylogeny, composition, and microbial load, Absolute UniFrac integrates three
33 dimensions of ecological change, better equipping microbial ecologists to quantitatively compare
34 microbial communities.

35 **Main Text**

36 Microbial ecologists routinely compare communities using β -diversity metrics derived
37 from relative abundances. Yet this approach overlooks a critical ecological dimension: microbial
38 load. High-throughput sequencing produces compositional data, in which each taxon's
39 abundance is constrained by all others [1]. However, quantitative profiling studies show that cell
40 abundance, not only composition, can drive major community differences [2]. In low-biomass
41 samples, relying on relative abundance can allow contaminants to appear biologically
42 meaningful despite absolute counts too low for concern [3].

43 Sequencing-based microbiome studies therefore rely on relative abundance even when
44 the hypotheses of interest implicitly concern absolute changes in biomass. This creates a
45 mismatch between ecological framing (growth, bloom magnitude, pathogen proliferation,
46 disturbance recovery, or colonization pressure) and the information the β -diversity metric
47 encodes [4]. As a result, β -diversity is often treated as if it includes biomass, even when absolute
48 abundance is either not measured at all or is measured but excluded from the calculation (as in
49 conventional UniFrac). Many studies therefore test biomass-linked hypotheses using a metric
50 that normalizes biomass away [4]. A conceptual correction is needed in which β -diversity is
51 understood as variation along three axes: composition, phylogeny and absolute abundance.

52 Absolute microbial load measurements are now increasingly obtainable through flow
53 cytometry, qPCR, and genomic spike-ins, allowing biomass to be quantified alongside taxonomic
54 composition [4, 5]. These approaches improve detection of functionally relevant taxa and
55 mitigate the compositional constraints imposed by sequencing [1, 2]. Most studies that
56 incorporate absolute abundance counts currently rely on Bray-Curtis dissimilarity, which can
57 capture load but does not consider phylogenetic similarity [5–7]. Unifrac distances provide the
58 opposite strength, incorporating phylogeny but discarding absolute abundance, as they are
59 restricted to relative abundance data by construction [8]. This leaves no phylogenetically
60 informed β -diversity metric that operates on absolute counts, despite the fact that biomass is
61 central to many ecological hypotheses.

62 To evaluate the implications of incorporating absolute abundance into phylogenetic β -
63 diversity, we use both simulations and reanalysis of four 16S rRNA amplicon datasets. The
64 simulations use a simple four-taxon community with controlled abundance shifts to directly
65 compare both Bray-Curtis and UniFrac in their relative and absolute forms, illustrating how each
66 metric responds when abundance, composition, or evolutionary relatedness differ. We then
67 reanalyze four real-world datasets spanning nuclear reactor cooling water [5], the mouse gut [3],
68 a freshwater lake [9], and rhizosphere soil [10]. These differ widely in richness, biomass range,
69 and ecological context, allowing us to test when absolute abundance changes align with or
70 diverge from phylogenetic turnover. Together, these simulations and reanalyses provide the
71 empirical foundation for interpreting Absolute UniFrac relative to existing β -diversity measures
72 across the three axes of ecological difference: abundance, composition, and phylogeny.

73 We also extend Absolute UniFrac as was proposed by [11] to Generalized Absolute
74 UniFrac that incorporates a tunable ecological dimension, α , and evaluate its impact across
75 simulated and real-world datasets. As α increases, β -diversity is increasingly correlated with
76 differences in absolute abundance, allowing researchers to fine tune the relative weight their
77 analyses place on microbial load versus composition.

78 **Defining Absolute UniFrac**

79 The UniFrac distance was first introduced by Lozupone & Knight (2005) and has since
 80 become enormously popular as a measure of β -diversity within the field of microbial ecology
 81 [12]. A benefit of the UniFrac distance is that it considers phylogenetic information when
 82 estimating the distance between two communities. After first generating a phylogenetic tree
 83 representing species (or amplicon sequence variants, “ASVs”) from all samples, the UniFrac
 84 distance computes the fraction of branch-lengths which is *shared* between communities, relative
 85 to the total branch length represented in the tree. UniFrac can be both unweighted, in which only
 86 the incidence of species is considered, or weighted, wherein a branch’s contribution is weighted
 87 by the proportional abundance of taxa on that branch [8]. The Weighted UniFrac is derived:

$$88 \quad U^R = \frac{\sum_{i=1}^n b_i |p_i^a - p_i^b|}{\sum_{i=1}^n b_i (p_i^a + p_i^b)}$$

89 where the contribution of each branch length, b_i , is weighted by the difference in the relative
 90 abundance of all species (p_i) descended from that branch in sample a or sample b . Here, we
 91 denote this distance as U^R , for “Relative UniFrac”. Popular packages which calculate weighted
 92 UniFrac—including the diversity-lib QIIME plug-in and the R packages phyloseq and
 93 GUniFrac—run this normalization by default [11, 13, 14].

94 Importantly, U^R is most sensitive to changes in abundant lineages, which can sometimes
 95 obscure compositional differences driven by rare to moderately-abundant taxa [11]. To address
 96 this weakness, Chen et al. (2012) introduced the generalized UniFrac distance (GU^R), in which
 97 the impact of abundant lineages can be mitigated by decreasing the parameter α :

$$98 \quad GU^R = \frac{\sum_{i=1}^n b_i (p_i^a + p_i^b)^\alpha \left| \frac{p_i^a - p_i^b}{p_i^a + p_i^b} \right|}{\sum_{i=1}^n b_i (p_i^a + p_i^b)^\alpha}$$

99 where α ranges from 0 (close to Unweighted UniFrac) up to 1 (identical to U^R , above). However,
 100 if one wishes to use absolute abundances, both U^R and GU^R can be derived without normalizing
 101 to proportions:

$$102 \quad U^A = \frac{\sum_{i=1}^n b_i |c_i^a - c_i^b|}{\sum_{i=1}^n b_i (c_i^a + c_i^b)} \quad GU^A = \frac{\sum_{i=1}^n b_i (c_i^a + c_i^b)^\alpha \left| \frac{c_i^a - c_i^b}{c_i^a + c_i^b} \right|}{\sum_{i=1}^n b_i (c_i^a + c_i^b)^\alpha}$$

103 Where c_i^a and c_i^b denote for the absolute counts of species descending from branch b_i in
 104 communities a and b , respectively. We refer to these distances as *Absolute UniFrac* (U^A) and
 105 *Generalized Absolute UniFrac* (GU^A). Although substituting absolute for relative abundances is
 106 mathematically straightforward, we found no prior work that examines UniFrac in the context of
 107 absolute abundance, either conceptually or in application. Incorporating absolute abundances
 108 introduces a third axis of ecological variation: beyond differences in composition and
 109 phylogenetic similarity, U^A also captures divergence in microbial load. This makes interpretation
 110 of U^A nontrivial, particularly in complex microbiomes.

111 **Demonstrating β -diversity metrics’ behavior with a simple simulation**

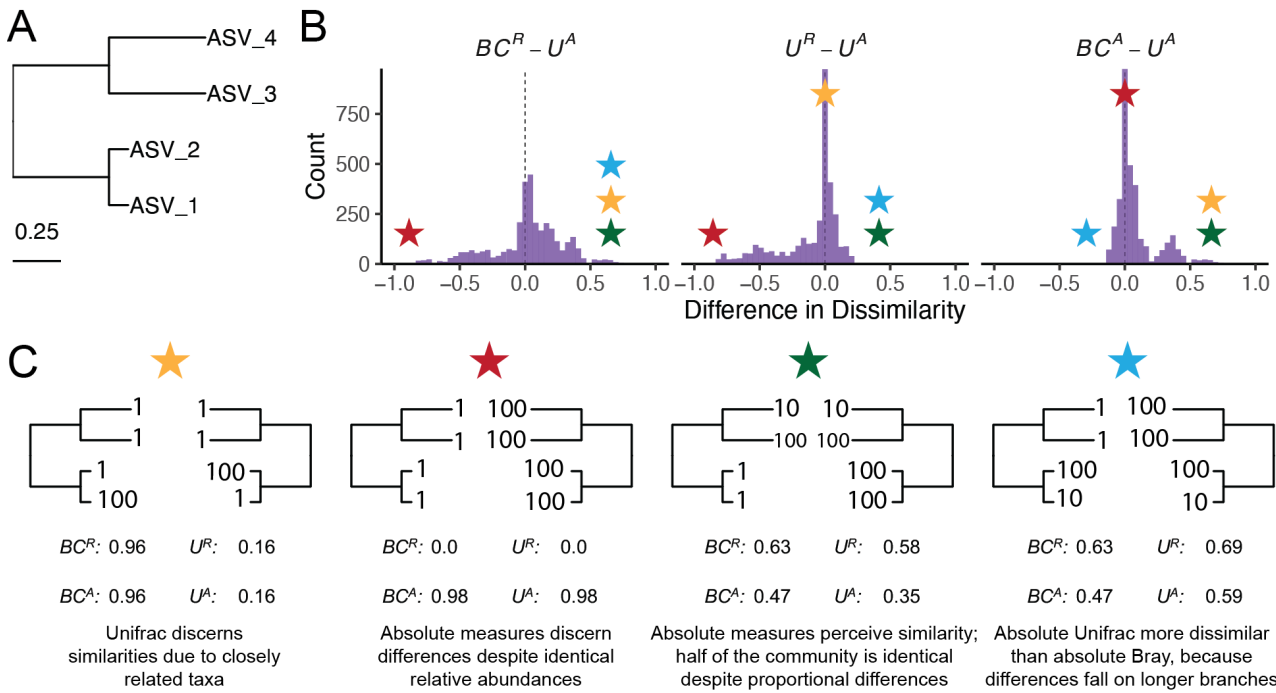
To clarify how U^A behaves relative to existing β -diversity metrics, we first constructed a simple four-taxon simulated community arranged in a small phylogeny (Fig. 1A). By varying the absolute abundance of each ASV (1, 10, or 100), we generated 81 samples and 3,240 pairwise comparisons. For each pair, we computed four dissimilarity metrics: Bray-Curtis with relative abundance (BC^R), Bray-Curtis with absolute abundance (BC^A), Weighted UniFrac with relative abundance (U^R), and Weighted UniFrac with absolute abundance (U^A). These comparisons help to illustrate how each axis of ecological difference—abundance, composition, and phylogeny—is expressed by the different metrics.

U^A does not consistently yield higher or lower distances compared to other metrics, but instead varies depending on how abundance and phylogeny intersect (Fig. 1B). In the improbable scenario that all branch lengths are equal, U^A is always less than or equal to BC^A (Fig. S1). These comparisons emphasize that once branch lengths differ, incorporating phylogeny and absolute abundance alters the structure of the distance space. The direction and magnitude of that change depend on which branches carry the abundance shifts. U^A is also usually smaller than BC^A and is more strongly correlated with BC^A (Pearson's $r = 0.82$, $p < 0.0001$) than with BC^R ($r = 0.41$) and U^R ($r = 0.55$).

To better understand how these metrics diverge, we examined individual sample pairs (Fig. 1C). Scenario 1 (gold star) illustrates the classic advantage of UniFrac: ASV_1 and ASV_2 are phylogenetically close, so U^R and U^A discern greater similarity between samples than BC^R and BC^A , which ignore phylogenetic structure. Scenario 2 (red star) highlights a limitation of relative metrics: two samples with identical relative composition but a 100-fold difference in biomass appear identical to BC^R and U^R , but not to their absolute counterparts. In Scenario 3 (green star), incorporating absolute abundance decreases dissimilarity. BC^A and U^A are lower than their relative counterparts because half the community is identical in absolute abundance, even though their proportions differ. In contrast, Scenario 4 (blue star) shows that U^A can exceed BC^A when abundance differences occur on long branches, amplifying phylogenetic dissimilarity.

These scenarios demonstrate that U^A integrates variation along three ecologically relevant axes: composition, phylogenetic similarity, and microbial load, rather than isolating any single dimension. Because a given U^A value can reflect multiple drivers of community change, interpreting it requires downstream analyses to disentangle the relative contributions of these three axes. To evaluate how this plays out in real systems we next reanalyzed four previously published datasets spanning diverse microbial environments.

144
145
146

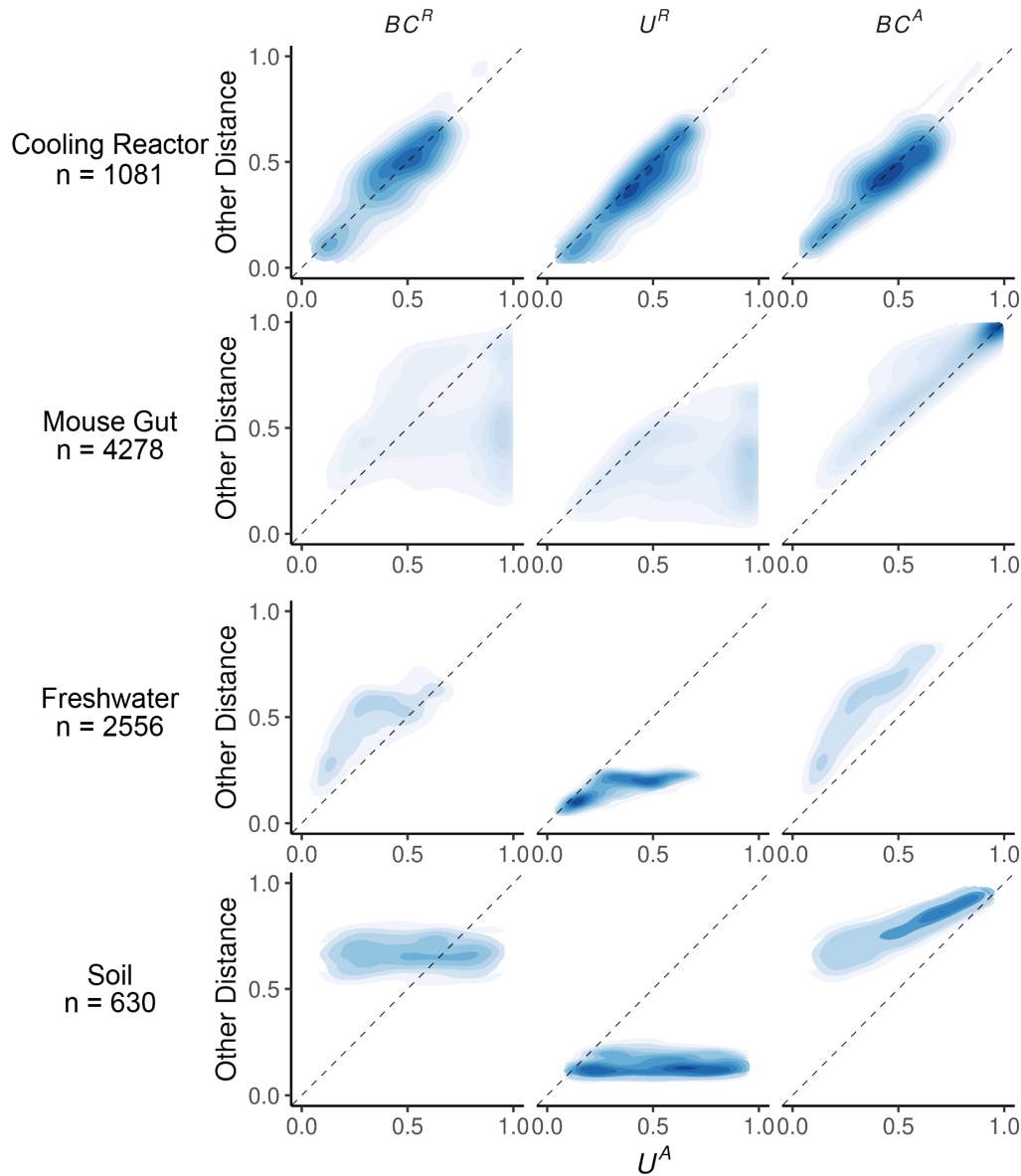


147 *Figure 1. Simulated communities reveal how absolute abundance affects phylogenetic and non-phylogenetic β -*
148 *diversity measures.* (A) We constructed a simple four-ASV community with a known phylogeny and generated all
149 permutations of each ASV having an absolute abundance of 1, 10, or 100, resulting in 81 unique communities and
150 3,240 pairwise comparisons. (B) Distributions of pairwise differences between weighted UniFrac using absolute
151 abundance (U^A) and three other metrics: Bray-Curtis using relative abundance (BC^R), weighted UniFrac using
152 relative abundance (UR), and Bray-Curtis using absolute abundance (BC^A). (C) Illustrative sample pairs demonstrate
153 how absolute abundances and phylogenetic structure interact to increase or decrease dissimilarity across metrics.
154 Stars indicate where each scenario falls within the distributions shown in panel B. Actual values for each metric are
155 displayed beneath each scenario.

156 Application of Absolute UniFrac to Four Real-World Microbiome Datasets

157 To illustrate the sensitivity of U^A to both variation in composition and absolute
158 abundance, we re-analyzed four previously published datasets from diverse microbial systems.
159 These datasets included: (i) nuclear reactor cooling water sampled across three reactor cycle
160 phases [5]; (ii) the mouse gut sampled across multiple regions and between two diets [3]; (iii)
161 depth-stratified freshwater communities sampled across two months [9]; and (iv) peanut
162 rhizospheres under two crop rotation schemes (conventional rotation (CR) vs. sod-based rotation
163 (SBR)), plant maturities, and irrigation treatments [10]. Absolute abundance was quantified by
164 flow cytometry for the cooling water and freshwater datasets, droplet digital PCR for the mouse
165 gut, and by qPCR for the rhizosphere dataset. Together these span a wide range of richness—from
166 215 ASVs in the cooling water to 24,000 ASVs in the soil—and microbial load—from as low as
167 4×10^5 cells/ml (cooling water) up to 2×10^{12} 16S rRNA copies/gram (mouse gut). Additional

168 details of the re-analysis workflow, including ASV generation and phylogenetic inference, are
169 provided in the Supporting Methods.



170 *Figure 2. Absolute UniFrac (U^A) compared with other β -diversity metrics across four real microbial datasets.* Each
171 panel shows pairwise sample distances for U^A (x-axis) against another metric (y-axis): Bray-Curtis using relative
172 abundance (BC^R , first column), weighted UniFrac using relative abundances (U^R , second column), and Bray-curtis
173 using absolute abundances (BC^A , third column). Contours indicate the relative density of pairwise comparisons (n
174 shown for each dataset, left), with darker shading corresponding to more observations. The dashed line marks the
175 1:1 relationship. Points above the line indicate cases where U^A is smaller than the comparator metric, while points
176 below indicate cases where U^A is larger.

177 We first calculated four β -diversity metrics for all sample pairs in each dataset and
178 compared them to U^A (Fig. 2). The degree of concordance between U^A and other metrics was
179 highly context dependent. In the cooling water dataset, U^A closely tracked all three alternatives,
180 whereas in the remaining systems it diverged substantially. U^A also spanned a similar or wider

181 range of distances than the other metrics. For example, in the soil dataset BC^R and U^R occupied a
182 narrow range relative to the broad separation observed under U^A .

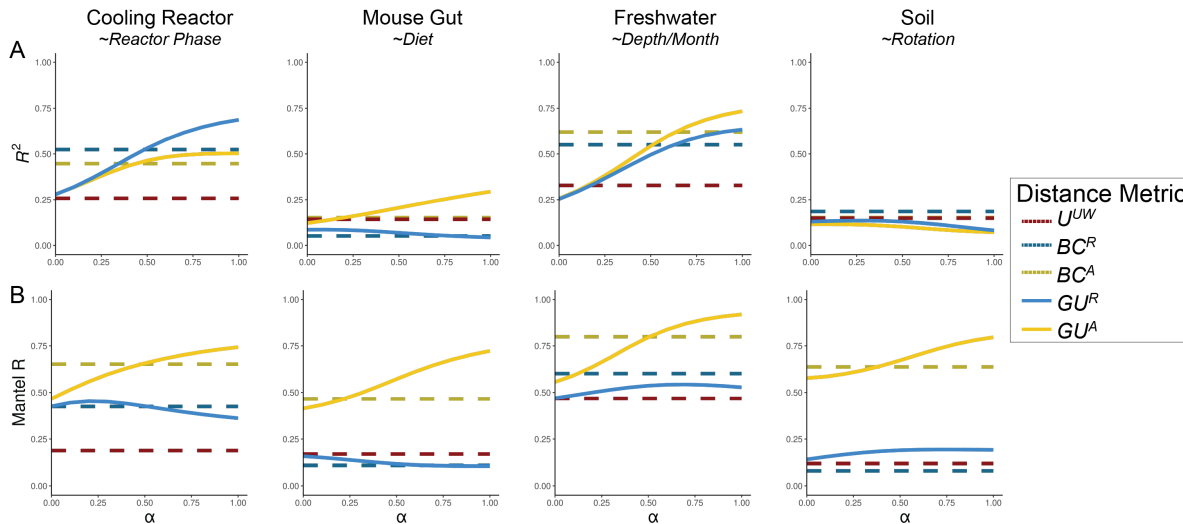
183 U^A generally reported distances that were similar to or greater than U^R , consistent with
184 the simulations shown in Fig. 1B. This reflects the ability of U^A to discern dissimilarity due to
185 differences in microbial load, even when community composition is conserved. In contrast, U^A
186 yielded distances that were similar to or lower than BC^A , again matching the simulated behavior
187 in Fig 1B. In these cases, phylogenetic proximity between abundant, closely-related ASVs leads
188 U^A to register greater similarity than BC^A .

189 Given these differences, we next quantified how well each metric discriminates among
190 categorical sample groups. For each dataset, we ran PERMANOVAs to measure the proportion
191 of variance (R^2) and statistical power (*pseudo-F*, *p*-value) attributable to group structure, using
192 groupings that were determined to be significant in the original publications. To evaluate how
193 strongly absolute abundance contributed to this discrimination, we also calculated GU^A across a
194 range of α values. The resulting R^2 values are displayed in Fig. 3A, with the corresponding
195 *pseudo-F* statistics and *p*-values provided in Fig. S2.

196 As in Fig. 2, the performance of each metric was strongly context dependent (Fig. 3A). In the
197 mouse gut and freshwater datasets, absolute-abundance-aware metrics (BC^A and GU^A) explained
198 the greatest proportion of variance (R^2), and R^2 generally increasing as α increased. In contrast,
199 relative metrics captured more variation in the cooling water dataset (again at higher α), and all
200 metrics explained comparably little variance in the soil dataset. Taken at face value, these trends
201 might suggest that higher α values typically improve group differentiation.

202 However, this comes with a major caveat: at high α values, GU^A becomes strongly
203 correlated with total cell count alone (Fig. 3B). Mantel tests confirmed that absolute-abundance
204 metrics are far more sensitive to differences in microbial load than their relative counterparts.
205 This behavior is intuitive, and to some extent desirable, because these metrics are designed to
206 detect changes in microbial load even when composition remains constant. Yet at $\alpha = 1$, U^A
207 approaches a proxy for sample absolute abundance itself. In ordination space (Fig. S3), this can
208 cause Axis 1 to correlate with absolute abundance and in some cases (freshwater and soil)
209 produces strong horseshoe effects [15], potentially distorting ecological interpretation.

210



211 *Figure 3. Discriminatory performance of U^A and related metrics across four microbial systems.* (A) PERMANOVAs
212 were used to quantify the percent variance (R^2) explained by predefined categorical groups (shown in italics beneath
213 each dataset name), with 1,000 permutations. PERMANOVA results were evaluated across five metrics and, where
214 applicable, across eleven α values (0-1 in 0.1 increments). For consistency with the original studies, only samples
215 from Reactor cycle 1 were used for the cooling-water dataset, only stool samples for the mouse gut dataset, and only
216 mature rhizosphere samples for the dataset. (B) Mantel correlation (R) between each distance metric and the
217 pairwise differences in absolute abundance (cell counts or 16S copy number), illustrating the degree to which each
218 metric is driven by biomass differences.

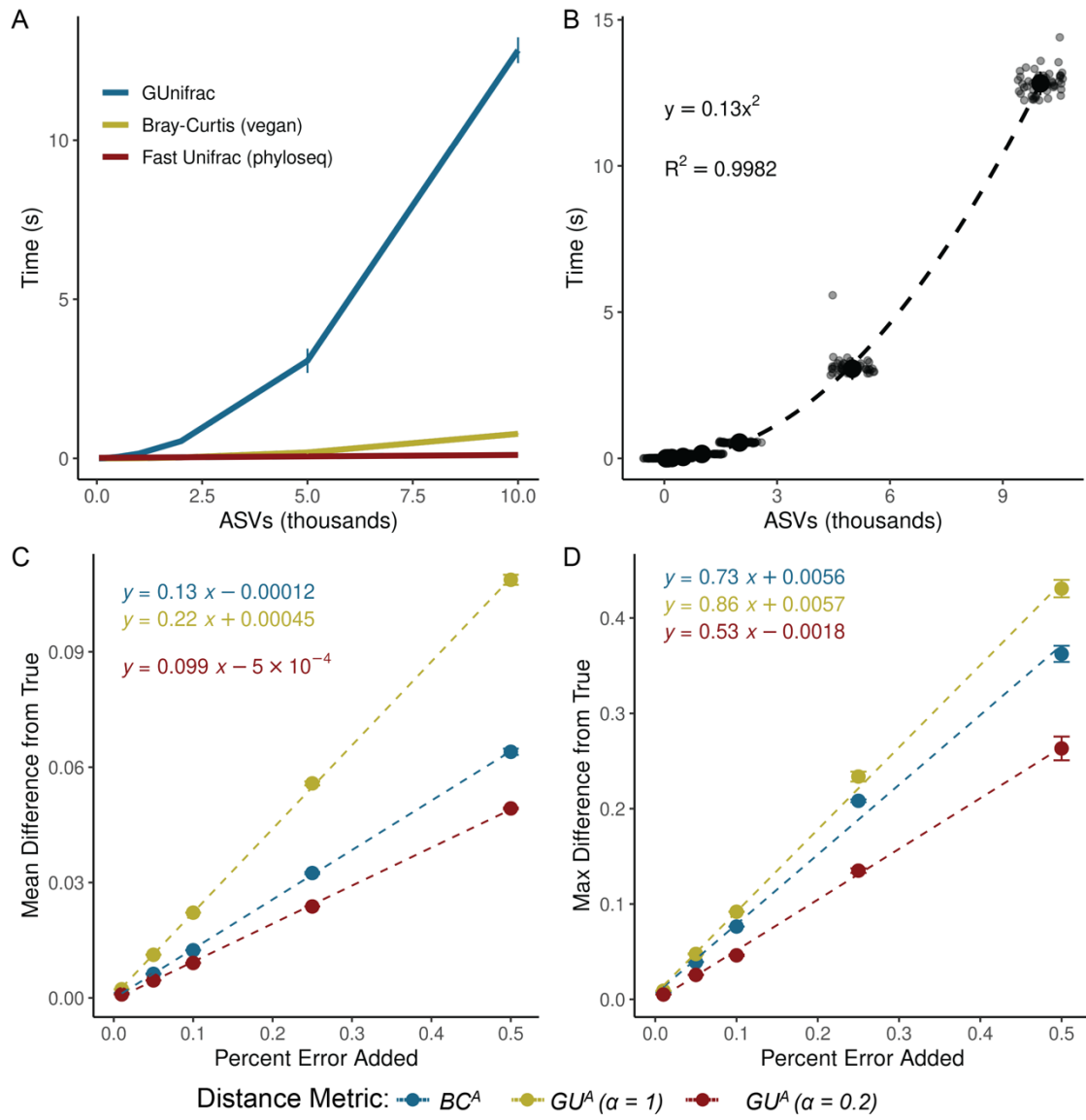
219 We recommend calibrating α based on research goals, modulating this effect by using
220 GU^A across a range of α rather than relying on U^A ($\alpha = 1$). Researchers should consider how
221 much emphasis they want their dissimilarity metric to place on microbial load (Box 1). When
222 biomass differences are central to the hypothesis being tested (for example, detecting
223 cyanobacterial blooms), high α are recommended. In contrast, if microbial load is irrelevant or
224 independent of the hypothesis in question, low α (or U^R) may be preferred; for example in the
225 soil dataset, fine-scale differences in composition may be obscured by random variation in
226 microbial load.

227 In many systems, microbial biomass is one piece of the story, likely correlated to other
228 variables being tested. If the importance of microbial load in the system is unknown, one
229 potential approach is to calculate correlations as demonstrated in Fig. 3B and select an α prior to
230 any ordinations or statistical testing. Again, correlation to cell count is valuable and is intrinsic to
231 absolute abundance-aware measures, especially when microbial load is relevant to the
232 hypotheses being tested. Correlations to cell count in BC^A , an accepted approach in the literature,
233 ranged from ~0.5 up to ~0.8. As a general recommendation from these analyses, we recommend
234 α values in an intermediate range from 0.1 up to 0.6, wherein GU^A has similar correlation to cell
235 count as BC^A .

236 Computational and Methodological Considerations

237 Applying GU^A in practice raises several considerations related to sequencing depth,
238 richness, and computational cost. Both Bray-Curtis and UniFrac can be sensitive to sequencing
239 depth because richness varies with read count [16–18]. Methods to address these concerns,
240 including rarefaction, remain debated and are challenging to benchmark rigorously [19]. We do
241 not evaluate the sensitivity of U^A or GU^A to different rarefaction strategies here, but we do

242 provide a workflow and code for how we incorporated rarefaction into our own analyses (Box 2
 243 and available code). This approach minimizes sequencing-depth biases while preserving
 244 abundance scaling for downstream β -diversity analysis.



245
 246 *Figure 4. GU^A requires more computational time but remains resilient to quantification error.* (A) Runtime for GU^A
 247 (GUniFrac package), U^R (FastUniFrac in the phyloseq package) and BC^A (vegan package) was benchmarked across
 248 50 iterations on a sub-sampled soil dataset (mature samples only) [10], using increasing ASV richness (50, 100, 200,
 249 500, 1,000, 2,000, 5,000, 10,000), with 10 samples and one α value per run (unweighted UniFrac is also calculated
 250 by default). Error bars represent standard deviation. (B) Quadratic relationship between GU^A computation time and
 251 ASV richness. Large center point represents median across 50 iterations, error bars (standard deviation) are too
 252 small to be seen. (C-D) Sensitivity of GU^A ($\alpha = 1$ and 0.2) and BC^A to measurement error was evaluated by adding
 253 random variation ($\pm 1\%$ to $\pm 50\%$; Supporting Methods) to 16S copy number estimates in stool samples from the
 254 mouse gut dataset [3]. For each error level, 50 replicate matrices were generated and compared to the original
 255 values. Panels reflect the (C) mean difference and (D) max difference between the error-added metrics compared to
 256 the originals. Error bars represent the standard deviation of the average mean and max difference across 50
 257 iterations.

258 GU^A is slower to compute than both BC^A and U^R because it must traverse the phylogenetic
259 tree to calculate branch lengths for each iteration. Computational time of GU^A increases
260 quadratically with ASV number and is 10-20 times slower, though up to 50 times slower, than
261 BC^A (Fig. 4A-B). The number of samples or α values, however, have relatively little effect on
262 runtime (Fig. S4). For a dataset of 24,000 ASVs, computing on a single CPU is still reasonable
263 (1.4 minutes), but repeated rarefaction increases runtime substantially because branch lengths are
264 redundantly calculated with each iteration. Allowing branch-length objects to be cached or
265 incorporated directly into the GUnifrac workflow would considerably improve computational
266 efficiency.

267 We also evaluated the sensitivity of GU^A to measurement error in absolute abundance due
268 to uncertainty arising from the quantification of cell number of 16S copy number. To assess the
269 sensitivity of GU^A and BC^A to measurement error, we added random error to the 16S copy
270 number measurements from the mouse gut dataset, limiting our analyses to the stool samples
271 where copy numbers varied by an order of magnitude. Across 50 iterations, each copy number
272 could randomly vary by a given percentage of error in either direction. We re-calculated β -
273 diversity (BC^A and GU^A at $\alpha = 1$ and $\alpha = 0.2$) and compared these measurements to the original
274 dataset.

275 Introducing random variation into measured 16S copy number altered GU^A values only
276 modestly, and the effect was proportional to the magnitude of the added noise (Fig. 4C-D). At α
277 = 1, each 1% of quantification error introduced an average difference of 0.0022 in GU^A ; at $\alpha =$
278 0.2, GU^A was even less sensitive. Thus, moderate α values provide a balance between
279 interpretability and robustness to noise in absolute quantification. The max deviation from true
280 that added error could inflict on a given metric was also proportional (and always less) than the
281 magnitude of the error itself (Fig. 4D). A more rigorous approach to assessing error propagation
282 within these metrics, including mathematical proofs of the relationships estimated above, is
283 outside the scope of this paper but would be helpful.

284 Ecological Interpretation and conceptual significance

285 Absolute UniFrac reframes the interpretation of β -diversity by making biomass an explicit
286 ecological axis rather than an unmeasured or normalized-away quantity. Conventional UniFrac
287 captures composition and shared evolutionary history, but implicitly invites interpretation as if it
288 also encodes differences on microbial load. By incorporating absolute abundance directly,
289 Absolute UniFrac helps to resolve this mismatch and restores alignment between ecological
290 hypotheses and the quantities represented in the metric. In this view, β -diversity becomes a three-
291 axis ecological measure, incorporating composition, phylogeny and biomass, rather than a two-
292 axis approximation. That said, the additional dimension of microbial load also increases the
293 complexity of applying and interpreting this metric.

294 There are many cases where the incorporation of absolute abundance allows microbial
295 ecologists to assess more realistic, ecologically-relevant differences in microbial communities,
296 especially when microbial load is mechanistically central. Outside of the datasets re-analyzed
297 here [3, 5, 9, 10]; the temporal development of the infant gut microbiome involves both a rise in
298 absolute abundance and compositional changes [6]; bacteriophage predation in wastewater
299 bioreactors can be understood only when microbial load is considered [20]; and antibiotic-driven
300 declines in specific swine gut taxa were missed using relative abundance approaches [21]. As β -

301 diversity metrics (and UniFrac specifically) remain central to microbial ecology, these findings
302 highlight how interpretation changes once biomass is incorporated. Broader adoption of absolute
303 abundance profiling will also depend on data availability. Few studies currently make absolute
304 quantification data publicly accessible, underscoring the need to deposit absolute measurements
305 alongside sequencing reads for reproducibility, ideally as metadata within SRA submissions.

306 While demonstrated here with 16S rRNA data, the approach should extend to other marker
307 genes or (meta)genomic features, provided absolute abundance estimates are available. In this
308 sense, GU^A offers a more ecologically grounded view of lineage turnover by jointly reflecting
309 variation in biomass and phylogenetic structure.

310 No single metric (or α in GU^A), however, is universally “best”. Each β -diversity metric
311 emphasizes a different dimension of community change. Researchers should therefore select
312 metrics based on the ecological quantity that is hypothesized to matter most (Box 1). Here, we
313 demonstrate not that GU^A outperforms other measures, but that it faithfully incorporates the three
314 axes of variation it was designed to incorporate: composition, phylogenetic similarity, and
315 absolute abundance (Fig. 1 and Fig. 2). As with any β -diversity analysis, interpretation requires
316 matching the metric to the ecological question at hand, and exploring sensitivity across different
317 metrics where appropriate [22]. By providing demonstrations and code for the application and
318 interpretation of U^A/GU^A , we hope to encourage the use of these metrics as a tool of microbial
319 ecology.

320 Conclusion

321 By explicitly incorporating absolute abundance, Absolute UniFrac shifts phylogenetic β -
322 diversity from a two-axis approximation to a three-axis ecological measure. This reframing
323 connects the metric to the underlying biological questions that motivate many microbiome
324 studies. As methods for quantifying microbial load continue to expand, the ability to interpret β -
325 diversity in a biomass-aware framework will become increasingly important for distinguishing
326 true ecological turnover from proportional change alone. In this way, Absolute UniFrac is not
327 simply an alternative distance metric but a tool for aligning statistical representation with
328 ecological mechanism.

329

330

331 **Box 1: β -diversity metrics should reflect the hypothesis being tested**

332 Absolute UniFrac is most informative when variation in microbial load is expected to carry
 333 ecological meaning rather than being a nuisance variable. The choice of α determines how
 334 strongly abundance differences influence the metric, and should therefore be selected based on
 335 the hypothesis, not by convention. In settings where biomass is central to the mechanism under
 336 study, higher α values appropriately foreground that signal, whereas in cases where load
 337 variation is incidental or confounding, lower α values maintain interpretability. Framing α as a
 338 hypothesis-driven choice repositions β -diversity from a default normalization step to an explicit
 339 ecological decision.

				Metric to Use	Hypothetical Example
Treat closely related lineages as similar?	Yes	How relevant is microbial load?	Central to hypothesis	$GU^A, \alpha > 0.5$	Cyanobacterial bloom, pathogen proliferation
			Relevant, but associated with other variables of interest	$GU^A, 0.1 < \alpha < 0.5$	Compositional shifts in response to nutrient addition
			Irrelevant	Dominant	$GU^R, \alpha > 0.5$
				Rare	$GU^R, \alpha < 0.5$
			Unknown	GU^A at multiple α	Random variation in microbial load obscured compositional shifts in soil communities
	No	Microbial load relevant?	Yes	BC^A	Strain turnover and proliferation in the infant gut
	No	BC^R	Temporal succession in chemostat		

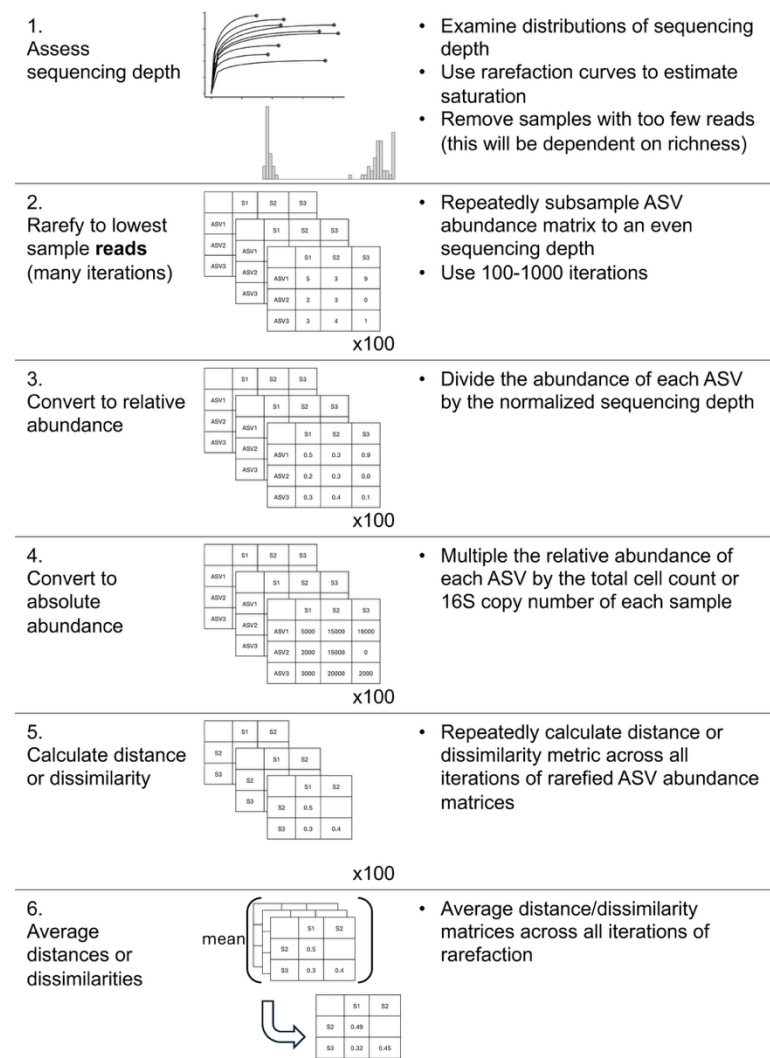
340

341

343 **Box 2: Rarefaction workflow for incorporating absolute abundance**

344 While we refrain from an in-depth
 345 analysis of rarefaction approaches,
 346 here we present our workflow for
 347 incorporating rarefaction alongside
 348 absolute abundance. First, samples
 349 were assessed for anomalously low
 350 read counts and discarded
 351 (sequencing blanks and controls
 352 were also removed). For rarefaction,
 353 each sample in the ASV table was
 354 subsampled to equal *sequencing*
 355 depth (# of reads) across 100
 356 iterations, creating 100 rarefied ASV
 357 tables. These tables were then
 358 converted to relative abundance by
 359 dividing each ASV's count by the
 360 equal sequencing depth (rounding
 361 was not performed). Then, each
 362 ASV's absolute abundance within a
 363 given sample was calculated by
 364 multiplying its relative abundance
 365 by that sample's total cell count or
 366 16S copy number. Methods to
 367 predict genomic 16S copy number
 368 for a given ASV were not used [23].

369 Each distance/dissimilarity metric was then calculated across all 100 absolute-normalized ASV
 370 tables. The final distance/dissimilarity matrix was calculated by averaging all 100 iterations of
 371 each distance/dissimilarity calculation. Of note for future users: pruning the phylogenetic tree
 372 after rarefaction for each iteration is not necessary – ASVs removed from the dataset do not
 373 contribute nor change the calculated of UniFrac distances.



- 375
- 376
- 377 **References**
- 378 1. Gloor GB et al. Microbiome Datasets Are Compositional: And This Is Not Optional. *Front*
379 *Microbiol* 2017;8:2224. <https://doi.org/10.3389/fmicb.2017.02224>
- 380 2. Vandepitte D et al. Stool consistency is strongly associated with gut microbiota richness
381 and composition, enterotypes and bacterial growth rates. *Gut* 2016;65:57–62.
382 <https://doi.org/10.1136/gutjnl-2015-309618>
- 383 3. Barlow JT, Bogatyrev SR, Ismagilov RF. A quantitative sequencing framework for absolute
384 abundance measurements of mucosal and luminal microbial communities. *Nat Commun*
385 2020;11:2590. <https://doi.org/10.1038/s41467-020-16224-6>
- 386 4. Wang X et al. Current Applications of Absolute Bacterial Quantification in Microbiome
387 Studies and Decision-Making Regarding Different Biological Questions. *Microorganisms*
388 2021;9:1797. <https://doi.org/10.3390/microorganisms9091797>
- 389 5. Props R et al. Absolute quantification of microbial taxon abundances. *ISME J* 2017;11:584–
390 587. <https://doi.org/10.1038/ismej.2016.117>
- 391 6. Rao C et al. Multi-kingdom ecological drivers of microbiota assembly in preterm infants.
392 *Nature* 2021;591:633–638. <https://doi.org/10.1038/s41586-021-03241-8>
- 393 7. Bray JR, Curtis JT. An Ordination of the Upland Forest Communities of Southern
394 Wisconsin. *Ecological Monographs* 1957;27:326–349. <https://doi.org/10.2307/1942268>
- 395 8. Lozupone CA et al. Quantitative and Qualitative β Diversity Measures Lead to Different
396 Insights into Factors That Structure Microbial Communities. *Applied and Environmental*
397 *Microbiology* 2007;73:1576–1585. <https://doi.org/10.1128/AEM.01996-06>

- 398 9. Pendleton A, Wells M, Schmidt ML. Upwelling periodically disturbs the ecological
399 assembly of microbial communities in the Laurentian Great Lakes. 2025. bioRxiv, 2025. ,
400 2025.01.17.633667
- 401 10. Zhang K et al. Absolute microbiome profiling highlights the links among microbial
402 stability, soil health, and crop productivity under long-term sod-based rotation. *Biol Fertil
403 Soils* 2022;58:883–901. <https://doi.org/10.1007/s00374-022-01675-4>
- 404 11. Chen J et al. Associating microbiome composition with environmental covariates using
405 generalized UniFrac distances. *Bioinformatics* 2012;28:2106–2113.
406 <https://doi.org/10.1093/bioinformatics/bts342>
- 407 12. Lozupone C, Knight R. UniFrac: a New Phylogenetic Method for Comparing Microbial
408 Communities. *Applied and Environmental Microbiology* 2005;71:8228–8235.
409 <https://doi.org/10.1128/AEM.71.12.8228-8235.2005>
- 410 13. McMurdie PJ, Holmes S. phyloseq: An R package for reproducible interactive analysis and
411 graphics of microbiome census data. *PLoS ONE* 2013;8:e61217.
- 412 14. Bolyen E et al. Reproducible, interactive, scalable and extensible microbiome data science
413 using QIIME 2. *Nat Biotechnol* 2019;37:852–857. [https://doi.org/10.1038/s41587-019-0209-9](https://doi.org/10.1038/s41587-019-
414 0209-9)
- 415 15. Morton JT et al. Uncovering the Horseshoe Effect in Microbial Analyses. *mSystems*
416 2017;2:10.1128/msystems.00166-16. <https://doi.org/10.1128/msystems.00166-16>
- 417 16. Schloss PD. Evaluating different approaches that test whether microbial communities have
418 the same structure. *The ISME Journal* 2008;2:265–275.
419 <https://doi.org/10.1038/ismej.2008.5>

- 420 17. Fukuyama J et al. Comparisons of distance methods for combining covariates and
421 abundances in microbiome studies. *Biocomputing 2012*. WORLD SCIENTIFIC, 2011,
422 213–224.
- 423 18. McMurdie PJ, Holmes S. Waste Not, Want Not: Why Rarefying Microbiome Data Is
424 Inadmissible. *PLOS Computational Biology* 2014;10:e1003531.
425 <https://doi.org/10.1371/journal.pcbi.1003531>
- 426 19. Schloss PD. Waste not, want not: revisiting the analysis that called into question the
427 practice of rarefaction. *mSphere* 2023;9:e00355-23. <https://doi.org/10.1128/mSphere.00355-23>
- 429 20. Shapiro OH, Kushmaro A, Brenner A. Bacteriophage predation regulates microbial
430 abundance and diversity in a full-scale bioreactor treating industrial wastewater. *The ISME
431 Journal* 2010;4:327–336. <https://doi.org/10.1038/ismej.2009.118>
- 432 21. Wagner S et al. Absolute abundance calculation enhances the significance of microbiome
433 data in antibiotic treatment studies. *Front Microbiol* 2025;16.
434 <https://doi.org/10.3389/fmicb.2025.1481197>
- 435 22. Kers JG, Saccenti E. The Power of Microbiome Studies: Some Considerations on Which
436 Alpha and Beta Metrics to Use and How to Report Results. *Front Microbiol* 2022;12.
437 <https://doi.org/10.3389/fmicb.2021.796025>
- 438 23. Douglas GM et al. PICRUSt2 for prediction of metagenome functions. *Nat Biotechnol*
439 2020;38:685–688. <https://doi.org/10.1038/s41587-020-0548-6>
- 440



1 **Interpreting UniFrac with Absolute Abundance: A Conceptual and Practical Guide**

2 Augustus Pendleton^{1*} & Marian L. Schmidt^{1*}

3 ¹Department of Microbiology, Cornell University, 123 Wing Dr, Ithaca, NY 14850, USA

4 **Corresponding Authors:** Augustus Pendleton: arp277@cornell.edu; Marian L. Schmidt:
5 marschmi@cornell.edu

6 **Author Contribution Statement:** Both authors contributed equally to the manuscript.

7 **Preprint servers:** This article was submitted to *bioRxiv* (doi: 10.1101/2025.07.18.665540) under
8 a CC-BY-NC-ND 4.0 International license.

9 **Keywords:** Microbial Ecology - Beta Diversity - Absolute Abundance - Bioinformatics -
10 UniFrac

11 **Data Availability:** All data and code used to produce the manuscript are available at
12 https://github.com/MarschmiLab/Pendleton_2025_Absolute_Unifrac_Paper, in addition to a
13 reproducible renv environment. All packages used for analysis are listed in Table S1.

14

Formatted: Font: Bold

Formatted: Line spacing: single

15 **Abstract**

16 β -diversity is central to microbial ecology, yet commonly used metrics overlook changes in
17 microbial load, limiting their ability to detect ecologically meaningful shifts. Popular for
18 incorporating phylogenetic relationships, UniFrac distances currently default to relative
19 abundance and therefore omit important variation in microbial abundances. As quantifying
20 absolute abundance becomes more accessible, integrating this information into β -diversity
21 analyses is essential. Here, we introduce *Absolute UniFrac* (GU^A), a variant of Weighted UniFrac
22 that incorporates absolute abundances. Using simulations and a reanalysis of four 16S rRNA
23 metabarcoding datasets (from a nuclear reactor cooling tank, the mouse gut, a freshwater lake,
24 and the peanut rhizosphere), we demonstrate that *Absolute UniFrac* captures microbial load,
25 composition, and phylogenetic relationships. While this can improve statistical power to detect
26 ecological shifts, we also find *Absolute UniFrac* can be strongly correlated to differences in cell
27 abundances alone. To balance these effects, we also incorporate absolute abundance into the
28 generalized extension (GU^A) that has a tunable α parameter to adjust the influence of abundance
29 and composition. Finally, we benchmark GU^A and show that although computationally slower
30 than conventional alternatives, GU^A is comparably insensitive to realistic noise in load estimates
31 compared to conventional alternatives like Bray-Curtis dissimilarities, particularly at lower α . By
32 coupling phylogeny, composition, and microbial load, *Absolute UniFrac* integrates three
33 dimensions of ecological change, better equipping microbial ecologists to quantitatively compare
34 microbial communities.

Deleted: Microbial ecologists routinely use
Deleted: metrics to compare communities, yet these metrics vary in the ecological dimensions they capture.
Deleted: , omitting
Deleted: load
Deleted: methods for
Deleted: estimating
Deleted: gain traction, incorporating
Deleted: becomes
Deleted: present
Deleted: uses
Deleted: Through
Deleted: freshwater case study.
Deleted: show that
Deleted: captures both
Deleted: s
Deleted: ,
Deleted: ing
Deleted: .
Deleted: However, it is also sensitive to variation in microbial load, especially when abundance changes occur along long branches, potentially amplifying differences. We therefore recommend a...
Deleted: form
Deleted: with
Deleted: balance sensitivity and interpretability
Deleted: .
Deleted: ¶

63 **Main Text**

64 Microbial ecologists routinely compare communities using β -diversity metrics derived
 65 from relative abundances. Yet this approach overlooks a critical ecological dimension: microbial
 66 load. High-throughput sequencing produces compositional data, in which each taxon's
 67 abundance is constrained by all others [1]. However, quantitative profiling studies show that cell
 68 abundance, not only composition, can drive major community differences [2]. In low-biomass
 69 samples, relying on relative abundance can allow contaminants to appear biologically
 70 meaningful despite absolute counts too low for concern [3].

Deleted:

71 Sequencing-based microbiome studies therefore rely on relative abundance even when
 72 the hypotheses of interest implicitly concern absolute changes in biomass. This creates a
 73 mismatch between ecological framing (growth, bloom magnitude, pathogen proliferation,
 74 disturbance recovery, or colonization pressure) and the information the β -diversity metric
 75 encodes [4]. As a result, β -diversity is often treated as if it includes biomass, even when absolute
 76 abundance is either not measured at all or is measured but excluded from the calculation (as in
 77 conventional UniFrac). Many studies therefore test biomass-linked hypotheses using a metric
 78 that normalizes biomass away [4]. A conceptual correction is needed in which β -diversity is
 79 understood as variation along three axes: composition, phylogeny and absolute abundance.

Deleted: {Citation}

80 Absolute microbial load measurements are now increasingly obtainable through flow
 81 cytometry, qPCR, and genomic spike-ins, allowing biomass to be quantified alongside taxonomic
 82 composition [4, 5]. These approaches improve detection of functionally relevant taxa and
 83 mitigate the compositional constraints imposed by sequencing [1, 2]. Most studies that
 84 incorporate absolute abundance counts currently rely on Bray-Curtis dissimilarity, which can
 85 capture load but does not consider phylogenetic similarity [5–7]. UniFrac distances provide the
 86 opposite strength, incorporating phylogeny but discarding absolute abundance, as they are
 87 restricted to relative abundance data by construction [8]. This leaves no phylogenetically
 88 informed β -diversity metric that operates on absolute counts, despite the fact that biomass is
 89 central to many ecological hypotheses.

Deleted: 1

To overcome compositional constraints, researchers increasingly use

Deleted: to quantify microbial load

Deleted: tools

Deleted: using

Deleted: dat

Deleted: a have used

Deleted: does not necessarily expect normalization to proportions

Formatted: Font: Italic

Deleted: But in the field of microbial ecology, UniFrac distances remain popular when working with relative abundance data. Here, we present *Absolute UniFrac*, a direct extension of Weighted UniFrac that incorporates total abundance, and evaluate its impact across simulated and real-world datasets.

90 To evaluate the implications of incorporating absolute abundance into phylogenetic β -
 91 diversity, we use both simulations and reanalysis of four 16S rRNA amplicon datasets. The
 92 simulations use a simple four-taxon community with controlled abundance shifts to directly
 93 compare both Bray-Curtis and UniFrac in their relative and absolute forms, illustrating how each
 94 metric responds when abundance, composition, or evolutionary relatedness differ. We then
 95 reanalyze four real-world datasets spanning nuclear reactor cooling water [5], the mouse gut [3],
 96 a freshwater lake [9], and rhizosphere soil [10]. These differ widely in richness, biomass range,
 97 and ecological context, allowing us to test when absolute abundance changes align with or
 98 diverge from phylogenetic turnover. Together, these simulations and reanalyses provide the
 99 empirical foundation for interpreting *Absolute UniFrac* relative to existing β -diversity measures
 100 across the three axes of ecological difference: abundance, composition, and phylogeny.

Formatted: Indent: First line: 0.5", Line spacing: single

101 We also extend *Absolute UniFrac* as was proposed by [11] to Generalized *Absolute*
 102 *UniFrac* that incorporates a tunable ecological dimension, α , and evaluate its impact across
 103 simulated and real-world datasets. As α increases, β -diversity is increasingly correlated with
 104 differences in absolute abundance, allowing researchers to fine tune the relative weight their
 105 analyses place on microbial load versus composition.

124 **Defining Absolute UniFrac**

125 The UniFrac distance was first introduced by Lozupone & Knight (2005) and has since
 126 become enormously popular as a measure of β -diversity within the field of microbial ecology
 127 [12]. A benefit of the UniFrac distance is that it considers phylogenetic information when
 128 estimating the distance between two communities. After first generating a phylogenetic tree
 129 representing species (or amplicon sequence variants, “ASVs”) from all samples, the UniFrac
 130 distance computes the fraction of branch-lengths which is *shared* between communities, relative
 131 to the total branch length represented in the tree. UniFrac can be both unweighted, in which only
 132 the incidence of species is considered, or weighted, wherein a branch’s contribution is weighted
 133 by the proportional abundance of taxa on that branch [8]. The Weighted UniFrac is derived:

$$U^R = \frac{\sum_{i=1}^n b_i |p_i^a - p_i^b|}{\sum_{i=1}^n b_i (p_i^a + p_i^b)}$$

134 where the contribution of each branch length, b_i , is weighted by the difference in the relative
 135 abundance of all species (p_i) descended from that branch in sample a or sample b . Here, we
 136 denote this distance as U^R , for “Relative UniFrac”. Popular packages which calculate weighted
 137 UniFrac—including the diversity-lib QIIME plug-in and the R packages phyloseq and
 138 GUniFrac—run this normalization by default [11, 13, 14].

139
 140 Importantly, U^R is most sensitive to changes in abundant lineages, which can sometimes
 141 obscure compositional differences driven by rare to moderately-abundant taxa [11]. To address
 142 this weakness, Chen et al. (2012) introduced the generalized UniFrac distance (GU^R), in which
 143 the impact of abundant lineages can be mitigated by decreasing the parameter α :

$$GU^R = \frac{\sum_{i=1}^n b_i (p_i^a + p_i^b)^\alpha |p_i^a - p_i^b|}{\sum_{i=1}^n b_i (p_i^a + p_i^b)^\alpha}$$

144 where α ranges from 0 (close to Unweighted UniFrac) up to 1 (identical to U^R , above). However,
 145 if one wishes to use absolute abundances, both U^R and GU^R can be derived without normalizing
 146 to proportions:

$$U^A = \frac{\sum_{i=1}^n b_i |c_i^a - c_i^b|}{\sum_{i=1}^n b_i (c_i^a + c_i^b)} \quad GU^A = \frac{\sum_{i=1}^n b_i (c_i^a + c_i^b)^\alpha |c_i^a - c_i^b|}{\sum_{i=1}^n b_i (c_i^a + c_i^b)^\alpha}$$

147 Where c_i^a and c_i^b denote for the absolute counts of species descending from branch b_i in
 148 communities a and b , respectively. We refer to these distances as *Absolute UniFrac* (U^A) and
 149 *Generalized Absolute UniFrac* (GU^A). Although substituting absolute for relative abundances is
 150 mathematically straightforward, we found no prior work that examines UniFrac in the context of
 151 absolute abundance, either conceptually or in application. Incorporating absolute abundances
 152 introduces a third axis of ecological variation: beyond differences in composition and
 153 phylogenetic similarity, U^A also captures divergence in microbial load. This makes interpretation
 154 of U^A nontrivial, particularly in complex microbiomes.

155 **Demonstrating β -diversity metrics’ behavior with a simple simulation**

156 Formatted: No underline
 Formatted: Line spacing: single
 Deleted:
 Formatted: Indent: First line: 0.5", Line spacing: single
 Deleted: s

Deleted: we weight the length

Deleted: f

Deleted: Because
 Deleted: it
 Formatted: Indent: First line: 0.5", Line spacing: single

Formatted: Line spacing: single

Deleted: stands

Deleted: ed

Deleted: y

Deleted: f

Deleted:

Deleted: U^A and

Formatted: No underline

Formatted: Font: Bold

170 To clarify how U^A behaves relative to existing β -diversity metrics, we first constructed a
171 simple four-taxon simulated community arranged in a small phylogeny (Fig. 1A). By varying the
172 absolute abundance of each ASV (1, 10, or 100), we generated 81 samples and 3,240 pairwise
173 comparisons. For each pair, we computed four dissimilarity metrics: Bray-Curtis with relative
174 abundance (BC^R), Bray-Curtis with absolute abundance (BC^A), Weighted UniFrac with relative
175 abundance (U^R), and Weighted UniFrac with absolute abundance (U^A). These comparisons help
176 to illustrate how each axis of ecological difference—abundance, composition, and phylogeny—is
177 expressed by the different metrics.

178 U^A does not consistently yield higher or lower distances compared to other metrics, but
179 instead varies depending on how abundance and phylogeny intersect (Fig. 1B). In the improbable
180 scenario that all branch lengths are equal, U^A is always less than or equal to BC^A (Fig. S1).
181 These comparisons emphasize that once branch lengths differ, incorporating phylogeny and
182 absolute abundance alters the structure of the distance space. The direction and magnitude of that
183 change depend on which branches carry the abundance shifts. U^A is also usually smaller than
184 BC^A and is more strongly correlated with BC^A (Pearson's $r = 0.82$, $p < 0.0001$) than with BC^R (r
185 = 0.41) and U^R ($r = 0.55$).

186 To better understand how these metrics diverge, we examined individual sample pairs
187 (Fig. 1C). Scenario 1 (gold star) illustrates the classic advantage of UniFrac: ASV_1 and ASV_2
188 are phylogenetically close, so U^R and U^A discern greater similarity between samples than BC^R
189 and BC^A , which ignore phylogenetic structure. Scenario 2 (red star) highlights a limitation of
190 relative metrics: two samples with identical relative composition but a 100-fold difference in
191 biomass appear identical to BC^R and U^R , but not to their absolute counterparts. In Scenario 3
192 (green star), incorporating absolute abundance decreases dissimilarity. BC^A and U^A are lower
193 than their relative counterparts because half the community is identical in absolute abundance,
194 even though their proportions differ. In contrast, Scenario 4 (blue star) shows that U^A can exceed
195 BC^A when abundance differences occur on long branches, amplifying phylogenetic dissimilarity.

196 These scenarios demonstrate that U^A integrates variation along three ecologically
197 relevant axes: composition, phylogenetic similarity, and microbial load, rather than isolating any
198 single dimension. Because a given U^A value can reflect multiple drivers of community change,
199 interpreting it requires downstream analyses to disentangle the relative contributions of these
200 three axes. To evaluate how this plays out in real systems we next reanalyzed four previously
201 published datasets spanning diverse microbial environments.

Formatted: Indent: First line: 0.5", Line spacing: single

Deleted: To illustrate how U^A behaves, we constructed a simulated community of four ASVs arranged in a simple phylogeny (Fig. 1A).

Deleted:

Deleted: reshapes distance estimates in nontrivial ways.

Deleted:

Deleted: terms, despite proportional differences

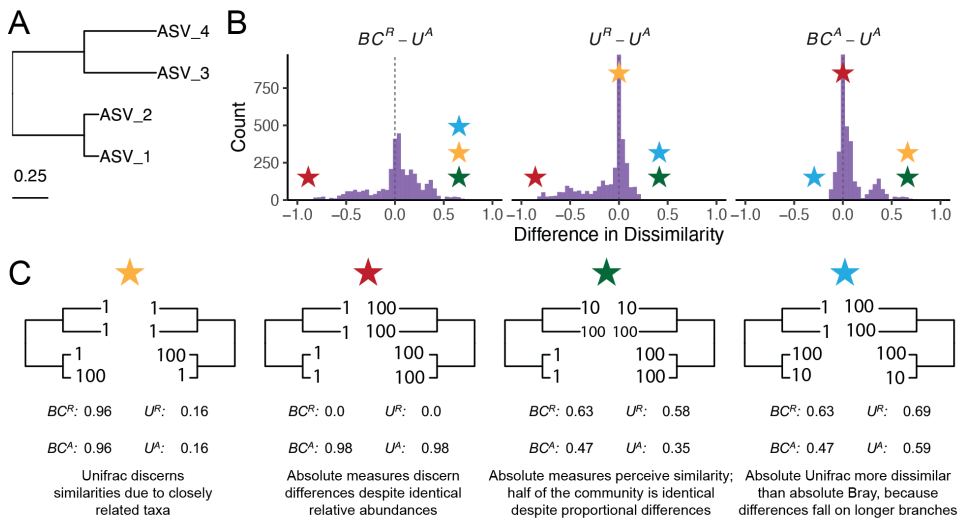
Deleted: increase dissimilarity relative to

Deleted: ¶

Formatted: Indent: First line: 0"

Formatted: Indent: First line: 0.5", Line spacing: single

Deleted: ¶



215 *Figure 1. Simulated communities reveal how absolute abundance affects phylogenetic and non-phylogenetic β -*
216 *diversity measures.* (A) We constructed a simple four-ASV community with a known phylogeny and generated all
217 permutations of each ASV having an absolute abundance of 1, 10, or 100, resulting in 81 unique communities and
218 3,240 pairwise comparisons. (B) Distributions of pairwise differences between weighted UniFrac using absolute
219 abundance (U^A) and three other metrics: Bray-Curtis using relative abundance (BC^R), weighted UniFrac using
220 relative abundance (U^R), and Bray-Curtis using absolute abundance (BC^A). (C) Illustrative sample pairs demonstrate
221 how absolute abundances and phylogenetic structure interact to increase or decrease dissimilarity across metrics.
222 Stars indicate where each scenario falls within the distributions shown in panel B. Actual values for each metric are
223 displayed beneath each scenario.

224 Application of Absolute UniFrac to Four Real-World Microbiome Datasets

225 To illustrate the sensitivity of U^A to both variation in composition and absolute
226 abundance, we re-analyzed four previously published datasets from diverse microbial systems.
227 These datasets included: (i) nuclear reactor cooling water sampled across three reactor cycle
228 phases [5]; (ii) the mouse gut sampled across multiple regions and between two diets [3]; (iii)
229 depth-stratified freshwater communities sampled across two months [9]; and (iv) peanut
230 rhizospheres under two crop rotation schemes (conventional rotation (CR) vs. sod-based rotation
231 (SBR)), plant maturities, and irrigation treatments [10]. Absolute abundance was quantified by
232 flow cytometry for the cooling water and freshwater datasets, droplet digital PCR for the mouse
233 gut, and by qPCR for the rhizosphere dataset. Together these span a wide range of richness—from
234 215 ASVs in the cooling water to 24,000 ASVs in the soil—and microbial load—from as low as
235 4×10^5 cells/ml (cooling water) up to 2×10^{12} 16S rRNA copies/gram (mouse gut). Additional

Formatted: Line spacing: single

Deleted: Example comparisons i

Deleted: ng specific scenarios where U^A yields greater or smaller dissimilarity than other metrics.

Deleted: Colored s

Deleted: Across all 3,240 pairwise comparisons, U^A is usually smaller than and strongly correlated with BC^A (Pearson's $r = 0.82$, $p < 0.0001$) than with BC^R ($r = 0.41$) and U^R ($r = 0.55$), reflecting the effect illustrated in Scenario 1. However, exceptions like Scenario 4 show that U^A can also yield larger distances than BC^A when abundance differences occur on long branches. These scenarios demonstrate that U^A

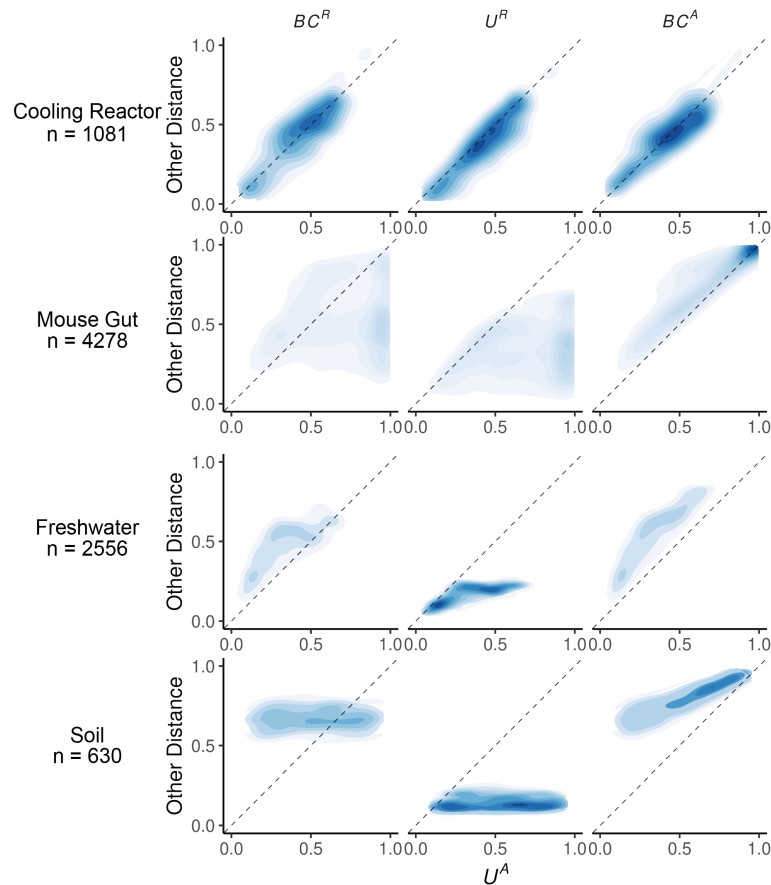
Formatted: Font: Bold

Formatted: Indent: First line: 0", Line spacing: single

248
249

details of the re-analysis workflow, including ASV generation and phylogenetic inference, are provided in the Supporting Methods.

Formatted: Font: 10 pt



250
251
252
253
254
255
256

Figure 2. Absolute UniFrac (U^A) compared with other β -diversity metrics across four real microbial datasets. Each panel shows pairwise sample distances for U^A (x-axis) against another metric (y-axis): Bray-Curtis using relative abundance (BC^R , first column), weighted UniFrac using relative abundances (U^R , second column), and Bray-Curtis using absolute abundances (BC^A , third column). Contours indicate the relative density of pairwise comparisons (n shown for each dataset, left), with darker shading corresponding to more observations. The dashed line marks the 1:1 relationship. Points above the line indicate cases where U^A is smaller than the comparator metric, while points below the line indicate cases where U^A is larger.

Formatted: Indent: First line: 0", Line spacing: single

257
258
259
260

We first calculated four β -diversity metrics for all sample pairs in each dataset and compared them to U^A (Fig. 2). The degree of concordance between U^A and other metrics was highly context dependent. In the cooling water dataset, U^A closely tracked all three alternatives, whereas in the remaining systems it diverged substantially. U^A also spanned a similar or wider

Formatted: Font: 10 pt

Formatted: Line spacing: single

range of distances than the other metrics. For example, in the soil dataset BC^R and U^R occupied a narrow range relative to the broad separation observed under U^A .

U^A generally reported distances that were similar to or greater than U^R , consistent with the simulations shown in Fig. 1B. This reflects the ability of U^A to discern dissimilarity due to differences in microbial load, even when community composition is conserved. In contrast, U^A yielded distances that were similar to or lower than BC^A , again matching the simulated behavior in Fig 1B. In these cases, phylogenetic proximity between abundant, closely-related ASVs leads U^A to register greater similarity than BC^A .

Given these differences, we next quantified how well each metric discriminates among categorical sample groups. For each dataset, we ran PERMANOVAs to measure the proportion of variance (R^2) and statistical power (*pseudo-F*, *p*-value) attributable to group structure, using groupings that were determined to be significant in the original publications. To evaluate how strongly absolute abundance contributed to this discrimination, we also calculated GU^A across a range of α values. The resulting R^2 values are displayed in Fig. 3A, with the corresponding *pseudo-F* statistics and *p*-values provided in Fig. S2.

As in Fig. 2, the performance of each metric was strongly context dependent (Fig. 3A). In the mouse gut and freshwater datasets, absolute-abundance-aware metrics (BC^A and GU^A) explained the greatest proportion of variance (R^2), and R^2 generally increasing as α increased. In contrast, relative metrics captured more variation in the cooling water dataset (again at higher α), and all metrics explained comparably little variance in the soil dataset. Taken at face value, these trends might suggest that higher α values typically improve group differentiation.

However, this comes with a major caveat: at high α values, GU^A becomes strongly correlated with total cell count alone (Fig. 3B). Mantel tests confirmed that absolute-abundance metrics are far more sensitive to differences in microbial load than their relative counterparts. This behavior is intuitive, and to some extent desirable, because these metrics are designed to detect changes in microbial load even when composition remains constant. Yet at $\alpha = 1$, U^A approaches a proxy for sample absolute abundance itself. In ordination space (Fig. S3), this can cause Axis 1 to correlate with absolute abundance and in some cases (freshwater and soil) produces strong horseshoe effects [15], potentially distorting ecological interpretation.

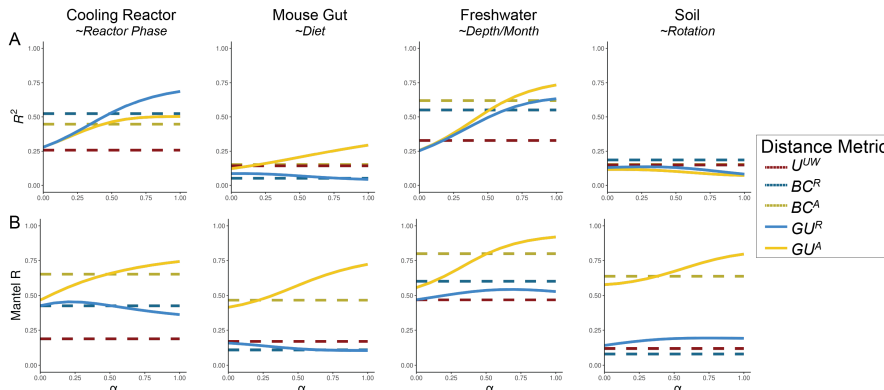
Deleted: integrates ecological realism by capturing differences in both lineage identity and total biomass.[¶]

Moved (insertion) [1]

Deleted: We next evaluated how U^A influences group separation in a real-world dataset. Using a previously published 16S rRNA gene dataset from Lake Ontario, we analyzed 66 samples and >7,000 ASVs. Samples clustered into three groups defined by depth and month, reflecting shifts in both taxonomic composition and microbial load (Fig. S2, [10]). Our goal was to determine whether weighting phylogenetic distances by absolute abundance enhances interpretability and statistical power to distinguish sample groups.[¶]

with total cell count alone (Fig. 2D). Mantel tests showed that absolute distance metrics are much more sensitive to differences in cell counts than their relative counterparts. This is intuitive, and to a degree, intentional: these metrics aim to detect changes in biomass even when composition remains constant. Yet at $\alpha = 1$, U^A is nearly a proxy for sample biomass. In ordination space, this manifests as Axis 1 being almost perfectly correlated with absolute abundance (Spearman's $\rho = -1.0$), whereas at $\alpha = 0.0$, the correlation is moderate ($\rho = 0.58$). The structure observed in Fig. 2A at $\alpha = 1$ may largely reflect a horseshoe effect [14], where a strong gradient (here, cell counts) becomes curved in ordination space, potentially distorting ecological interpretation.[¶]

UniFrac (GU^A) across three levels of α : 0.0 (approximating unweighted UniFrac), 0.5, and 1.0 (equivalent to U^A). As α increased, PCoA ordinations revealed stronger similarity between Shallow May and Shallow September samples, reflecting their higher cell counts compared to the Deep samples (Fig. 2A). Notably, the proportion of variation explained by the first PCoA axis increased substantially with α , going from 18.3% at $\alpha = 0$ up to 76.7% $\alpha = 1$. This trend was also true for U^R across multiple α , but to a much weaker degree (Fig. S3).



327 **Figure 3. Discriminatory performance of U^A and related metrics across four microbial systems.** (A) PERMANOVAs
328 were used to quantify the percent variance (R^2) explained by predefined categorical groups (shown in italics beneath
329 each dataset name), with 1,000 permutations. PERMANOVA results were evaluated across five metrics and, where
330 applicable, across eleven α values (0-1 in 0.1 increments). For consistency with the original studies, only samples
331 from Reactor cycle 1 were used for the cooling-water dataset, only stool samples for the mouse gut dataset, and only
332 mature rhizosphere samples for the dataset. (B) Mantel correlation (R) between each distance metric and the
333 pairwise differences in absolute abundance (cell counts or 16S copy number), illustrating the degree to which each
334 metric is driven by biomass differences.

335 We recommend calibrating α based on research goals, modulating this effect by using
336 GU^A across a range of α rather than relying on U^A ($\alpha = 1$). Researchers should consider how
337 much emphasis they want their dissimilarity metric to place on microbial load (Box 1). When
338 biomass differences are central to the hypothesis being tested (for example, detecting
339 cyanobacterial blooms), high α are recommended. In contrast, if microbial load is irrelevant or
340 independent of the hypothesis in question, low α (or U^R) may be preferred; for example in the
341 soil dataset, fine-scale differences in composition may be obscured by random variation in
342 microbial load.

343 In many systems, microbial biomass is one piece of the story, likely correlated to other
344 variables being tested. If the importance of microbial load in the system is unknown, one
345 potential approach is to calculate correlations as demonstrated in Fig. 3B and select an α prior to
346 any ordinations or statistical testing. Again, correlation to cell count is valuable and is intrinsic to
347 absolute abundance-aware measures, especially when microbial load is relevant to the
348 hypotheses being tested. Correlations to cell count in BC^A , an accepted approach in the literature,
349 ranged from ~0.5 up to ~0.8. As a general recommendation from these analyses, we recommend
350 α values in an intermediate range from 0.1 up to 0.6, wherein GU^A has similar correlation to cell
351 count as BC^A .

352 Computational and Methodological Considerations

353 Applying GU^A in practice raises several considerations related to sequencing depth,
354 richness, and computational cost. Both Bray-Curtis and UniFrac can be sensitive to sequencing
355 depth because richness varies with read count [16–18]. Methods to address these concerns,
356 including rarefaction, remain debated and are challenging to benchmark rigorously [19]. We do
357 not evaluate the sensitivity of U^A or GU^A to different rarefaction strategies here, but we do

Formatted: Font: 10 pt

Formatted: Indent: First line: 0", Line spacing: single

Moved up [1]: at high α values, GU^A became strongly correlated with total cell count alone (Fig. 2D). Mantel tests showed that absolute distance metrics are much more sensitive to differences in cell counts than their relative counterparts. This is intuitive, and to a degree, intentional: these metrics aim to detect changes in biomass even when composition remains constant. Yet at $\alpha = 1$, U^A is nearly a proxy for sample biomass. In ordination space, this manifests as Axis 1 being almost perfectly correlated with absolute abundance (Spearman's $\rho = -1.0$), whereas at $\alpha = 0.0$, the correlation is moderate ($\rho = 0.58$). The structure observed in Fig. 2A at $\alpha = 1$ may largely reflect a horseshoe effect [12], where a strong gradient (here, cell counts) becomes curved in ordination space, potentially distorting ecological interpretation.

Deleted:

To quantify the impact on group differentiation, we performed PERMANOVA across depth-month groupings using GU^R , GU^A , BC^R , and BC^A at varying α (Fig. 2B–C). Across all metrics, incorporating absolute abundance increased both the proportion of explained variance (R^2) and the pseudo F -statistic. GU^A achieved a maximum R^2 of 75.8% and a pseudo F -statistic 1.56 times greater than GU^R , highlighting the ability of GU^A to detect group differences driven by microbial load.¹

However, a major caveat emerged:

Deleted:

Deleted: urge careful calibration of

Deleted: thereby mitigating

Formatted: Line spacing: single

Deleted:

Formatted: Indent: First line: 0.5", Line spacing: single

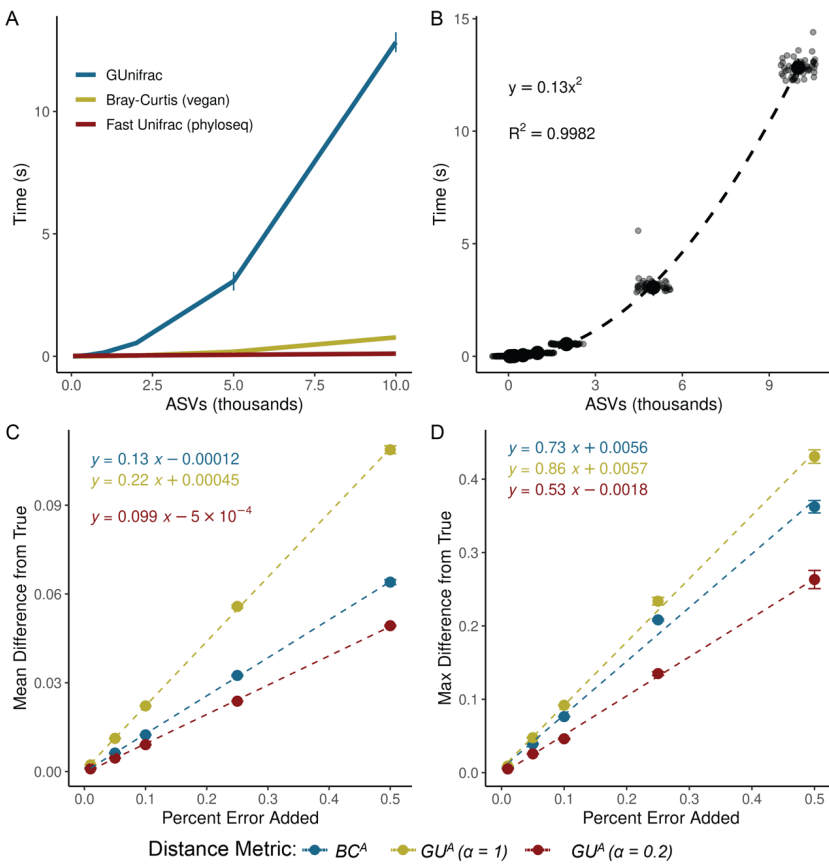
Deleted: In this dataset, we recommend an intermediate α of 0.5, consistent with prior guidance [9], but especially important when using absolute abundance data.

Deleted:

Formatted: Font: Bold

Formatted: Line spacing: single

431 provide a workflow and code for how we incorporated rarefaction into our own analyses (Box 2
 432 and available code). This approach minimizes sequencing-depth biases while preserving
 433 abundance scaling for downstream β -diversity analysis.



434

435 *Figure 4. GU^A requires more computational time but remains resilient to quantification error. (A) Runtime for GU^A*
 436 (*GUUnifrac package*), U^R (*FastUniFrac* in the *phyloseq* package) and BC^A (*vegan* package) was benchmarked across
 437 50 iterations on a sub-sampled soil dataset (mature samples only) [10], using increasing ASV richness (50, 100, 200,
 438 500, 1,000, 2,000, 5,000, 10,000), with 10 samples and one α value per run (unweighted UniFrac is also calculated
 439 by default). Error bars represent standard deviation. (B) Quadratic relationship between GU^A computation time and
 440 ASV richness. Large center point represents median across 50 iterations, error bars (standard deviation) are too
 441 small to be seen. (C-D) Sensitivity of GU^A ($\alpha = 1$ and 0.2) and BC^A to measurement error was evaluated by adding
 442 random variation ($\pm 1\%$ to $\pm 50\%$; Supporting Methods) to 16S copy number estimates in stool samples from the
 443 mouse gut dataset [3]. For each error level, 50 replicate matrices were generated and compared to the original
 444 values. Panels reflect the (C) mean difference and (D) max difference between the error-added metrics compared to
 445 the originals. Error bars represent the standard deviation of the average mean and max difference across 50
 446 iterations.

447 *GU^A* is slower to compute than both BC^A and U^R because it must traverse the phylogenetic
448 tree to calculate branch lengths for each iteration. Computational time of GU^A increases
449 quadratically with ASV number and is 10-20 times slower, though up to 50 times slower, than
450 BC^A (Fig. 4A-B). The number of samples or α values, however, have relatively little effect on
451 runtime (Fig. S4). For a dataset of 24,000 ASVs, computing on a single CPU is still reasonable
452 (1.4 minutes), but repeated rarefaction increases runtime substantially because branch lengths are
453 redundantly calculated with each iteration. Allowing branch-length objects to be cached or
454 incorporated directly into the GUnifrac workflow would considerably improve computational
455 efficiency.

456 We also evaluated the sensitivity of GU^A to measurement error in absolute abundance due to
457 uncertainty arising from the quantification of cell number of 16S copy number. To assess the
458 sensitivity of GU^A and BC^A to measurement error, we added random error to the 16S copy
459 number measurements from the mouse gut dataset, limiting our analyses to the stool samples
460 where copy numbers varied by an order of magnitude. Across 50 iterations, each copy number
461 could randomly vary by a given percentage of error in either direction. We re-calculated β -
462 diversity (BC^A and GU^A at $\alpha = 1$ and $\alpha = 0.2$) and compared these measurements to the original
463 dataset.

464 Introducing random variation into measured 16S copy number altered GU^A values only
465 modestly, and the effect was proportional to the magnitude of the added noise (Fig. 4C-D). At α
466 = 1, each 1% of quantification error introduced an average difference of 0.0022 in GU^A ; at $\alpha =$
467 0.2, GU^A was even less sensitive. Thus, moderate α values provide a balance between
468 interpretability and robustness to noise in absolute quantification. The max deviation from true
469 that added error could inflict on a given metric was also proportional (and always less) than the
470 magnitude of the error itself (Fig. 4D). A more rigorous approach to assessing error propagation
471 within these metrics, including mathematical proofs of the relationships estimated above, is
472 outside the scope of this paper but would be helpful.

473 Ecological Interpretation and conceptual significance

474 Absolute UniFrac reframes the interpretation of β -diversity by making biomass an explicit
475 ecological axis rather than an unmeasured or normalized-away quantity. Conventional UniFrac
476 captures composition and shared evolutionary history, but implicitly invites interpretation as if it
477 also encodes differences on microbial load. By incorporating absolute abundance directly,
478 Absolute UniFrac helps to resolve this mismatch and restores alignment between ecological
479 hypotheses and the quantities represented in the metric. In this view, β -diversity becomes a three-
480 axis ecological measure, incorporating composition, phylogeny and biomass, rather than a two-
481 axis approximation. That said, the additional dimension of microbial load also increases the
482 complexity of applying and interpreting this metric.

483 There are many cases where the incorporation of absolute abundance allows microbial
484 ecologists to assess more realistic, ecologically-relevant differences in microbial communities,
485 especially when microbial load is mechanistically central. Outside of the datasets re-analyzed
486 here [3, 5, 9, 10], the temporal development of the infant gut microbiome involves both a rise in
487 absolute abundance and compositional changes [6]; bacteriophage predation in wastewater
488 bioreactors can be understood only when microbial load is considered [20]; and antibiotic-driven
489 declines in specific swine gut taxa were missed using relative abundance approaches [21]. As β -

Formatted: Indent: First line: 0.5", Space After: 8 pt,
Adjust space between Latin and Asian text, Adjust space
between Asian text and numbers, Tab stops: Not at 0.39" +
0.78" + 1.17" + 1.56" + 1.94" + 2.33" + 2.72" + 3.11" +
3.5" + 3.89" + 4.28" + 4.67"

Formatted: Font: Not Italic

Formatted: Font: Not Italic

Formatted: Font: (Default) Times New Roman

Formatted: Font: (Default) Times New Roman

Formatted: Font: (Default) Times New Roman

Formatted: Line spacing: single

Formatted: Font: (Default) Times New Roman

Formatted: Font: (Default) Times New Roman

Formatted: No underline

Formatted: Indent: First line: 0.35", Line spacing: single

Formatted: Font: 10 pt

Deleted: [11][3]

491 diversity metrics (and UniFrac specifically) remain central to microbial ecology, these findings
492 highlight how interpretation changes once biomass is incorporated. Broader adoption of absolute
493 abundance profiling will also depend on data availability. Few studies currently make absolute
494 quantification data publicly accessible, underscoring the need to deposit absolute measurements
495 alongside sequencing reads for reproducibility, ideally as metadata within SRA submissions.

496 While demonstrated here with 16S rRNA data, the approach should extend to other marker
497 genes or (meta)genomic features, provided absolute abundance estimates are available. In this
498 sense, GU^A offers a more ecologically grounded view of lineage turnover by jointly reflecting
499 variation in biomass and phylogenetic structure.

500 No single metric (or α in GU^A), however, is universally “best”. Each β -diversity metric
501 emphasizes a different dimension of community change. Researchers should therefore select
502 metrics based on the ecological quantity that is hypothesized to matter most (Box 1). Here, we
503 demonstrate not that GU^A outperforms other measures, but that it faithfully incorporates the three
504 axes of variation it was designed to incorporate: composition, phylogenetic similarity, and
505 absolute abundance (Fig. 1 and Fig. 2). As with any β -diversity analysis, interpretation requires
506 matching the metric to the ecological question at hand, and exploring sensitivity across different
507 metrics where appropriate [22]. By providing demonstrations and code for the application and
508 interpretation of U^A/GU^A , we hope to encourage the use of these metrics as a tool of microbial
509 ecology.

510 Conclusion

511 By explicitly incorporating absolute abundance, Absolute UniFrac shifts phylogenetic β -
512 diversity from a two-axis approximation to a three-axis ecological measure. This reframing
513 connects the metric to the underlying biological questions that motivate many microbiome
514 studies. As methods for quantifying microbial load continue to expand, the ability to interpret β -
515 diversity in a biomass-aware framework will become increasingly important for distinguishing
516 true ecological turnover from proportional change alone. In this way, Absolute UniFrac is not
517 simply an alternative distance metric but a tool for aligning statistical representation with
518 ecological mechanism.

519

Formatted: Indent: First line: 0.35", Line spacing: single

Deleted:

Formatted: Line spacing: single

Formatted: Font: Not Italic

522 **Box 1: β -diversity metrics should reflect the hypothesis being tested**

Formatted: Font: Bold

523 Absolute UniFrac is most informative when variation in microbial load is expected to carry
 524 ecological meaning rather than being a nuisance variable. The choice of α determines how
 525 strongly abundance differences influence the metric, and should therefore be selected based on
 526 the hypothesis, not by convention. In settings where biomass is central to the mechanism under
 527 study, higher α values appropriately foreground that signal, whereas in cases where load
 528 variation is incidental or confounding, lower α values maintain interpretability. Framing α as a
 529 hypothesis-driven choice repositions β -diversity from a default normalization step to an explicit
 530 ecological decision.

			Metric to Use			Hypothetical Example
Treat closely related lineages as similar?	Yes	How relevant is microbial load?	Central to hypothesis			<i>GU^A, $\alpha > 0.5$</i>
			Relevant, but associated with other variables of interest			<i>GU^A, $0.1 < \alpha < 0.5$</i>
			Irrelevant	Emphasize rare or dominant taxa?	Dominant	<i>GU^R, $\alpha > 0.5$</i>
					Rare	<i>GU^R, $\alpha < 0.5$</i>
			Unknown			<i>GU^A at multiple α</i>
	No	Microbial load relevant?	Yes		<i>BC^A</i>	Random variation in microbial load obscured compositional shifts in soil communities
	No		<i>BC^R</i>	Strain turnover and proliferation in the infant gut		
				Temporal succession in chemostat		

Formatted: Font: 10 pt

Formatted: Font: 10 pt

Formatted: Centered

Formatted: Font: 10 pt

Formatted: Font: 10 pt

Formatted: Centered

Formatted: Font: 10 pt, Not Italic

Formatted: Font: 10 pt

Formatted: Centered

533

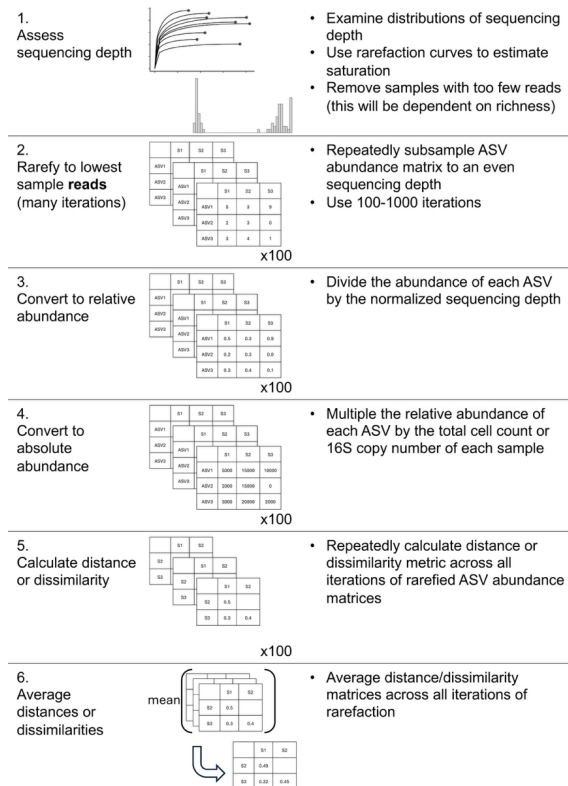
534 **Box 2: Rarefaction workflow for incorporating absolute abundance**

Formatted: Font: Bold

535 While we refrain from an in-depth
 536 analysis of rarefaction approaches,
 537 here we present our workflow for
 538 incorporating rarefaction alongside
 539 absolute abundance. First, samples
 540 were assessed for anomalously low
 541 read counts and discarded
 542 (sequencing blanks and controls
 543 were also removed). For rarefaction,
 544 each sample in the ASV table was
 545 subsampled to equal sequencing
 546 depth (# of reads) across 100
 547 iterations, creating 100 rarefied ASV
 548 tables. These tables were then
 549 converted to relative abundance by
 550 dividing each ASV's count by the
 551 equal sequencing depth (rounding
 552 was not performed). Then, each
 553 ASV's absolute abundance within a
 554 given sample was calculated by
 555 multiplying its relative abundance
 556 by that sample's total cell count or
 557 16S copy number. Methods to
 558 predict genomic 16S copy number
 559 for a given ASV were not used [23].

560 Each distance/dissimilarity metric was then calculated across all 100 absolute-normalized ASV
 561 tables. The final distance/dissimilarity matrix was calculated by averaging all 100 iterations of
 562 each distance/dissimilarity calculation. Of note for future users: pruning the phylogenetic tree
 563 after rarefaction for each iteration is not necessary – ASVs removed from the dataset do not
 564 contribute nor change the calculated UniFrac distances.

565



566

567

568 **References**

- 569 1. Gloor GB et al. Microbiome Datasets Are Compositional: And This Is Not Optional. *Front
570 Microbiol* 2017;8:2224. <https://doi.org/10.3389/fmicb.2017.02224>
- 571 2. Vandepitte D et al. Stool consistency is strongly associated with gut microbiota richness
572 and composition, enterotypes and bacterial growth rates. *Gut* 2016;65:57–62.
573 <https://doi.org/10.1136/gutjnl-2015-309618>
- 574 3. Barlow JT, Bogatyrev SR, Ismagilov RF. A quantitative sequencing framework for absolute
575 abundance measurements of mucosal and luminal microbial communities. *Nat Commun*
576 2020;11:2590. <https://doi.org/10.1038/s41467-020-16224-6>
- 577 4. Wang X et al. Current Applications of Absolute Bacterial Quantification in Microbiome
578 Studies and Decision-Making Regarding Different Biological Questions. *Microorganisms*
579 2021;9:1797. <https://doi.org/10.3390/microorganisms9091797>
- 580 5. Props R et al. Absolute quantification of microbial taxon abundances. *ISME J* 2017;11:584–
581 587. <https://doi.org/10.1038/ismej.2016.117>
- 582 6. Rao C et al. Multi-kingdom ecological drivers of microbiota assembly in preterm infants.
583 *Nature* 2021;591:633–638. <https://doi.org/10.1038/s41586-021-03241-8>
- 584 7. Bray JR, Curtis JT. An Ordination of the Upland Forest Communities of Southern
585 Wisconsin. *Ecological Monographs* 1957;27:326–349. <https://doi.org/10.2307/1942268>
- 586 8. Lozupone CA et al. Quantitative and Qualitative β Diversity Measures Lead to Different
587 Insights into Factors That Structure Microbial Communities. *Applied and Environmental
588 Microbiology* 2007;73:1576–1585. <https://doi.org/10.1128/AEM.01996-06>

Formatted: Line spacing: single

Deleted: That said, interpretation of GU^A requires care. When biomass differences dominate, ordinations may largely reflect microbial load rather than lineage turnover, particularly at $\alpha = 1$ and with long phylogenetic branches. In such cases, higher statistical power may come at the cost of biological nuance. We also do not address related concerns, such as how sequencing depth influences richness estimates or whether rarefaction should be applied before calculating GU^A [15]. As with any β -diversity study, researchers should interpret results critically, explore sensitivity across metrics, and justify their choice of α [16]. Our results suggest that an intermediate α value offers a practical compromise that balances sensitivity to biomass with robustness to overdominance by total load, especially when lineage turnover is also of interest. We anticipate that GU^A will become an essential tool for microbiome researchers seeking to incorporate absolute abundance into ecologically grounded β -diversity comparisons.¶

- 607 9. Pendleton A, Wells M, Schmidt ML. Upwelling periodically disturbs the ecological
608 assembly of microbial communities in the Laurentian Great Lakes. 2025. bioRxiv, 2025. ,
609 2025.01.17.633667
- 610 10. Zhang K et al. Absolute microbiome profiling highlights the links among microbial
611 stability, soil health, and crop productivity under long-term sod-based rotation. *Biol Fertil
612 Soils* 2022;58:883–901. <https://doi.org/10.1007/s00374-022-01675-4>
- 613 11. Chen J et al. Associating microbiome composition with environmental covariates using
614 generalized UniFrac distances. *Bioinformatics* 2012;28:2106–2113.
615 <https://doi.org/10.1093/bioinformatics/bts342>
- 616 12. Lozupone C, Knight R. UniFrac: a New Phylogenetic Method for Comparing Microbial
617 Communities. *Applied and Environmental Microbiology* 2005;71:8228–8235.
618 <https://doi.org/10.1128/AEM.71.12.8228-8235.2005>
- 619 13. McMurdie PJ, Holmes S. phyloseq: An R package for reproducible interactive analysis and
620 graphics of microbiome census data. *PLoS ONE* 2013;8:e61217.
- 621 14. Bolyen E et al. Reproducible, interactive, scalable and extensible microbiome data science
622 using QIIME 2. *Nat Biotechnol* 2019;37:852–857. [https://doi.org/10.1038/s41587-019-0209-9](https://doi.org/10.1038/s41587-019-
623 0209-9)
- 624 15. Morton JT et al. Uncovering the Horseshoe Effect in Microbial Analyses. *mSystems*
625 2017;2:10.1128/msystems.00166-16. <https://doi.org/10.1128/msystems.00166-16>
- 626 16. Schloss PD. Evaluating different approaches that test whether microbial communities have
627 the same structure. *The ISME Journal* 2008;2:265–275.
628 <https://doi.org/10.1038/ismej.2008.5>

- 629 17. Fukuyama J et al. Comparisons of distance methods for combining covariates and
630 abundances in microbiome studies. *Biocomputing* 2012. WORLD SCIENTIFIC, 2011,
631 213–224.
- 632 18. McMurdie PJ, Holmes S. Waste Not, Want Not: Why Rarefying Microbiome Data Is
633 Inadmissible. *PLOS Computational Biology* 2014;10:e1003531.
634 <https://doi.org/10.1371/journal.pcbi.1003531>
- 635 19. Schloss PD. Waste not, want not: revisiting the analysis that called into question the
636 practice of rarefaction. *mSphere* 2023;9:e00355-23. <https://doi.org/10.1128/mSphere.00355-23>
- 637 20. Shapiro OH, Kushmaro A, Brenner A. Bacteriophage predation regulates microbial
638 abundance and diversity in a full-scale bioreactor treating industrial wastewater. *The ISME
639 Journal* 2010;4:327–336. <https://doi.org/10.1038/ismej.2009.118>
- 640 21. Wagner S et al. Absolute abundance calculation enhances the significance of microbiome
641 data in antibiotic treatment studies. *Front Microbiol* 2025;16.
642 <https://doi.org/10.3389/fmicb.2025.1481197>
- 643 22. Kers JG, Saccenti E. The Power of Microbiome Studies: Some Considerations on Which
644 Alpha and Beta Metrics to Use and How to Report Results. *Front Microbiol* 2022;12.
645 <https://doi.org/10.3389/fmicb.2021.796025>
- 646 23. Douglas GM et al. PICRUSt2 for prediction of metagenome functions. *Nat Biotechnol*
647 2020;38:685–688. <https://doi.org/10.1038/s41587-020-0548-6>
- 648
- 649

Page 9: [1] Deleted

Augustus Raymond Pendleton

9/28/25 9:44:00 PM



Click here to access/download

Supplemental Material

Pendleton_ISME_PostReview_SupportingInformation.pdf

¹ **Interpreting UniFrac with Absolute Abundance: A Conceptual
2 and Practical Guide**

³ Augustus Pendleton^{1*} & Marian L. Schmidt^{1*}

⁴ ¹Department of Microbiology, Cornell University, 123 Wing Dr, Ithaca, NY 14850, USA

⁵ **Corresponding Authors:** Augustus Pendleton: arp277@cornell.edu; Marian L.
⁶ Schmidt: marschmi@cornell.edu

⁷ **Author Contribution Statement:** Both authors contributed equally to the
⁸ manuscript.

⁹ **Preprint servers:** This article was submitted to *bioRxiv* (doi:) under a CC-BY-NC-ND
¹⁰ 4.0 International license.

¹¹ **Keywords:** Microbial Ecology - Beta Diversity - Absolute Abundance - Bioinformatics
¹² - UniFrac

¹³ **Data Availability:** All data and code used to produce the manuscript are available at
¹⁴ https://github.com/MarschmiLab/Pendleton_2025_Absolute_Unifrac_Paper, in addition
¹⁵ to a reproducible `renv` environment. All packages used for analysis are listed in
¹⁶ Table S1.

¹⁷ **Abstract**

¹⁸ Microbial ecologists routinely use β -diversity metrics to compare communities, yet these
¹⁹ metrics vary in the ecological dimensions they capture. Popular for incorporating phyloge-
²⁰ netic relationships, UniFrac distances default to relative abundance, omitting important
²¹ variation in microbial load. As methods for estimating absolute abundance gain trac-
²² tion, incorporating this information into β -diversity analyses becomes essential. Here,
²³ we present *Absolute UniFrac* (U^A), a variant of Weighted UniFrac that uses absolute
²⁴ abundances. Through simulations and a freshwater case study, we show that Absolute
²⁵ UniFrac captures both microbial load and phylogenetic relationships, improving statisti-
²⁶ cal power to detect ecological shifts. However, it is also sensitive to variation in microbial
²⁷ load, especially when abundance changes occur along long branches, potentially ampli-
²⁸ fying differences. We therefore recommend a generalized form (GU^A) with a tunable α
²⁹ parameter to balance sensitivity and interpretability.

30 **Main Text**

31 Microbial ecologists routinely compare communities using β -diversity metrics derived
32 from relative abundances. Yet this approach overlooks a critical ecological dimension:
33 microbial load. High-throughput sequencing produces compositional data, in which each
34 taxon's abundance is constrained by all others [1]. However, quantitative profiling studies
35 show that cell abundance, not only composition, can drive major community differences
36 [2]. In low-biomass samples, relying on relative abundance can allow contaminants to
37 appear biologically meaningful despite absolute counts too low for concern [3].

38 To overcome compositional constraints, researchers increasingly use flow cytometry,
39 qPCR, and genomic spike-ins to quantify microbial load [4, 5]. These tools improve detection
40 of functionally relevant taxa and mitigate the compositional constraints imposed by
41 sequencing [1, 2]. Most studies using absolute data have used Bray-Curtis dissimilarity,
42 which does not necessarily expect normalization to proportions [e.g. 4, 6]. But in the
43 field of microbial ecology, UniFrac distances remain popular when working with relative
44 abundance data. Here, we present *Absolute UniFrac*, a direct extension of Weighted
45 UniFrac that incorporates total abundance, and evaluate its impact across simulated and
46 real-world datasets.

47 The UniFrac distance was first introduced by Lozupone & Knight (2005), and has
48 since become enormously popular as a measure of β -diversity within the field of microbial
49 ecology [7]. A benefit of the UniFrac distance is that it considers phylogenetic information
50 when estimating the distance between two communities. After first generating a
51 phylogenetic tree representing species (or amplicon sequence variants, “ASVs”) from all
52 samples, the UniFrac distance computes the fraction of branch-lengths which is *shared*
53 between communities, relative to the total branch length represented in the tree. UniFrac
54 can be both unweighted, in which only the incidence of species is considered, or weighted,
55 wherein a branch's contribution is weighted by the proportional abundance of taxa on
56 that branch [8]. The weighted UniFrac is derived:

$$U^R = \frac{\sum_{i=1}^n b_i |p_i^a - p_i^b|}{\sum_{i=1}^n b_i (p_i^a + p_i^b)}$$

57 where we weight the length of each branch, b_i , by the difference in the relative abundance
58 of all species (p_i) descended from that branch in sample a or sample b . Here,
59 we denote this distance as U^R , for “Relative UniFrac”. Popular packages which calculate
60 weighted UniFrac-including `diversity-lib` QIIME plug-in and the R packages `phyloseq`
61 and `GUniFrac-run` this normalization by default.

62 Because U^R is most sensitive to changes in abundant lineages, it can sometimes
63 obscure compositional differences driven by rare to moderately-abundant taxa [9]. To
64 address this weakness, Chen et al. (2012) introduced the generalized UniFrac distance
65 (GU^R), in which the impact of abundant lineages can be mitigated by decreasing the
66 parameter α :

$$GU^R = \frac{\sum_{i=1}^n b_i (p_i^a + p_i^b)^\alpha \left| \frac{p_i^a - p_i^b}{p_i^a + p_i^b} \right|}{\sum_{i=1}^n b_i (p_i^a + p_i^b)^\alpha}$$

67 where α ranges from 0 (close to unweighted UniFrac) up to 1 (identical to U^R , above).
 68 However, if one wishes to use absolute abundances, both U^R and GU^R can be derived
 69 without normalizing to proportions:

$$U^A = \frac{\sum_{i=1}^n b_i |c_i^a - c_i^b|}{\sum_{i=1}^n b_i (c_i^a + c_i^b)} \quad GU^A = \frac{\sum_{i=1}^n b_i (c_i^a + c_i^b)^\alpha \left| \frac{c_i^a - c_i^b}{c_i^a + c_i^b} \right|}{\sum_{i=1}^n b_i (c_i^a + c_i^b)^\alpha}$$

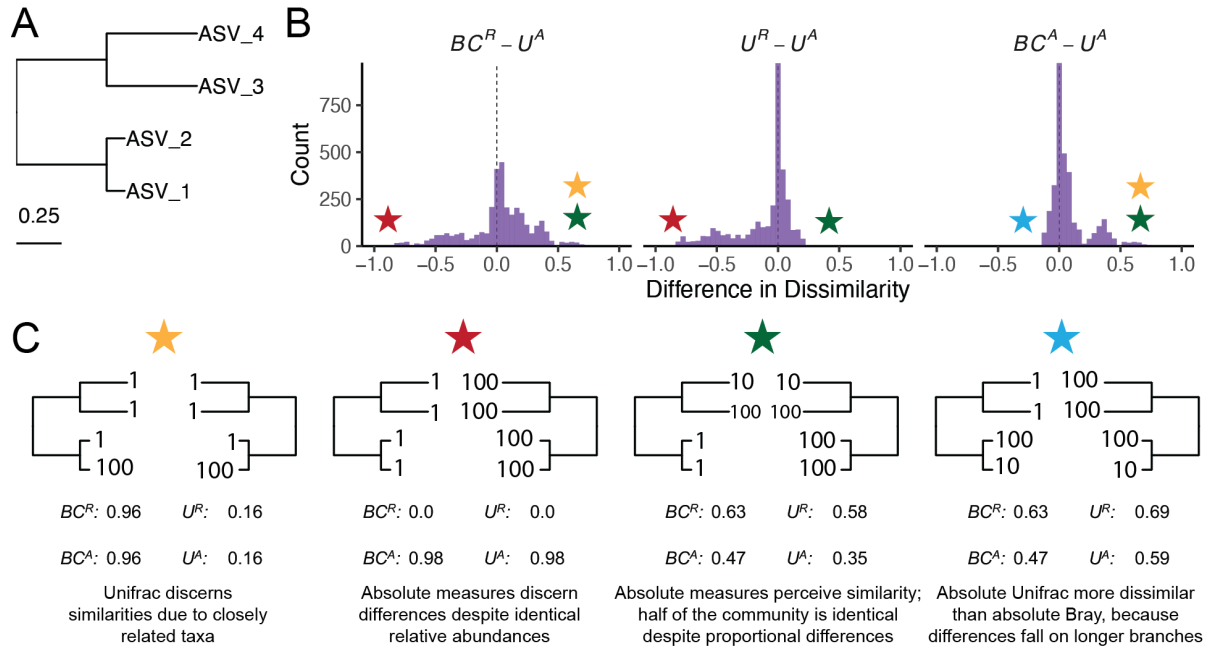
70 Where c_i^a and c_i^b stands for the absolute counts of species descended from branch b_i in
 71 community a and b , respectively. We refer to these distances as *Absolute Unifrac* and
 72 *Generalized Absolute Unifrac* (U^A and GU^A) .

73 To illustrate how U^A behaves, we constructed a simulated community of four ASVs
 74 arranged in a simple phylogeny (Fig. 1A). By varying the absolute abundance of each
 75 ASV (1, 10, or 100), we generated 81 samples and 3,240 pairwise comparisons. For
 76 each pair, we computed four dissimilarity metrics: Bray-Curtis with relative abundance
 77 (BC^R), Bray-Curtis with absolute abundance (BC^A), Weighted UniFrac with relative
 78 abundance (U^R), and Weighted UniFrac with absolute abundance (U^A).

79 U^A does not consistently yield higher or lower distances but instead varies depending
 80 on how abundance and phylogeny intersect (Fig. 1B). In the improbable scenario that
 81 all branch lengths are equal, U^A is always less than or equal to BC^A (Fig. S1). These
 82 comparisons emphasize that incorporating phylogeny and absolute abundance reshapes
 83 distance estimates in nontrivial ways.

84 To better understand how these metrics diverge, we examined individual sample pairs
 85 (Fig. 1C). Scenario 1 (gold star) illustrates the classic advantage of UniFrac: ASV_1
 86 and ASV_2 are phylogenetically close, so U^R and U^A discern greater similarity between
 87 samples than BC^R and BC^A , which ignore phylogenetic structure. Scenario 2 (red star)
 88 highlights a limitation of relative metrics: two samples with identical relative composition
 89 but a 100-fold difference in biomass appear identical to BC^R and U^R , but not to their
 90 absolute counterparts. In Scenario 3 (green star), incorporating absolute abundance
 91 decreases dissimilarity. BC^A and U^A are lower than their relative counterparts because
 92 half the community is identical in absolute terms, despite proportional differences. In
 93 contrast, Scenario 4 (blue star) shows that U^A can increase dissimilarity relative to BC^A
 94 when abundance differences occur on long branches, amplifying phylogenetic dissimilarity.

95 Across all 3,240 pairwise comparisons, U^A is usually smaller than and strongly corre-
 96 lated with BC^A (Pearson's $r = 0.82$, $p < 0.0001$) than with BC^R ($r = 0.41$) and U^R ($r =$
 97 0.55), reflecting the effect illustrated in Scenario 1. However, exceptions like Scenario 4
 98 show that U^A can also yield larger distances than BC^A when abundance differences occur
 99 on long branches. These scenarios demonstrate that U^A integrates ecological realism by
 100 capturing differences in both lineage identity and total biomass.



101

102 *Figure 1. Simulated communities reveal how absolute abundance affects phylogenetic and non-phylogenetic*
103 *-diversity measures.* (A) We constructed a simple four-ASV community with a known phylogeny and
104 generated all permutations of each ASV having an absolute abundance of 1, 10, or 100, resulting in 81
105 unique communities and 3,240 pairwise comparisons. (B) Distributions of pairwise differences between
106 weighted UniFrac using absolute abundance (U^A) and three other metrics: Bray-Curtis using relative
107 abundance (BC^R), weighted UniFrac using relative abundance (U^R), and Bray-Curtis using absolute
108 abundance (BC^A). (C) Example comparisons illustrating specific scenarios where U^A yields greater
109 or smaller dissimilarity than other metrics. Colored stars indicate where each scenario falls within the
110 distributions shown in panel B. Actual values for each metric are displayed beneath each scenario.

111 We next evaluated how U^A influences group separation in a real-world dataset. Using a
112 previously published 16S rRNA gene dataset from Lake Ontario, we analyzed 66 samples
113 and >7,000 ASVs. Samples clustered into three groups defined by depth and month,
114 reflecting shifts in both taxonomic composition and microbial load (Fig. S2, [10]). Our
115 goal was to determine whether weighting phylogenetic distances by absolute abundance
116 enhances interpretability and statistical power to distinguish sample groups.

117 We calculated generalized absolute UniFrac (GU^A) across three levels of α : 0.0 (approx-
118 imating unweighted UniFrac), 0.5, and 1.0 (equivalent to U^A). As α increased, PCoA
119 ordinations revealed stronger similarity between Shallow May and Shallow September
120 samples, reflecting their higher cell counts compared to the Deep samples (Fig. 2A). Not-
121 ably, the proportion of variation explained by the first PCoA axis increased substantially
122 with α , going from 18.3% at $\alpha = 0$ up to 76.7% $\alpha = 1$. This trend was also true for U^R
123 across multiple α , but to a much weaker degree (Fig. S3).

124 To quantify the impact on group differentiation, we performed PERMANOVA across
125 depth-month groupings using GU^R , GU^A , BC^R , and BC^A at varying α (Fig. 2B–C).
126 Across all metrics, incorporating absolute abundance increased both the proportion of
127 explained variance (R^2) and the *pseudo*–*F*-statistic. GU^A achieved a maximum R^2 of
128 75.8% and a *pseudo*–*F*-statistic 1.56× greater than GU^R , highlighting the ability of
129 GU^A to detect group differences driven by microbial load.

130 However, a major caveat emerged: at high α values, GU^A became strongly correlated
131 with total cell count alone (Fig. 2D). Mantel tests showed that absolute distance metrics

are much more sensitive to differences in cell counts than their relative counterparts. This is intuitive, and to a degree, intentional: these metrics aim to detect changes in biomass even when composition remains constant. Yet at $\alpha = 1$, U^A is nearly a proxy for sample biomass. In ordination space, this manifests as Axis 1 being almost perfectly correlated with absolute abundance (Spearman's $\rho = -1.0$), whereas at $\alpha = 0.0$, the correlation is moderate ($\rho = 0.58$). The structure observed in Fig. 2A at $\alpha = 1$ may largely reflect a horseshoe effect [11], where a strong gradient (here, cell counts) becomes curved in ordination space, potentially distorting ecological interpretation.

We urge careful calibration of α based on research goals, thereby mitigating this effect using GU^A rather than U^A . Researchers should consider how much emphasis they want their dissimilarity metric to place on microbial load. In this dataset, we recommend an intermediate α of 0.5, consistent with prior guidance [9], but especially important when using absolute abundance data.

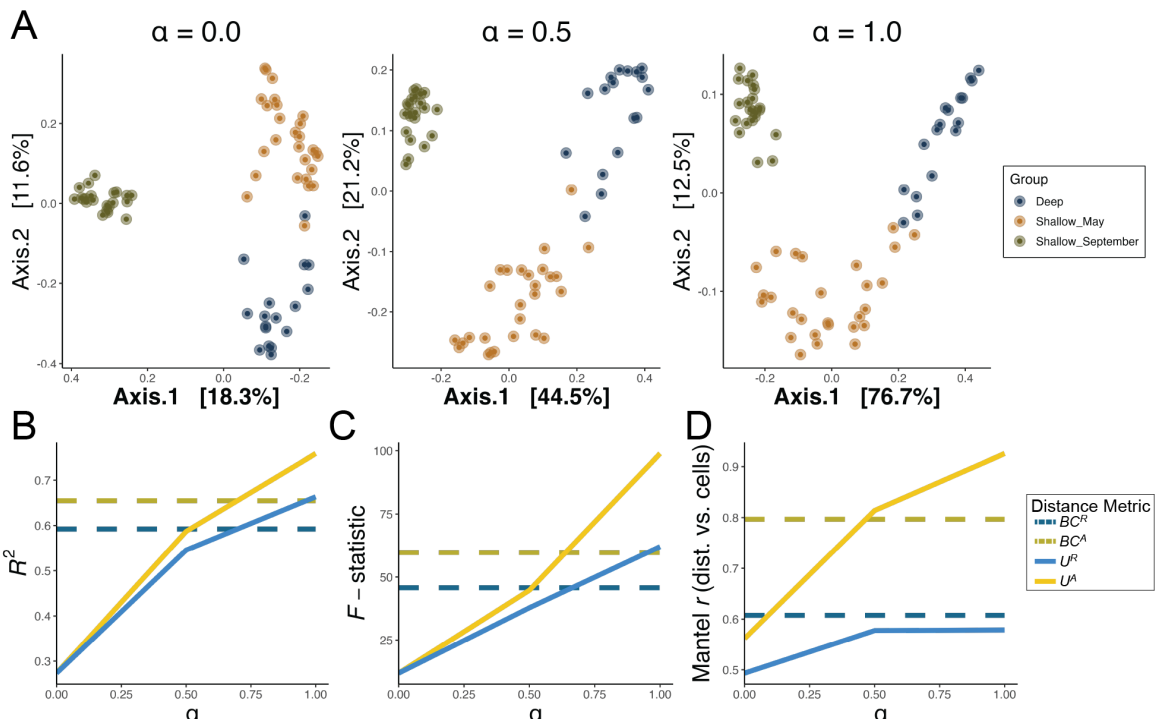


Figure 2. Absolute abundance sharpens ecological signal in freshwater microbial communities but increases sensitivity to biomass. (A) Principal Coordinates Analysis (PCoA) of microbial communities from Lake Ontario, sampled in May and September at two depths (Shallow and Deep) [10]. Ordinations are based on generalized UniFrac with absolute abundance (GU^A) at α values of 0.0, 0.5, and 1.0. Variance explained by each axis is shown in brackets. The x-axis is reversed in the first panel to provide visual symmetry across ordinations. (B-C) Results of PERMANOVA analyses quantifying (B) variance explained (R^2) and (C) statistical power (*pseudo* – F -statistic) across depth-month groups for four distance metrics: GU^R , GU^A , BC^R , and BC^A , each evaluated at multiple α values. (D) Mantel correlations between each distance matrix and differences in cell abundances.

The incorporation of absolute abundance allows microbial ecologists to assess more realistic, ecologically-relevant differences in microbial communities, especially in contexts where microbial load matters. For example, the temporal development of the infant microbiome involves both a rise in absolute abundance and compositional changes [6]; bacteriophage predation in wastewater bioreactors can be understood only when microbial load is considered [12]; and antibiotic-driven declines in specific swine gut taxa were

missed using relative abundance approaches [13]. As β -diversity metrics (and UniFrac specifically) remain central to microbial ecology, we encourage researchers to adopt GU^A when absolute abundance data are available. While demonstrated here with 16S rRNA data, the approach is generalizable to other marker genes or (meta)genomic features, provided absolute abundance estimates are available. In doing so, GU^A offers not only a more grounded picture of lineage differences but also sensitivity to both biomass variation and phylogenetic depth, enabling detection of subtle yet ecologically meaningful shifts.

That said, interpretation of GU^A requires care. When biomass differences dominate, ordinations may largely reflect microbial load rather than lineage turnover, particularly at $\alpha = 1$ and with long phylogenetic branches. In such cases, higher statistical power may come at the cost of biological nuance. We also do not address related concerns, such as how sequencing depth influences richness estimates or whether rarefaction should be applied before calculating GU^A [14]. As with any β -diversity study, researchers should interpret results critically, explore sensitivity across metrics, and justify their choice of α [15]. Our results suggest that an intermediate α value offers a practical compromise that balances sensitivity to biomass with robustness to overdominance by total load, especially when lineage turnover is also of interest. We anticipate that GU^A will become an essential tool for microbiome researchers seeking to incorporate absolute abundance into ecologically grounded β -diversity comparisons.

References

1. Gloor GB et al. Microbiome Datasets Are Compositional: And This Is Not Optional. *Front Microbiol* 2017;8:2224. <https://doi.org/10.3389/fmicb.2017.02224>
2. Vandeputte D et al. Quantitative microbiome profiling links gut community variation to microbial load. *Nature* 2017;551:507–511. <https://doi.org/10.1038/nature24460>
3. Barlow JT, Bogatyrev SR, Ismagilov RF. A quantitative sequencing framework for absolute abundance measurements of mucosal and luminal microbial communities. *Nat Commun* 2020;11:2590. <https://doi.org/10.1038/s41467-020-16224-6>
4. Props R et al. Absolute quantification of microbial taxon abundances. *ISME J* 2017;11:584–587. <https://doi.org/10.1038/ismej.2016.117>
5. Wang X et al. Current Applications of Absolute Bacterial Quantification in Microbiome Studies and Decision-Making Regarding Different Biological Questions. *Microorganisms* 2021;9:1797. <https://doi.org/10.3390/microorganisms9091797>
6. Rao C et al. Multi-kingdom ecological drivers of microbiota assembly in preterm infants. *Nature* 2021;591:633–638. <https://doi.org/10.1038/s41586-021-03241-8>
7. Lozupone C, Knight R. UniFrac: a New Phylogenetic Method for Comparing Microbial Communities. *Applied and Environmental Microbiology* 2005;71:8228–8235. <https://doi.org/10.1128/AEM.71.12.8228-8235.2005>
8. Lozupone CA et al. Quantitative and Qualitative Diversity Measures Lead to Different Insights into Factors That Structure Microbial Communities. *Applied and Environmental Microbiology* 2007;73:1576–1585. <https://doi.org/10.1128/AEM.01996-06>
9. Chen J et al. Associating microbiome composition with environmental covariates using generalized UniFrac distances. *Bioinformatics* 2012;28:2106–2113. <https://doi.org/10.1093/bioinformatics/bts342>

- 190 10. Pendleton A, Wells M, Schmidt ML. Upwelling periodically disturbs the ecological assembly of microbial communities in the Laurentian Great Lakes.
- 191 11. Morton JT et al. Uncovering the Horseshoe Effect in Microbial Analyses. *mSystems* 2017;2:10.1128/msystems.00166-16. <https://doi.org/10.1128/msystems.00166-16>
- 192 12. Shapiro OH, Kushmaro A, Brenner A. Bacteriophage predation regulates microbial abundance and diversity in a full-scale bioreactor treating industrial wastewater. *The ISME Journal* 2010;4:327–336. <https://doi.org/10.1038/ismej.2009.118>
- 193 13. Wagner S et al. Absolute abundance calculation enhances the significance of microbiome data in antibiotic treatment studies. *Front Microbiol* 2025;16. <https://doi.org/10.3389/fmicb.2025.1481197>
- 194 14. Schloss PD. Waste not, want not: revisiting the analysis that called into question the practice of rarefaction. *mSphere* 2023;9:e00355–23. <https://doi.org/10.1128/msphere.00355-23>
- 195 15. Kers JG, Saccenti E. The Power of Microbiome Studies: Some Considerations on Which Alpha and Beta Metrics to Use and How to Report Results. *Front Microbiol* 2022;12. <https://doi.org/10.3389/fmicb.2021.796025>



Click here to access/download
Supplemental Material
Supporting_Information.pdf

